2013

Callovian (upper Middle Jurassic) Magnetostratigraphy: A Composite Polarity Pattern From France, Britain and Germany, and its Correlation to the Pacific Marine Magnetic Anomaly Model

Rachel Anne Gipe
Purdue University, Rachel.Gipe@gmail.com

Graduate School ETD Form 9
(Revised 12/07)

PURDUE UNIVERSITY
GRADUATE SCHOOL
Thesis/Dissertation Acceptance

This is to certify that the thesis/dissertation prepared

By Rachel A. Gipe

Entitled
Callovian (upper Middle Jurassic) Magnetostratigraphy: A composite Polarity Pattern from France, Britain and Germany, and its correlation to the Pacific magnetic anomaly model

For the degree of Master of Science

Is approved by the final examining committee:

William Zinsmeister
Chair

James Ogg

Masako Tominaga

To the best of my knowledge and as understood by the student in the *Research Integrity and Copyright Disclaimer (Graduate School Form 20)*, this thesis/dissertation adheres to the provisions of Purdue University's "Policy on Integrity in Research" and the use of copyrighted material.

Approved by Major Professor(s): James Ogg

Approved by: Indrajeet Chaubey 10/04/2010
Head of the Graduate Program Date

CALLOVIAN (UPPER MIDDLE JURASSIC) MAGNETOSTRATIGRAPHY: A COMPOSITE POLARITY PATTERN FROM FRANCE, BRITAIN AND GERMANY, AND ITS CORRELATION TO THE PACIFIC MARINE MAGNETIC ANOMALY MODEL

A Thesis

Submitted to the Faculty

of

Purdue University

by

Rachel Gipe

In Partial Fulfillment of the

Requirements for the Degree

of

Master of Science

December 2013

Purdue University

West Lafayette, Indiana

ACKNOWLEDGEMENTS

I would like to thank my advisor, Professor James Ogg, for support and guidance through this project. I would like to thank Professor Masako Tominaga for providing me with the amazing opportunity to participate on the 2011 Jurassic Ocean Crust Magnetic Survey. I would also like to thank her for being on my committee and for providing valuable insights into geophysics and the study of the Earth's geomagnetic field. A sincere thanks also goes to Professor William Zinsmeister for taking the time to serve on my advisor committee.

Analytical facilities were generously provided by the paleomagnetic laboratories at the University of Michigan (Rob Van der Voo), the University of Oxford (Buffy McClelland) and GeoForschungZentrum Postdam, Germany (Manfred Menning and Nobert Nowaczyk). For assistance with the fieldwork and sample collection, I would like to thank Angela Coe (The Open University), Jean-Pierre Garcia (Universite de Bourgogne) and Gerd Dietl (Staatliches Museum für Naturkunde Stuttgart).

I would particularly like to thank my friend and family for the support they provided me through my graduate work at Purdue University.

TABLE OF CONTENTS

Page

Page

LIST OF TABLES

LIST OF FIGURES

Figure Page

Figure Page

ABSTRACT

Gipe, Rachel A. M.S., Purdue University, December 2013. Callovian (upper Middle Jurassic) Magnetostratigraphy: A composite polarity pattern from France, Britain and Germany, and its correlation to the Pacific marine magnetic anomaly mode. Major Professor: James Ogg.

Callovian strata from sixteen exposures across western Europe produced a nearly continuous composite geomagnetic polarity reference sequence spanning the latest Bathonian (*Clydoniceras discus* Zone) through the entire Callovian and into the earliest Oxfordian (*Quenstedtoceras mariae* zone). This sequence is compiled from multi-section sequences from France and England, a section in southern Germany, and a section on the Isle of Skye (Scotland). These sections are calibrated with ammonite biostratigraphy, brachiopod associations and sequence stratigraphy. Over 400 oriented core samples were subjected to progressive thermal demagnetization and filtered according to magnetic behavior; the highest quality suite produced mean paleopoles of 67.3°N, 174.8°E (δp: 5.0, δm: 7.6) for the English composite, 80.4°N, 137.4°E (δp: 2.7. δm: 3.6) for the French composite, 48°N, 137°E (δp: 8.0, δm: 13.8) on the Isle of Skye and 81.8°N, 171.1°E (δp: 7.6, δm: 10.1) in Southern Germany. The composite polarity pattern for the Callovian shows a trend of longer durations for the normally oriented zones that is interrupted by three clusters of Chrons dominated by their reversed-polarity. The observed Chron duration in addition to the overall trend in orientation mirrors the pattern found from M37 through M39 in the pre-M29 geomagnetic polarity block models based on marine magnetic anomaly analyses from the Pacific Ocean, with the Callovian-Oxfordian boundary occurring within anomaly M37n (tentatively within M37n.1n) and the Callovian-Bathonian boundary falling within M39n.

1 INTRODUCTION

Manuscript to be adapted for publication in Earth and Planetary Science Letters.

The application of magnetic stratigraphy as part of an integrated time scale, along with biostratigraphy and other stratigraphic methods, is a powerful tool for high-resolution global correlations. This sequence records the same global magnetic reversal history that is preserved in the marine magnetic anomaly sequence (Cox et al., 1963; Opdyke et al., 1966; Vine & Wilson, 1965). Numerous investigators, including Heirtzler et al. (1968), Larson and Hilde (1975), LaBrecque et al (1977), Cande and Kent (1992a, 1992b, 1995) and Sager et al (1998), have demonstrated the application of a simple polarity block model to understand the geomagnetic time scale. Of this well-studied aspect of the timescale, the oldest oceanic crust existing on the Earth formed during the Jurassic period and contain the least well-understood magnetic sequence (Tivey et al., 2006). In the central Atlantic, the Jurassic age oceanic crust was formed associating with the initiation of breakup of Pangaea, following a period of extensive rifting during the Triassic-Early Jurassic (Golonk & Ford, 2000). In the western Pacific, Jurassic age crust was formed at the ridge-ridge-ridge triple-junction. The extent of the Jruassic crust is currently recognized by the Japanese, Hawaiian, and Phoenix M-sequence magnetic lineation sets. The M-sequence magnetic polarity reversal record is modeled and numbered based on the pre-M28 marine magnetic anomalies from the Japanese lineation set, and is currently extended to M44 (Tivey et al., 2006; Tominaga et al., 2008). To identify and model these pre-M28 magnetic anomalies with the low amplitude, short-wavelength feature, the application of near-source data acquisition (i.e. deep-towed magnetic mapping) (Tivey et al., 2006; Tominaga et al., 2008). The age model for the M-sequence is mainly constrained by radiometric dating of basalts at ODP Sites 878 at MIT Guyot (122.9±09 Ma, Pringle & Duncan, 1995), 765 from anomaly M26r in Argo Abbysal Plain (155.3 ± 3.4 Ma, Ludden, 1992) and 801C at Chron M42 in the Pigafetta basin (167.7 ± 1.4 Ma, Koppers et al., 2003). This block model has been successfully correlated with biostratigraphy of the Late Jurassic through the application of magnetostratigraphic studies

(e.g., Channell et al., 1987; Ogg, 1988; Ogg et al., 2010; Przybylski et al., 2010a, 2010b; Speranza et al., 2005). Modeled anomalies older than the identified base of the Oxfordian, Chron M37n.1n.25, have remained biostratigraphically uncalibrated and unverified due to the absences of a complete Callovian (upper Middle Jurassic) paleomagnetic sequence with associated with well-resolved biological markers (Ogg et al., 2010).

Through the application of high-resolution magnetostratigraphic correlations, a nearly continuous magnetic polarity reference pattern from the Callovian is derived from outcrops in France, central England and southern Germany (Figure 1; Table 1). These outcrops contain ammonite biostratigraphy, brachiopod associations, regional sea-level oscillations and/or cyclostratigraphic sequences, allowing for the establishment and the verification of a paleomagnetic timescale for the entire Callovian. Here we have investigated over 400 paleomagnetic samples from these strata to construct a magnetostratigraphic sequence coeval to Chrons M37-M39. This magnetostratigraphic record of the Earth's field reversals is the principal method for the validation and improvement of the magnetic polarity reversal sequence models. In addition to paleomagnetic directions, the paleomagnetic pole for each sample is calculated, providing virtual geomagnetic pole measurements for the four regions in Europe.

Figure 1: Locations of the outcrops from Burgundy, France (Burgundy high, Eastern Paris Basin), Southeast France (Dauphinois basin), Swabian Alb, Germany (South German Basin) and southern England (Worchester Basin, East Midland Shelf and Cotswold) sampled for the magnetostratigraphy of this study, indicated in open circles.
Figure 1A provides the regional relationship between the sample lcoations. The English set of sampling locations contains four outcrops: Shipton-on-Cherwell Cement Works (SC), Shorncote Quarry (SK), King's Dyke Clay Pit (KD) and Dix Pit, Stanton Harcourt (SH). Southeastern France contains two outcrops (THX and SAV) within a few kilometers of each other. Swabian Alb (Swabia) and the Isle of Sky (STF) each contain a single sample location, as depicted. The Burgundy high region is expanded in Figure 1B depicting the distribution of the following 11 outcrops: Chassignelles (CHAS), Buffon (BUF), Chatillon-sur-Seine (CSS), Etrochey (ETR), Nuits-St-George (NSG), Val Suzon (VSZ), Ladoix (LAD), Veuxhaulles-sur-Aube (VSA), Saulx-le-Duc (SLD), Talant – Cormbe Valton (CVT) and Corelles – La Cras (CRAS). The extent of Middle Jurassic units of Great Britain, France and Germany are mapped in dark grey based on DiGMapGB-625 from the British Geological Survey and maps from the OneGeology-Europe project and the participating geological survey organization rightholders. See Table 1 for detailed information on individual sections.

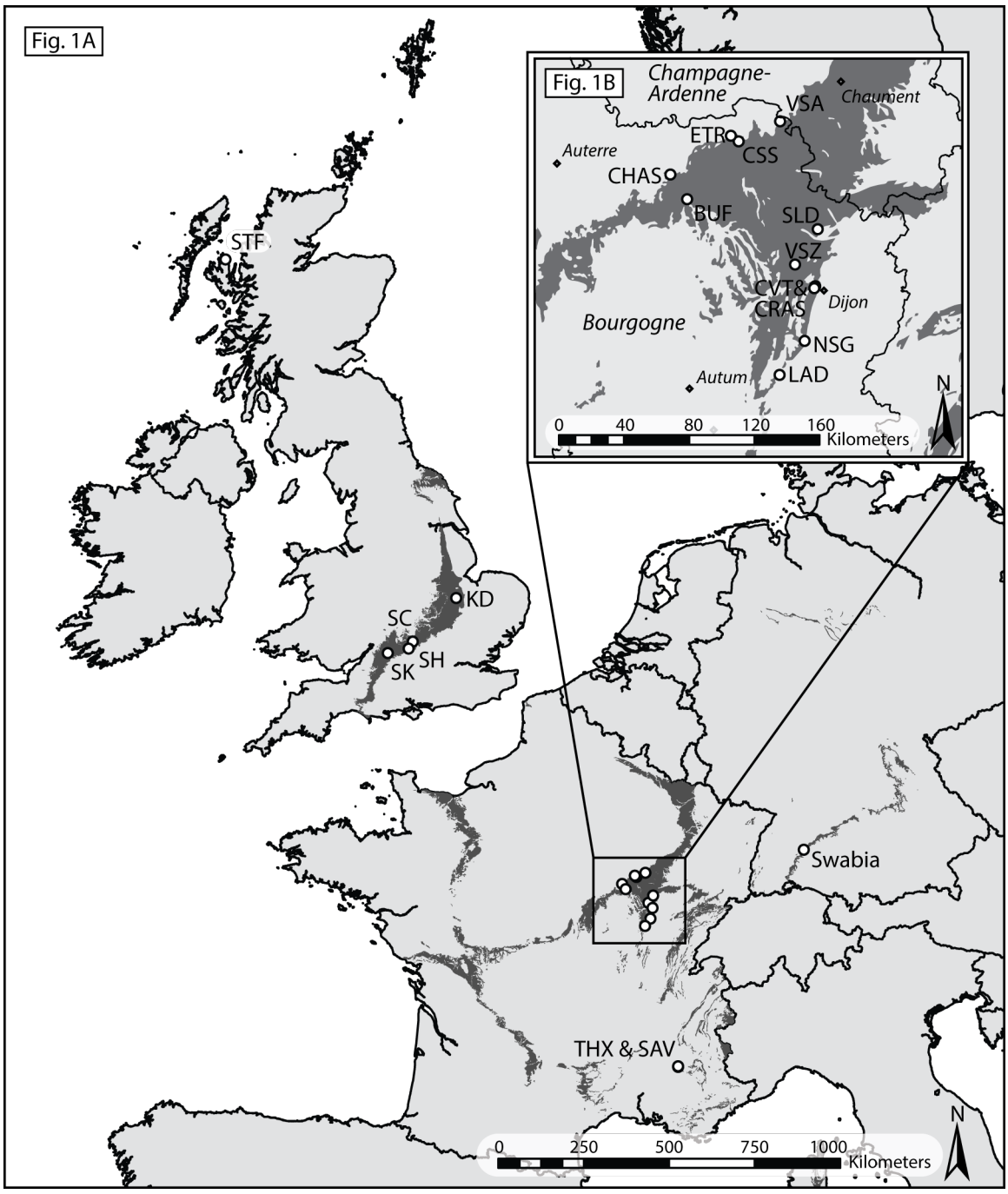
Fig. 1A
Fig. 1B
Champagne-
Ardenne
VSA
Chaumont
ETR
CSS
Auterre
CHAS
BUF
SLD
VSZ
CVT&
CRAS
Dijon
Bourgogne
NSG
Autum
LAD
N
0 40 80 120 160
Kilometers
STF
KD
SC
SH
SK
Swabia
THX & SAV
N
0 250 500 750 1000
Kilometers

Figure 1

Table 1: Summary information for the Callovian sampling sites.

Location		Position		Average Bedding		Magnetic Field		Sampling	
Outcrop	Abbr	Lat	Long	Dip	Dip Dir	Incl	Dec	Height	Samples
Burgundy, France		(°N)	(°E)	(°)	(°)	(°)	(°)	(m)	
Chassignelles	CHAS	47.7	4.2	1	330	63.3	-1.3	6.5	14
Buffon	BUF	47.7	4.3	Horizontal		63.4	-1.2	13.9	16
Châtillon-sur-Seine	CSS	47.9	4.6	2	360	63.5	-1.4	16.5	11
Etrochey	ETR	47.9	4.5	Horizontal		63.5	-1.4	10.4	14
Nuits-St-George	NSG	47.1	4.8	Horizontal		62.8	-1.2	13.1	25
Val Suzon	VSZ	47.4	4.9	2	150	63.1	-1.0	6.1	13
Ladoix	LAD	47.0	4.8	Horizontal		62.8	-1.2	13.1	9
Veuxhaulles-sur-Aube	VSA	47.9	4.8	Horizontal		63.6	-1.1	13.1	20
Saulx-le-Duc	SLD	47.5	5.0	Horizontal		63.2	-1.0	1.5	16
Talant -- Cormbe Valton	CVT	47.3	5.0	15	20	63.0	-1.0	4.1	10
Corelles -- La Cras	CRAS	47.3	5.0	3	330	63.0	-1.0	0.8	5
England									
Shipton-on-Cherwell	SC	51.9	358.7	2	135	66.8	-3.8	5.1	43
Shorncote Quarry	SK	51.7	358.0	3	215	66.6	-4.1	7.1	23
King's Dyke Pit	KD	52.6	359.8	Horizontal		67.3	-3.8	25.5	59
Dix Pit	SH	51.3	358.6	2	20	66.7	-4.1	3.8	37
Isle of Sky									
Staffin Bay	STF	57.6	353.8	39	291	70.5	-2.0	39.3	71
Germany									
Swabian Albstadt	SBC	48.4	9.0	Horizontal		64.2	-0.6	2.0	37

2 PALEOMAGNETIC ANALYTICAL PROCEDURE AND MAGNETIC PROPERTIES/ANALYSIS OF PALEOMAGNETIC SAMPLES

2.1 Demagnetization procedure and magnetic behavior

Paleomagnetic samples collected from various field locations were analyzed in magnetically shielded spaces at the University of Michigan (USA), Oxford University (Great Britain) and the University of Munich (Germany) using two- or three-axis cryogenic magnetometers.

The remnant magnetization of each sample was measured using progressive thermal demagnetization with temperature steps tailored to each lithology and region, as implied by a set of pilot studies. Samples were typically demagnetized beginning at 200°C, with temperature steps of 20-40°C. For the majority of samples, the bulk susceptibility was monitored at every other demagnetization step below 300°C and at each step that followed. At the University of Michigan and the University of Munich, the very fissile samples were wrapped in aluminum foil, to prevent disintegration when the clays dehydrated, without adding any measurable magnetization. At the University of Oxford, gluing was required to hold fissile samples together as the wrappings acquired spurious magnetizations in the Helmholtz-coil field-free zone.

There is variability in the response of samples to the demagnetization procedure resulting from variations in lithology and outcrop location, but generalized characteristics are identifiable. All of the samples began with an initial natural remnant magnetization (NRM) dominated by a normal direction corresponding to the modern magnetic field. Typical samples reveal their depositional remnant magnetization upon the removal of this secondary overprint between 240°C and 350°C. Continued heating led to a decrease in remnant magnetization at or below the level of magnetometer noise, a surge in susceptibility and/or the advent of viscous remnant magnetization (VRM). This temperature range is indicative of magnetite (a range of 200°C to 400°C). The observed surge in susceptibility and/or VRM is likely resulting from the combined effects of iron-rich clays dehydrating and iron sulfides oxidizing to produce new iron oxide minerals. Magnetic measurements at temperatures above 400°C typically only show random noise. Detailed progressive demagnetization data, lithological details and interpretations are available in the supplemental material.

2.2 Interpretation of magnetic behavior

With the aid of the Paleomagnetic Analysis Program, *Paleomag* (Zhang & Ogg, 2003), the demagnetization trends of samples were analyzed for the characteristic magnetic direction, polarity assignment and reliability. The visualization through Zijderveld (or modified Zijderveld) projection and stereographic projections in both geographical and tilt-corrected coordinates provided a tool to select the demagnetization steps used to compute the characteristic directions of each sample (Zhang & Ogg, 2003). Each sample's best three-dimensional least squares fit of the user-selected demagnetization steps was conducted within the *Paleomag* program through principal component analysis (PCA) as developed by Kirschvink (1980; Zhang & Ogg, 2003). A fisher statistics routine built into the *Paleomag* program conducted fisher statistics (Fisher, 1953) on the set of PCA least squares data, computing the mean directions for the normal and reversed polarities as well as the mean direction for the combined normal and antipode of the reversed polarities. Also calculated for comparison with the combined direction is the vector combination of the mean normal and mean reversed poles.

A combined polarity and reliability ranking system (e.g., Ogg, 2010; Przybylski et al., 2010a, b), was applied to assign a characteristic directions of either normal or reversed polarity to the observed demagnetization behavior as well as a ranking for the confidence of that orientation. Demagnetization behavior containing at least three successive demagnetization steps within 15 degrees of each other and showing the typical intensity decrease received an assignment of R or N (Figures 2a, 2b)). Demagnetization behavior that provided an obvious magnetic polarity but did not meet the standards for R and N, were assigned NP and RP (Figures 2c, 2d)), and these received a half weight in calculations of mean paleomagnetic directions. NPP- and RPP-rated samples showed a systematic trend towards a polarity end point in their demagnetization trend, but were omitted from mean pole computations. NPP and RPP demagnetization behavior either did not achieve enough cleaning during demagnetization or yielded a set of poles with a large amount of variability in orientation. Uncertain samples (N? and R?) and indeterminate samples (INT) were assigned to samples with poorly defined paleomagnetic polarities; these samples were not used to define polarity zones or for paleomagnetic direction analysis (Figures 2e, 2f)). Both the selection of demagnetization steps for computing characteristic directions and the assignment of pole direction and rank were conducted by two independent investigators and then compared to decrease bias.

Figure 2: Examples of the typical thermal demagnetization behavior for samples with various polarities and quality ratings.

Sample assessment and the assignment of polarity ratings is assisted by two display methods, a stereographic projection (right of each paired plot) and a projected vector (Zijderveld) diagram (left of each paired plot). Each measured step not utilized in characteristic direction calculation is plotted in grey, while those plotted in black were selected for the calculation of a characteristic direction. In the Zijderveld diagram the inclination is plotted with solid points and a solid line while the declination is plotted with hollow points and a dashed line. (a) Saulx-le-Duc quary sample SLD_8B (a densely packed iron-oolite) is rated 'R' based on the tight clustering and location of six thermal demagnetization steps (240°-400°C). The calculated characteristic vector has a 183.4°declination, -49.8° inclination and 4.46E-01 A/m intensity. (b) Ladoix quarry sample LAD_22 (a medium-gray grainstone) is rated 'N' based on the tight clustering of points and the intensity decay trend. Five temperature steps were selected (240°-360°C) produced a characteristic vector of 37.3° declination, 57.5 inclination and 3.84E-02 A/m intensity. (c) Nuits-St-George quarry sample NSG_15 (a medium-grey grainstone) is ranked 'RP' for the clump of four measurements across two temperature steps (300°C and 330°C) producing a characteristic vector of 188.0° declination, -54.3° inclination with and intensity of 8.68E-03 A/m. (d) King's Dyke Clay Pit sample KD_18.1 (a dark grey shale) is ranked 'NP' for three thermal demagnetization steps for the larger spread of the three points but still strongly normal orientation. The three temperature steps (240°-300°C) produces 1.1° declination and 59.0° inclination with an intensity of 3.03E-02 A/m. (e) Saulx-le-Duc quarry sample SLD_25A (a light tan-yellow wackestone) is ranked 'R?' for its likely trend towards reversed but lacks a stable orientation for the demagnetization endpoint due the sample's low intensity. The final demagnetization step at 240°C, measured twice, produces an orientation of 312.26° declination and -12.06° inclination with a very low intensity of 3.18E-03. (f) Saulx-le-Duc quarry sample SLD_12A (a light grey bioclastic limestone) produced an orientation of 'N?' for having a trend that is probably normal but low intensities, high error and a large amount of variation in measured direction make assessment of low quality. The three temperature steps (150°-240°C; 5 measurements) produced a 348.5° declination, 62.8° inclination and 1.09E-02 intensity.

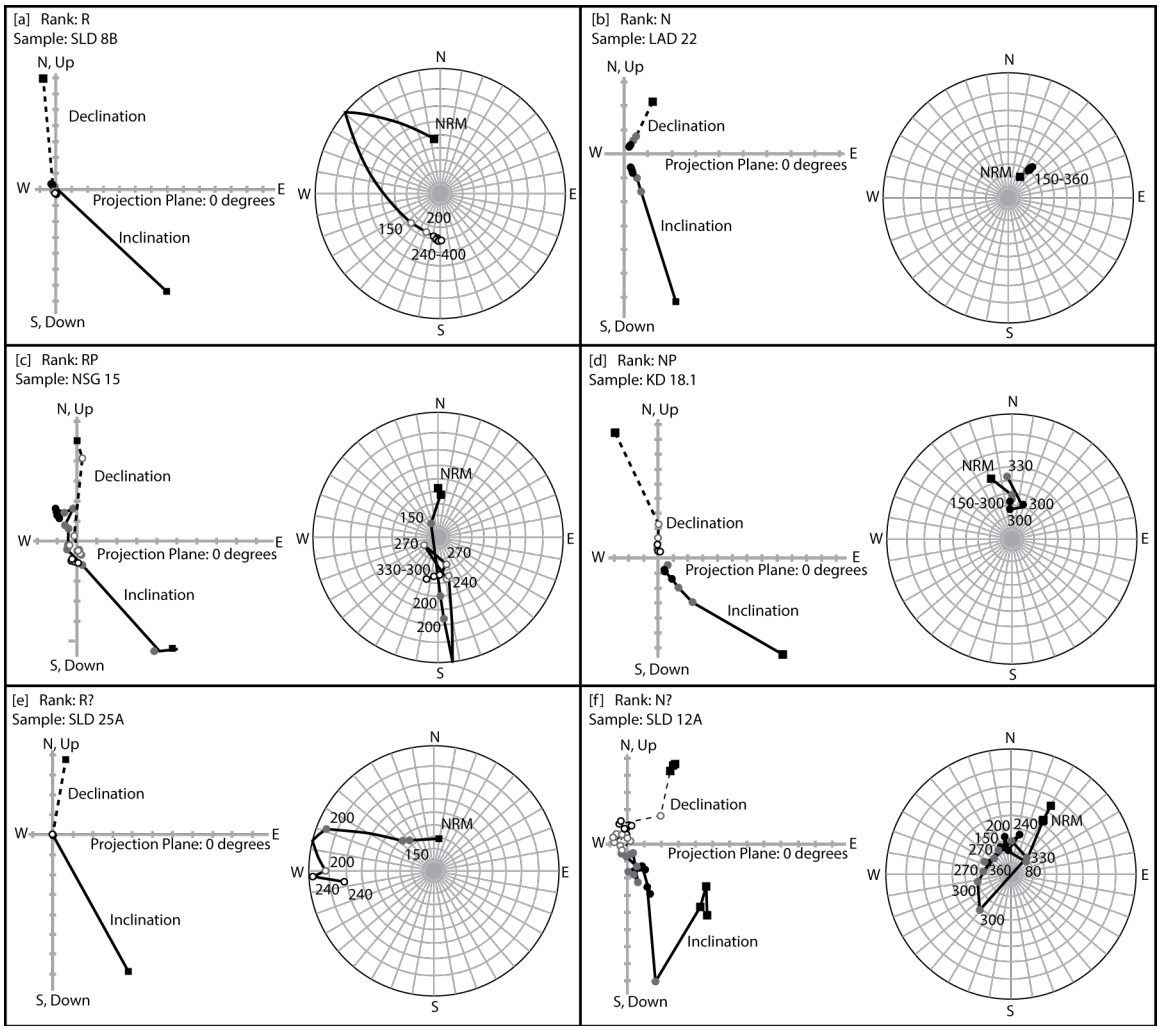
[a] Rank: R
Sample: SLD 8B
N, Up
Declination
W
E
Projection Plane: 0 degrees
Inclination
S, Down
N
W
E
S
NRM
200
150
240-400
[b] Rank: N
Sample: LAD 22
N, Up
Declination
W
E
Projection Plane: 0 degrees
Inclination
S, Down
N
W
E
S
NRM
150-360
[c] Rank: RP
Sample: NSG 15
N, Up
Declination
W
E
Projection Plane: 0 degrees
Inclination
S, Down
N
W
E
S
NRM
150
270
330-300
270
240
200
200
[d] Rank: NP
Sample: KD 18.1
N, Up
Declination
W
E
Projection Plane: 0 degrees
Inclination
S, Down
N
W
E
S
NRM
330
150-300
300
300
[e] Rank: R?
Sample: SLD 25A
N, Up
Declination
W
E
Projection Plane: 0 degrees
Inclination
S, Down
N
W
E
S
200
NRM
150
200
240
240
[f] Rank: N?
Sample: SLD 12A
N, Up
Declination
W
E
Projection Plane: 0 degrees
Inclination
S, Down
N
W
E
S
200
240
NRM
150
270
330
270
360
80
300
300

Figure 2

3 STRATIGRAPHIC SAMPLING

The abundance of ammonites in the Jurassic strata of Central Europe enables the high-resolution subdivision into ammonite assemblage zones (e.g., Arkell, 1956). Strata spanning the late Callovian into early Oxfordian contain the highest level of mixing of Boreal, Sub-Boreal and Sub-Mediterranean ammonoid faunal provinces, thereby enabling inter-bioprovincial correlations (Bradshaw, 1992; Pieńkowski et al., 2008; Ziegler et al., 1982). Increased precision on the duration of these zones and subzones has been improved through the incorporation of a floating astronomical timescales based on Milankovitch cycles (e.g., Boulila et al., 1997; Coe & Weedon, 2006).

Natural outcrops, quarries and road cuts in England, France and Southern Germany were selected for magnetostratigraphy based on the availability of biostratigraphy. These outcrops are located in Burgundy, France (Eastern Paris Basin), Swabia, Germany (South German Basin) and southern England (Worchester Basin, East Midland Shelf and Cotswold) (Figure 1). In the Mid-Jurassic, spreading in the Alpine Tethys and rifting in the Norwegian-Greenland Sea allowed for the maximum extent of the Paris and South German Basins despite the structural highs that dominated the rest of interconnected Central European basin system (Pieńkowski et al., 2008). A shallow, epicontinental sea connecting the Atlantic, Tethys and Northern Oceans was the dominant depositional environment in the region, influenced both locally by tectonic influences and at a regional scale by the transgression of the North Sea sea-level super-cycle (Brigaud, 2009; Cope, 2006; Jacquin et al., 1998; Jacquin & Graciansky, 1998a, 1998b; Hallam, 1978, 2001). Northern portions of these basins are dominated by Boreal biogeographic domain, with the Mediterranean domain located further south in the Tethyan basins (Pieńkowski et al., 2008).

4 FRANCE (BURGUNDY PLATFORM)

The outcrops in Burgundy are located along the eastern edge of the Paris Basin. This basin is a large, semicircular intraplate flexural basin presenting a surface pattern of concentric outcrops of Permo-Carboniferous, Mesozoic and minor Cenozoic sediments that unconformably overlay a Cadomian-Varscan basement (Beccaletto et al., 2011; Pomerol, 1978). Subsidence of this basin began with rifting in the Late Permian and was controlled through the Cenozoic by the combination of long-term thermal subsidence and numerous short-term influences from tectonic deformation of the western Eurasian plate (Beccaletto et al., 2011; Brunet & Pichon, 1982; Robin et al., 2000).

During the middle Jurassic, the dominant control on the depositional patterns within the Paris Basin was provided by the interaction of three semi-stable basement blocks producing a Y-pattern of faulting (Seine-Sennely, Saint-Martin de Bossenay, Bay and Vittel faults) (Guillocheau et al., 2000; Perrodon and Zabek, 1990). The Burgundy arch remained as a relative high through the Bathonian, resulting in the development of a typical subtropical to tropical bioclastic carbonate platform with oolites alongside the Tethyan seaway (Dromart et al., 2003; Gaumet et al., 1996). Slightly deeper basins bound this SW-NE elongated platform to the west (Loire Trough) and east (Lorraine Basin) that were dominated by the deposition of marls (Belkaaloul et al., 1997). A distinct set of facies was deposited as water depth increased from the Bathonian through early Callovian (Garcia & Dromart, 1997; Gaumet et al., 1996). By the Middle Callovian, the oolitic bioclastic deposits that capped the homoclinal, low-angle ramp, were completely drowned (Garcia & Dromart, 1997; Gaumet et al., 1996). This progressive drowning occurred during the backstepping sequences of the transgressive phase of the T/R cycle 8 within the North Sea Cycle (third Mesozoic transgressive/regressive cycle) (Garcia, 1993; Hallam, 2001; Jacquin & Graciansky, 1998a; Jacquin & Graciansky, 1998b; Jacquin et al., 1998).

Within the Callovian, six third-order sequences, at the outcrop scale, have been identified (e.g., Hardenbol et al., 1998). All six sequences are found in some parts of the Paris Basin, but at the Burgundy high, the Oolithe Ferugineuse marker bed tops the middle Callovian at sequence boundary Ca3, and a very condensed section was deposited during the upper Callovian through lower Oxfordian (Jacquin et al., 1998).

Lateral facies changes along the carbonate ramp influence the correlation of lithologic boundaries among outcrops as well as the interpretation of sequence boundaries within the units. The third-order sequences, regional lithologic trends, brachiopod associations and ammonite levels in these outcrops were established and corroborated by numerous studies (e.g., Brigaud et al., 2009; Collin, 1997; Collin & Courville, 2006; Delance et al., 1993; Garcia, 1993; Garcia & Dromart, 1997; Garcia et al, 1996; Gaumet et al., 1996; Jacquin et al., 1998b; Marchand & Thierry, 1997 and Thierry et al., 2006) (e.g., Figure 3). To improve correlation, the spatial location of the outcrops along the Burgundy platform ramp was considered in the correlation of the magnetostratigraphy sections. These correlation tools allowed the magnetostratigraphic sections to be tied to the standard ammonite biostratigraphy timescale.

The basal formation in our study is the micritic limestone of the Calcaire de Comblanchien formation. The distinct hardground at top of this formation is the Ca0 sequence boundary. In the Burgundy Platform domain, the Calcaire de Comblanchien is overlain directly by the Calcaires Bicolores unit of the Pierre de Dijon-Corton formation. In the transitional to distal domains, a set of marls, the Marnes à Eudesia, is between the upper and lower limestone units. The basal portion of the Pierre de Dijon-Corton formation in this domain is distinguished by Garcia (1993) as the Calcaires grenus unit. The presence of the ammonites *Eudesia multicostata* and *Burmirhynchia elegantula* within both the lower part of the Marnes à Eudesia formation and the base of the Calcaires Bicolores unit of the Pierre de Dijon-Corton formation indicates that lower part of the Pierre de Dijon-Corton within the ramp domain correlates with part of the Calcaires Bicolores unit of the Pierre de Dijon-Corton within the platform domain. This is supported by both the facies successions within the Ca1 sequence and the brachiopod association of *Lotharingella gremifera (sub-assemblage 1)*.

The marls of the Marnes à Digonelles unit of the Pierre de Dijon-Corton occurs next in both the domains, with its base located in the transgressive systems tract of the Ca1 sequence. The brachiopod associations of *Lotharingella gremifera (sub-assemblage 2)* and *Digonella divionensis* fall within these marls except at Val Suzon, where *Lotharingella gremifera (2)* is at the top of the coarser-grained underlying facies of the Pierre de Dijon-Corton. The upper

boundary of the Marnes à Digonelles is distinctly different between the ramp domain and the platform domain. In the ramp domain, the brachiopod association *Burmirhynchia latiscensiss* is below the hardground that caps the Pierre de Dijon formation and is overlain by the Pierre de Ladoix formation. In the platform domain, the Marnes à Digonelles unit is overlain by the Calcaires à Rhynchonelles formation within which the *Burmirhynchia latiscensiss* brachiopod association. Within the Burgundy platform domain the Calcaires à Rhynchonelles is overlain by the Calcaires à Plantes formation and the Calcaires à Coraux d'Etrochey formation. Capping the succession in all domains is a pitted hardground overlain by the condensed Ferruginous Oolite formation.

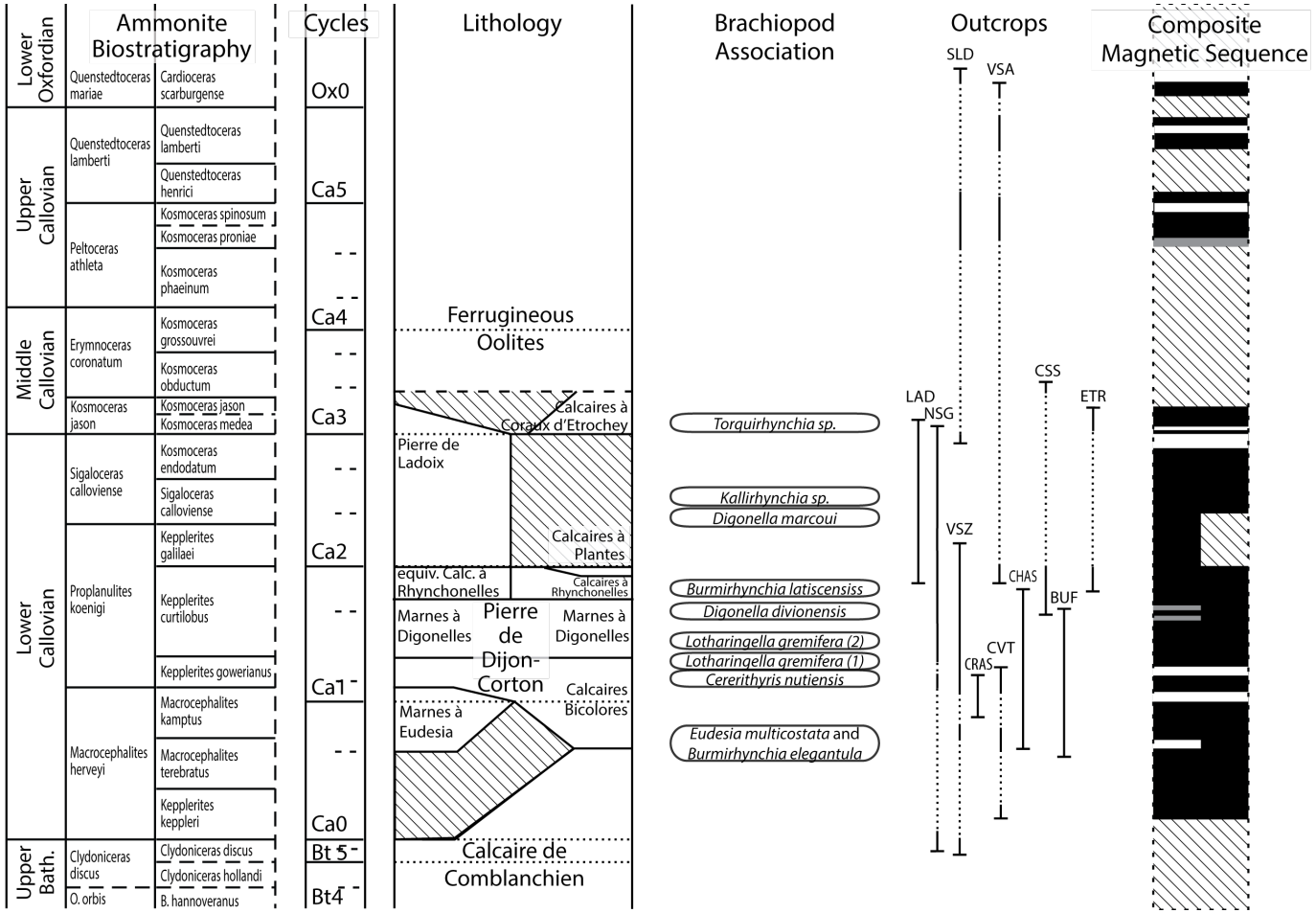

Figure 3: A composite magnetostratigraphic sequence constructed from the French Callovian outcrops is plotted against Sub-Boreal ammonite biostratigraphy and Boreal third order cycles as scaled by Hardenbol et al. (1998) and the GTS2012 (Ogg & Hinnov, 2012). The spans represented in each of the French outcrops and their observed brachiopod associations are indicated next to the interpreted composite sequence.

4.1 French Outcrops

The magnetic stratigraphy sequence from France is compiled from 11 Callovian outcrops across the Burgundy platform region and associated ramps. The Veuxhaulles-sur-Aube (VSA), Chatillon-sur-Seine (CSS), Etrochey (ETR), Chassignelles (CHAS) and Buffon (BUF) outcrops transect the western branch of the Burgundy high and ramp. A southern-trending transect includes the Talant – Cormbe Valton (CVT), Corelles – La Cras (CRAS), Saulx-le-Duc (SLD), Nuits-St-George (NSG), Ladoix (LAD) and Val Suzon (VSZ) outcrops (Figure 1B).

4.1.1 Chassignelles (CHAS); upper Bathonian-lower Callovian

The Chassignelles quarry (Figure 4) exposes the Calcaires Bicolores and the Marnes à Digonelles units of the Pierre de Dijon-Corton formation. A basal hardground is overlain by a bluish-grey bio-oo-sparite and oolitic grainstone beds. Onto a perforated surface below the base of bed 8 is a horizon of bioturbated pebbles and shelly debris that marks the onset of the first of two parasequences within the Calcaires Bicolores unit as well as a fauna renewal and third-order maximum flooding surface (Garcia, 1993). The pair of parasequences concludes with bioturbated biomicrite beds followed by a package of oo-bio-sparite beds. A third parasequence is present in the Marnes à Digonelles unit. Brachiopod associations of *Eudesia multicostata* and *Burmirhynchia elegantula, Cererithyris nutiensis, Lotharingella gremifera (1 & 2)* and *Digonella divionensis* occur at the levels shown in Figure 4 (Garcia, 1993).

Paleomagnetic analysis of 14 horizons spanning 8 meters of upper Bathonian-lower Callovian stratigraphy yielded a normal-polarity orientation for all but one sample. The single reversed-polarity sample contained a distinct trend away from a normal pole, but lacked the intensity for reliable orientation measurements. The 11 high-quality characteristic directions produced a tilt-corrected declination of 1.8° and an inclination of 56.6° (α95: 6.1°, K: 77). The modern magnetic pole is indistinguishable from the measured orientation of the non tilt-corrected best-fit orientation at the 95% confidence interval (2.6° declination, 57.4° inclination), indicating the likely presence of an unremoved modern overprint component.

Chassignelles (CHAS)

	Dec	Inc	α95	K	Intensity	Std.Dev (+/-)		R	N	Lat	Long	δp	δm	Paleolat
Normal	1.8	56.6	6.1	77.4	2.60E-02	2.22E-02	-1.20E-02	8.4	8.5	79.4	176.5	6.4	8.8	37.2
Reversed	-	-	-	-	-	-	-	-	-	-	-	-	-	-
Combined	-	-	-	-	-	-	-	-	-	-	-	-	-	-
Vector Comb.	-	-	-	-	-	-	-	-	-	-	-	-	-	-
2nd Vector Comb.	-	-	-	-	-	-	-	-	-	-	-	-	-	-

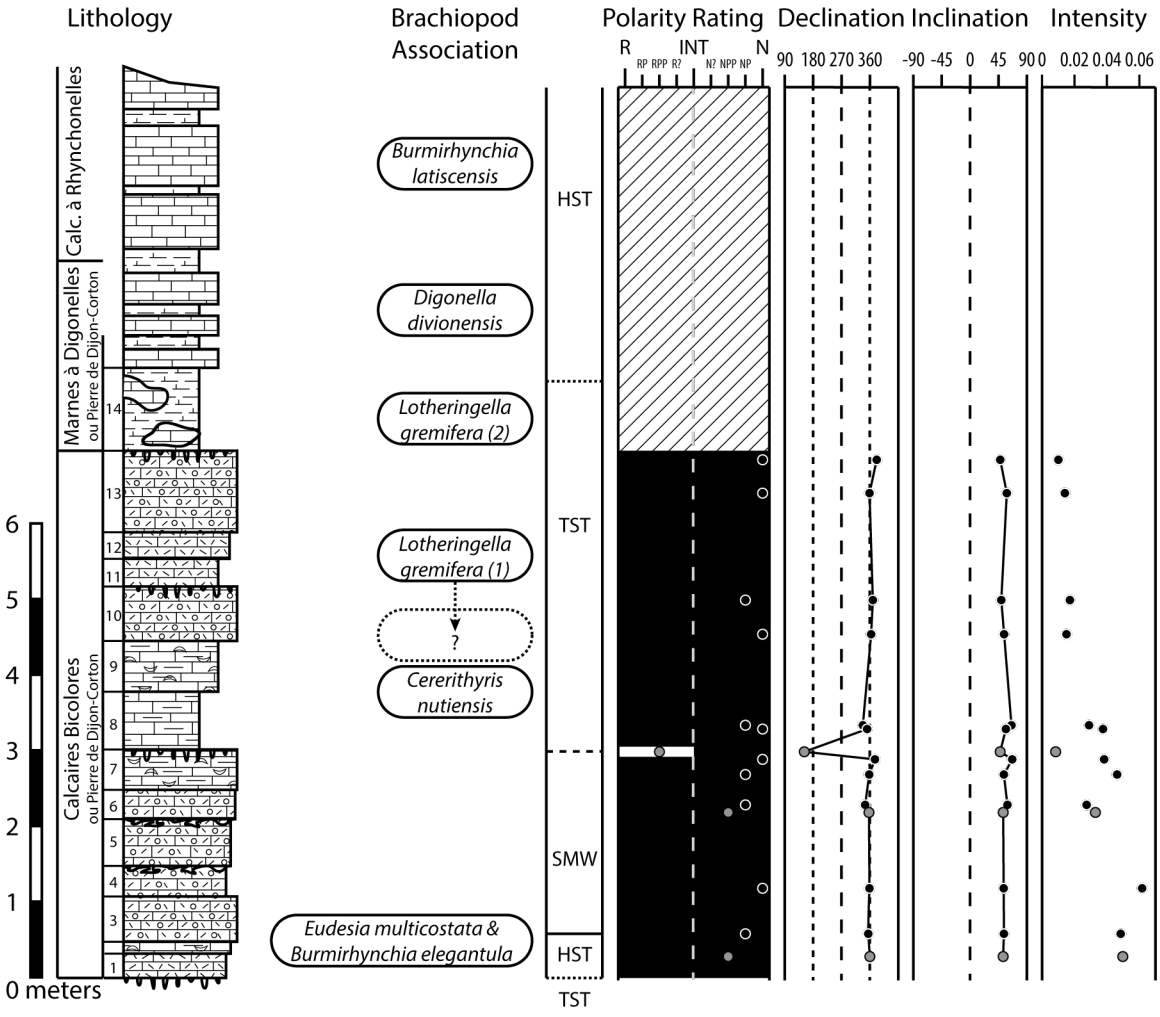

Figure 4: Paleomagnetic measurements from the Chassignelles quarry are plotted by sample location alongside the lithostraigrahy of the outcrop.

The brachiopod associations and sequence stratigraphic surfaces present in this outcrop are plotted at their stratigraphic locations, as interpreted by Garcia (1993) and Delance et al. (1993). Polarity ranking, from highly ranked reversed (R) to highly ranked normal (N) with indeterminate samples falling along the middle (INT), is plotted over the interpreted magnetic sequence. The characteristic direction (declination and inclination) as well as intensity of the calculated best fit vectors for each sample are plotted, corresponding with the location on the outcrop from which the sample was collected. The orientation of the normal vector calculated from the highly ranked (N & NP) samples is included in the table along with the produced virtual geomagnetic pole (VGP; latitude, longitude) and confidence levels (δp, δm).

4.1.2 Buffon (BUF); upper Bathonian-lower Callovian

The Buffon Quarry overlaps with Chassignelles quarry, but penetrates into the underlying Calcaires de Comblanchien formation. This formation has a lower subunit of white oolitic grainstone that terminates in an erosion surface marking a sequence boundary. The upper subunit of the Calcaires de Comblanchien is a pelsparite to oolitic-pellet grainstone that is capped by a hardground. The overlying Calcaires Bicolores member of the Pierre de Dijon-Corton formation is a fine- to medium-grained bio-packstone. Similar to its facies in the Chassignelles quarry, this Calcaires Bicolores unit consists of parasequence packages of a basal marly, bioturbated, reworked lag deposit that is typically covered by a marl bed and then capped with an oobioclastic calcarenite, that can contain cross-bedding. Similar to the CHAS quarry, the onset of marly Bed 13 above a bored surface is associated with a renewal of fauna, and is interpreted as a transgression following a sequence boundary. Another hardground separates the Calcaires Bicolores from the overlying Marnes à Digonelles unit of alternating marls and fine-grained grainstone. The lowermost Calcaires Bicolores contains the brachiopod associations of *Eudesia multicostata* and *Burmirhynchia elegantula* and the index species for the *Clydoniceras discus* ammonite zone (Garcia, 1993) (Figure 5). The *Cererithyris nutiensis* and *Lotharingella gremifera (1)* brachiopod association is in the upper Calcaires Bicolores. The Marnes à Digonelles contains the *Lotharingella gremifera (2)* and *Digonella divionensis* associations and ammonite genera of the *Macrocephalites herveyi* ammonite zone (Figure 5).

The entire suite of 16 paleomagnetic samples are normal polarity, of which 15 are assigned as high-quality characteristic directions. These yield a paleomagnetic declination of 10.0° and an inclination of 54.9° (α95: 7.0°, K: 48) that did not require a tilt-correction as the outcrop contained horizontal bedding. This best-fit orientation is unique from the modern magnetic pole at the 95% confidence interval.

Buffon (BUF)

	Dec	Inc	α95	K	Intensity	Std.Dev (+/-)		R	N	Lat	Long	δp	δm	Paleolat
Normal	10.0	54.9	7.0	48.2	2.33E-02	1.81E-02	-1.02E-02	9.8	10	75.7	149.3	7.1	10.0	35.45
Reversed	-	-	-	-	-	-	-	-	-	-	-	-	-	-
Combined	-	-	-	-	-	-	-	-	-	-	-	-	-	-
Vector Comb.	-	-	-	-	-	-	-	-	-	-	-	-	-	-
2nd Vector Comb.	-	-	-	-	-	-	-	-	-	-	-	-	-	-

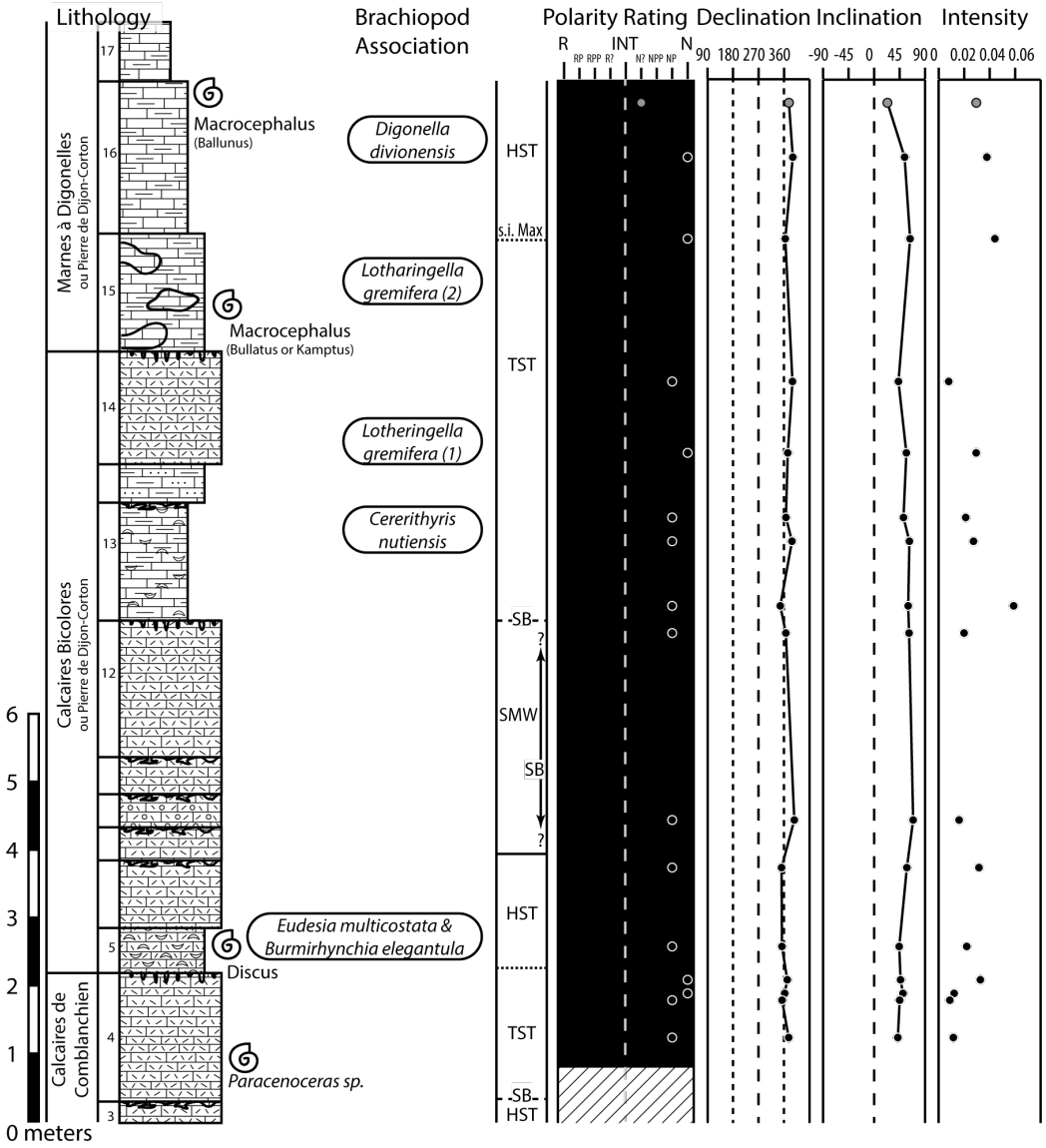

Figure 5: Paleomagnetic measurements from the Buffon quarry are plotted by sample location alongside the lithostraigrahy of the outcrop.

The brachiopod associations, points of dating for ammonite biostratigraphy and sequence stratigraphic surfaces present in this outcrop are plotted at their stratigraphic locations, as interpreted by Garcia (1993). Polarity ranking, from highly ranked reversed (R) to highly ranked normal (N) with indeterminate samples falling along the middle (INT), is plotted over the interpreted magnetic sequence. Characteristic direction (declination and inclination) as well as intensity of the calculated best fit vectors for each sample are plotted, corresponding with the location on the outcrop from which the sample was collected. The calculated normal vector is at the top along with the produced VGP (latitude, longitude) and confidence levels (δp, δm).

4.1.3 Châtillon-sur-Seine (CSS); lower-middle Callovian

The railroad cut near the Châtillon railway station spans the Calcaires à Rhynchonelles formation, plus about 1.5 meters of the uppermost biomicrite beds of the Marnes à Digonelles unit of the Pierre de Dijon-Corton formation (Figure 6). This Calcaires à Rhynchonelles formation is terminated by a karstified hardground that is overlain and a few centimeters of condensed ferruginous oolites. The parasequences of the Calcaires à Rhynchonelles include a range of lithologies from chalky bio-wackestone to bio-oolitic grainstone. Only the middle of the Calcaires à Rhynchonelles formation (Beds 10 and 11) has biostratigraphic age control from the *Burmirhynchia latiscensis* brachiopod association and ammonites representative of the lower Callovian (*Macrocephalites kamptus* Subzone of the *Macrocephalites gracilis* Zone) (Garcia, 1993).

All of the 11 paleomagnetic samples were interpreted as normal polarity. The nine high-quality characteristic directions yielded a tilt-corrected declination and inclination of 342.3° and 60.9° (α95: 7.6°, K: 70). The non tilt-corrected best-fit orientation is unique from the modern magnetic pole at the 95% confidence interval (346.4° declination, 61.5° inclination) but it should also be noted that this orientation is unique from orientations produced by over two thirds of the localities in France.

Figure 6: Paleomagnetic measurements from the Chatillon-sur-Seine Railway exposure are plotted by sample location alongside the lithostraigrahy of the outcrop.
The brachiopod association, points of dating for ammonite biostratigraphy and the sequence stratigraphic surface present in this outcrop are plotted at their stratigraphic locations, as interpreted by Garcia (1993). Polarity ranking, from highly ranked reversed (R) to highly ranked normal (N) with indeterminate samples falling along the middle (INT), is plotted over the interpreted magnetic sequence. The characteristic direction (declination and inclination) as well as intensity of the calculated best fit vectors for each sample are plotted, corresponding with the location on the outcrop from which the sample was collected. The orientation of the normal vector calculated from the highly ranked (N & NP) samples is included in the table along with the produced VGP (latitude, longitude) and confidence levels (δp, δm).

Chatillon-sur-Seine (CSS)

	Dec	Inc	α95	K	Intensity	Std.Dev (+/-)		R	N	Lat	Long	δp	δm	Paleolat
Normal	342.3	60.92	7.64	69.8	3.56E-02	4.88E-02	-2.06E-02	6.4	6.5	76.19	255.6	8.94	11.7	41.95
Reversed	-	-	-	-	-	-	-	-	-	-	-	-	-	-
Combined	-	-	-	-	-	-	-	-	-	-	-	-	-	-
Vector Comb.	-	-	-	-	-	-	-	-	-	-	-	-	-	-
2nd Vector Comb.	-	-	-	-	-	-	-	-	-	-	-	-	-	-

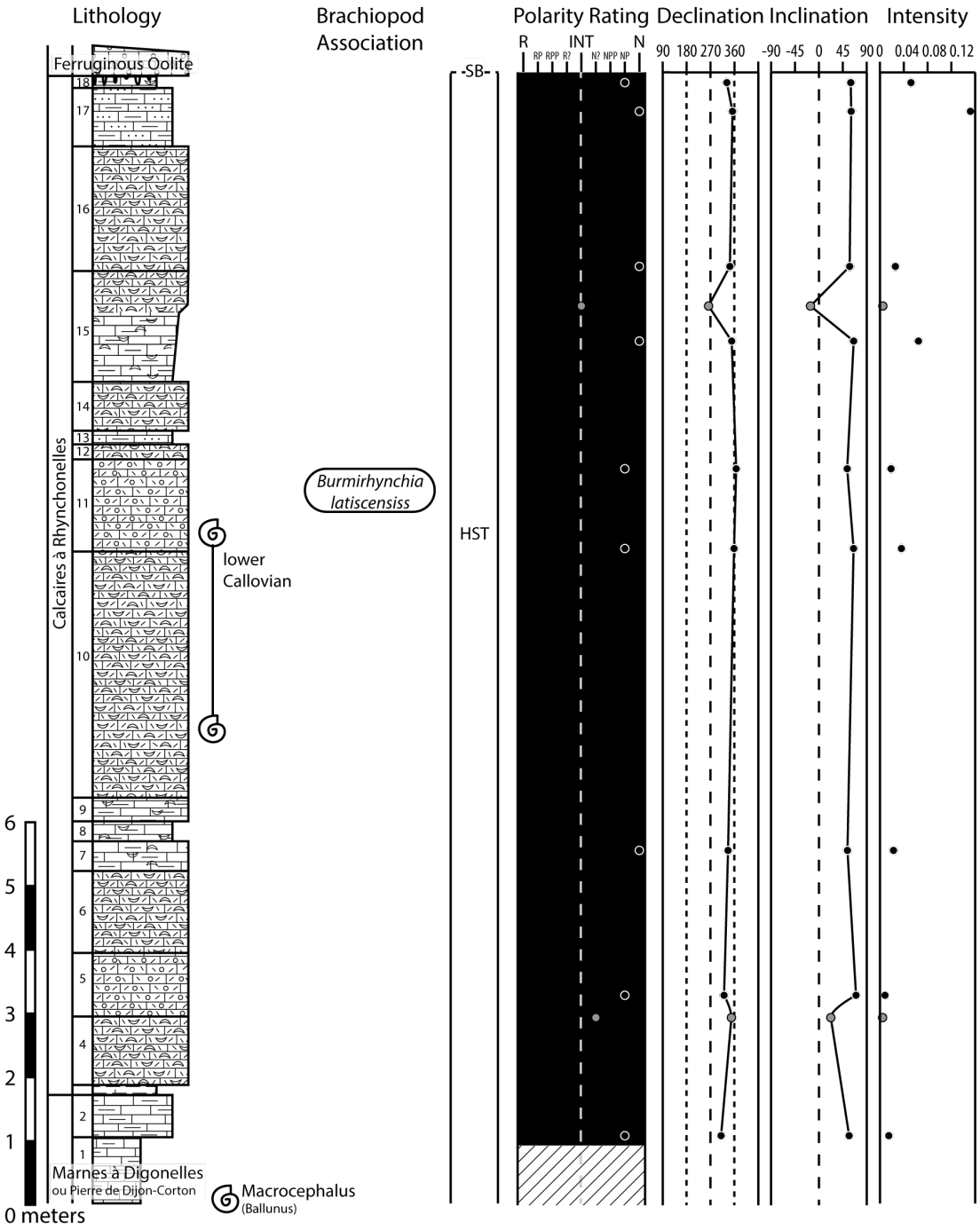

Figure 6

4.1.4 Etrochey (ETR); lower-middle Callovian

Three major stratigraphic units are exposed at Etrochey Quarry: Calcaires à Rhynchonelles, Calcaires à Plantes and Calcaires à Coraux d'Etrochey (Figure 7). The Calcaires à Rhynchonelles formation of gastropod, oncolite, coral-rich bioclastic packstones and wackestones along with occasional lagoonal micrites is similar to the facies at Châtillon-sur-Seine, but does not contain obvious sharp contacts or ravinement surface. The *Burmirhynchia latiscensis* brachiopod association occurs in several horizons (Garcia, 1993). The upward contact to Calcaires à Plantes is marked by a hardground and a transition to a calcarenite rich in bioclasts, oolites and plant fossils. The uppermost Calcaires à Plantes is fining upward to a truncation by a hardground that is interpreted as a major sequence boundary. The overlying Calcaires à Coraux d'Etrochey begins with a distinct faunal replacement to the *Torquirhynchia sp.* brachiopod association and ammonites of the Gracilis Zone (Calloviense or Patina subzone) ammonite surface (Garcia, 1993). The Calcaires à Coraux d'Etrochey has three distinct beds exposed in this quarry.

The 14 paleomagnetic samples were interpreted as normal polarity, of which 11 displayed high-quality characteristic directions. These yielded a paleomagnetic direction of 17.4° declination and 63.0° inclination ($\alpha 95$: 9.0°, K: 34) and did not require a tilt-correction. This orientation is unique from the modern magnetic pole at the 95% confidence interval.

Etrochey (ETR)

	Dec	Inc	α95	K	Intensity	Std.Dev (+/-)		R	N	Lat	Long	δp	δm	Paleolat
Normal	17.4	63.0	9.0	33.6	2.59E-02	1.92E-02	-1.10E-02	8.8	9.0	77.5	104.0	11.1	14.2	44.5
Reversed	-	-	-	-	-	-	-	-	-	-	-	-	-	-
Combined	-	-	-	-	-	-	-	-	-	-	-	-	-	-
Vector Comb.	-	-	-	-	-	-	-	-	-	-	-	-	-	-
2nd Vector Comb.	-	-	-	-	-	-	-	-	-	-	-	-	-	-

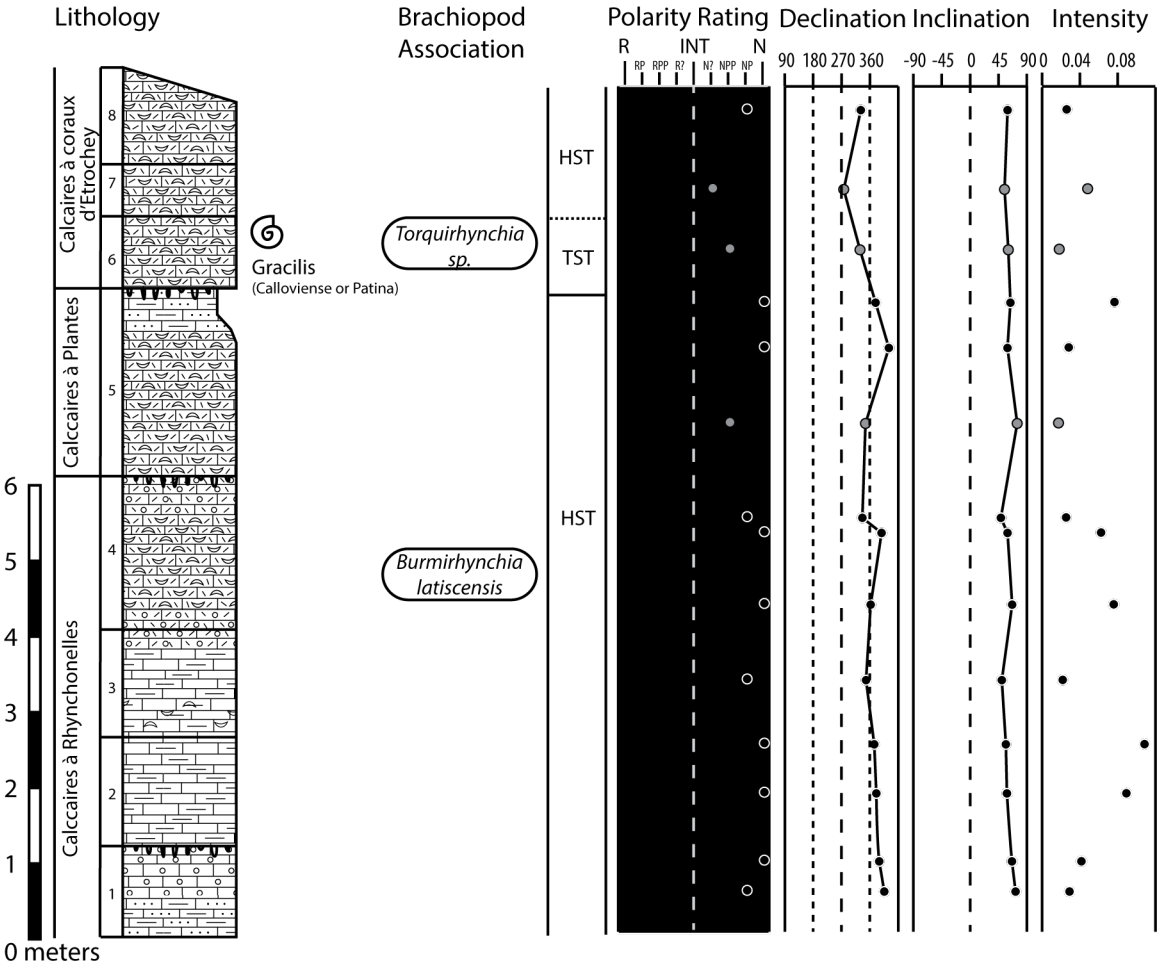

Figure 7: Paleomagnetic measurements from the Etrochey quarry are plotted by sample location alongside the lithostraigrahy of the outcrop.

The brachiopod association, the point of dating for ammonite biostratigraphy and sequence stratigraphic surfaces present in this outcrop are plotted at their stratigraphic locations, as interpreted by Garcia (1993). Polarity ranking, from highly ranked reversed (R) to highly ranked normal (N) with indeterminate samples falling along the middle (INT), is plotted over the interpreted magnetic sequence. The characteristic direction (declination and inclination) as well as intensity of the calculated best fit vectors for each sample are plotted, corresponding with the location on the outcrop from which the sample was collected. The orientation of the normal vector calculated from the highly ranked (N & NP) samples is included in the table along with the produced VGP (latitude, longitude) and confidence levels (δp, δm).

4.1.5 Nuits-St-George (NSG); lower Callovian

The large quarry west of Nuits Saint George exposes over 16 meters of upper Bathonian and lower Callovian (Figure 8). Only the uppermost portion of the Calcaires de Comblanchien formation is exposed, which is a micritic limestone capped with a hardground with burrows infilled by brown marls. The overlying Calcaires Bicolores member of Pierre de Dijon-Corton formation is a grey medium-grained packstone to grainstone that ends in a hardground. The Marnes à Digonelles member of the Pierre de Dijon-Corton formation begins with a lithological transition to wackestone and marls followed by an overall coarsening-upwards trend that is interrupted by an erosional surface in the middle of "Bed 9". The lithology transition at the top of "Bed 10" into a grainstone is interpreted as the beginning of the equivalent to the Calcaires à Rhynchonelles member of the Pierre de Dijon-Corton formation (Garcia, 1993). Brachiopods on the erosional surface at the top of Bed 11 are from the *Burmirhynchia latiscensis* association. The Pierre de Dijon formation ends in a hardground, and the onset of the overlying Pierre de Ladoix formation begins with 30 centimeters of marl that contains ammonites of the Gracilis Zone. This marl is followed by grainstone capped by a rippled surface, and the onset of the succeeding marly facies (Bed 16) is interpreted as a maximum flooding surface (Garcia, 1993). The exposure of the Pierre de Ladoix formation ends in a set of grey packstone to grainstone beds with rounded clasts and crossbedding that are interpreted as a type-two lowstand systems tract. Brachiopod associations include *Eudesia multicostata* and *Burmirhynchia elegantula* at the base of the Pierre de Dijon-Corton formation, *Lotharingella gremifera (2)* at the base and *Digonella divionensis* and *Burmirhynchia latiscensis* within the Marnes à Digonelles unit of the Pierre de Dijon-Corton formation, and *Kallirhynchia sp.* and *Digonella macroui* in the lowermost Pierre de Ladoix formation (Garcia, 1993).

The magnetic stratigraphy from 25 horizons indicated that the basal Pierre de Dijon-Corton formation is reversed polarity, but the overlying units and formations are predominantly of normal polarity with only single-sample levels suggesting brief reversed-polarity subzones (third bed of Pierre de Dijon-Corton formation, and two levels within the Beds 16 and 18 of the middle of the Pierre de Ladoix formation). The mean paleomagnetic direction from the 4 relatively high-quality characteristic directions of reversed polarity (186.8° declination, -42.8 inclination; α95: 57.3°, K: 33) is slightly shallower than the mean direction from the 15 higher-quality normal-polarity samples (7.1° declination, 56.6° inclination; α95: 8.4°, K: 27). The combined mean direction is 7.1° declination, 55.1° inclination (α95: 7.8°, K: 27). This orientation, which does not require a tilt-correction, is unique from the modern magnetic pole at the 95% confidence interval. It also passes the reversal test of McFadden and McElhinny (1990) with an intermediate classification (γ_o/γ_c: 13.8°/25.1°).

Figure 8: Paleomagnetic measurements from the Nuits-St-George quarry are plotted by sample location alongside the lithostraigrahy of the outcrop.
The brachiopod associations, points of dating for ammonite biostratigraphy and the sequence stratigraphic surfaces present in this outcrop are plotted at their stratigraphic locations, as interpreted by Garcia (1993). Polarity ranking, from highly ranked reversed (R) to highly ranked normal (N) with indeterminate samples falling along the middle (INT), is plotted over the interpreted magnetic sequence. The characteristic direction (declination and inclination) as well as intensity of the calculated best fit vectors for each sample are plotted, corresponding with the location on the outcrop from which the sample was collected. The normal, reversed and combined vectors calculated from the highly ranked (R, N, RP, NP) samples are included in the table along with the produced VGP (latitude, longitude) and confidence levels (δp, δm).

Nuits-St-George (NSG)

	Dec	Inc	α95	K	Intensity	Std.Dev (+/-)		R	N	Lat	Long	δp	δm	Paleolat
Normal	7.1	56.6	8.4	26.6	1.28E-02	5.95E-03	-4.06E-03	12.1	12.5	78.8	154.3	8.8	12.1	37.20
Reversed	186.9	-42.8	57.3	33.4	3.71E-02	9.35E-02	-2.66E-02	1.5	1.5	-67.1	-11.4	43.8	70.9	-24.86
Combined	7.1	55.1	7.8	26.7	1.43E-02	1.18E-02	-6.47E-03	13.5	14.0	77.4	157.5	7.9	11.1	35.65
Vector Comb.	6.9	46.3	-	-	2.48E-02	-	-	-	-	69.8	166.8	6.5	10.1	27.65
2nd Vector Comb.	186.8	-35.8	-	-	1.24E-02	-	-	-	-	-	-	-	-	-

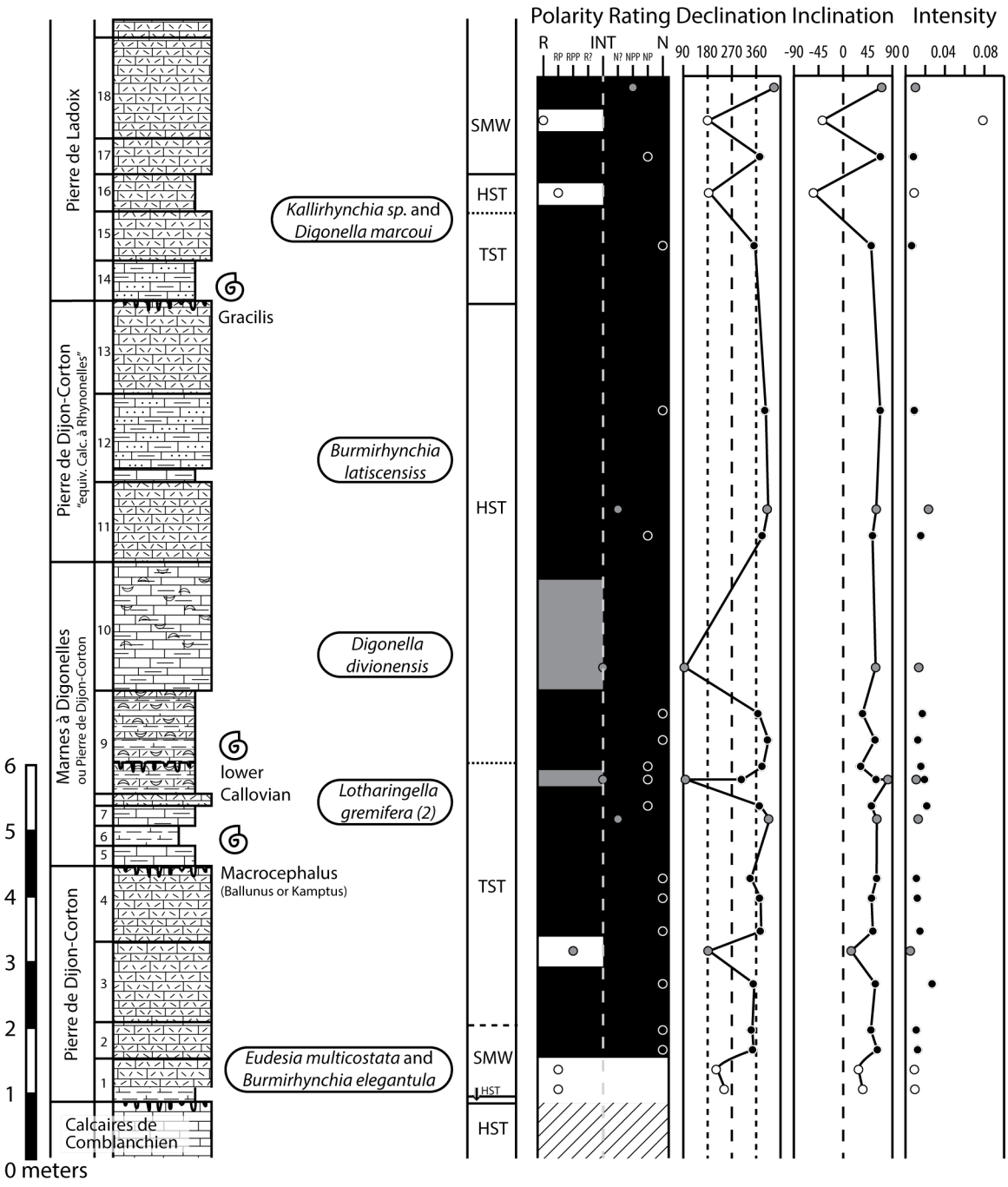

Figure 8

4.1.6 Val Suzon (VSZ); upper Bathonian-lower Callovian

The Val Suzon outcrop is a road cut exposing the very top of the Calcaire de Comblanchien, overlain by a relatively thick section of Marnes á Eudesia topped by the cross-bedded grainstone and pelmicrite of the Pierre de Dijon-Corton formation (Figure 9). The Marnes á Eudesia contains three distinct oolitic grainstone beds separated by marls. The top of the first grainstone bed within the marls is interpreted as the Ca0 third-order sequence boundary (Garcia, 1993). Identified brachiopod associations are the *Eudesia multicostata* and the *Burmirhynchia elegantula* in the first grainstone bed within the Eudesia marl, the *Lotharingella gremifera (1)* at the base of the second Pierre de Dijon-Corton bed, and the *Lotharingella gremifera (2)* at the base of the third bed of the Pierre de Dijon-Corton formation (Garcia, 1993).

All paleomagnetic samples were interpreted as normal polarity; however there are relatively large sample gaps in the upper Pierre de Dijon-Corton formation. The 13 high-quality characteristic directions yielded a tilt-corrected declination of 16.9° and an inclination of 64.4° ($\alpha 95$: 5.7°, K: 57). The non tilt-corrected orientation is unique from the modern magnetic pole at the 95% confidence interval (14.1° declination, 63.0° inclination).

Val Suzon (VSZ)

	Dec	Inc	α95	K	Intensity	Std.Dev (+/-)		R	N	Lat	Long	δp	δm	Paleolat
Normal	16.93	64.4	5.7	56.9	1.69E-02	1.45E-02	-7.80E-03	12.3	12.5	78.4	94.6	7.3	9.1	46.2
Reversed	-	-	-	-	-	-	-	-	-	-	-	-	-	-
Combined	-	-	-	-	-	-	-	-	-	-	-	-	-	-
Vector Comb.	-	-	-	-	-	-	-	-	-	-	-	-	-	-
2nd Vector Comb.	-	-	-	-	-	-	-	-	-	-	-	-	-	-

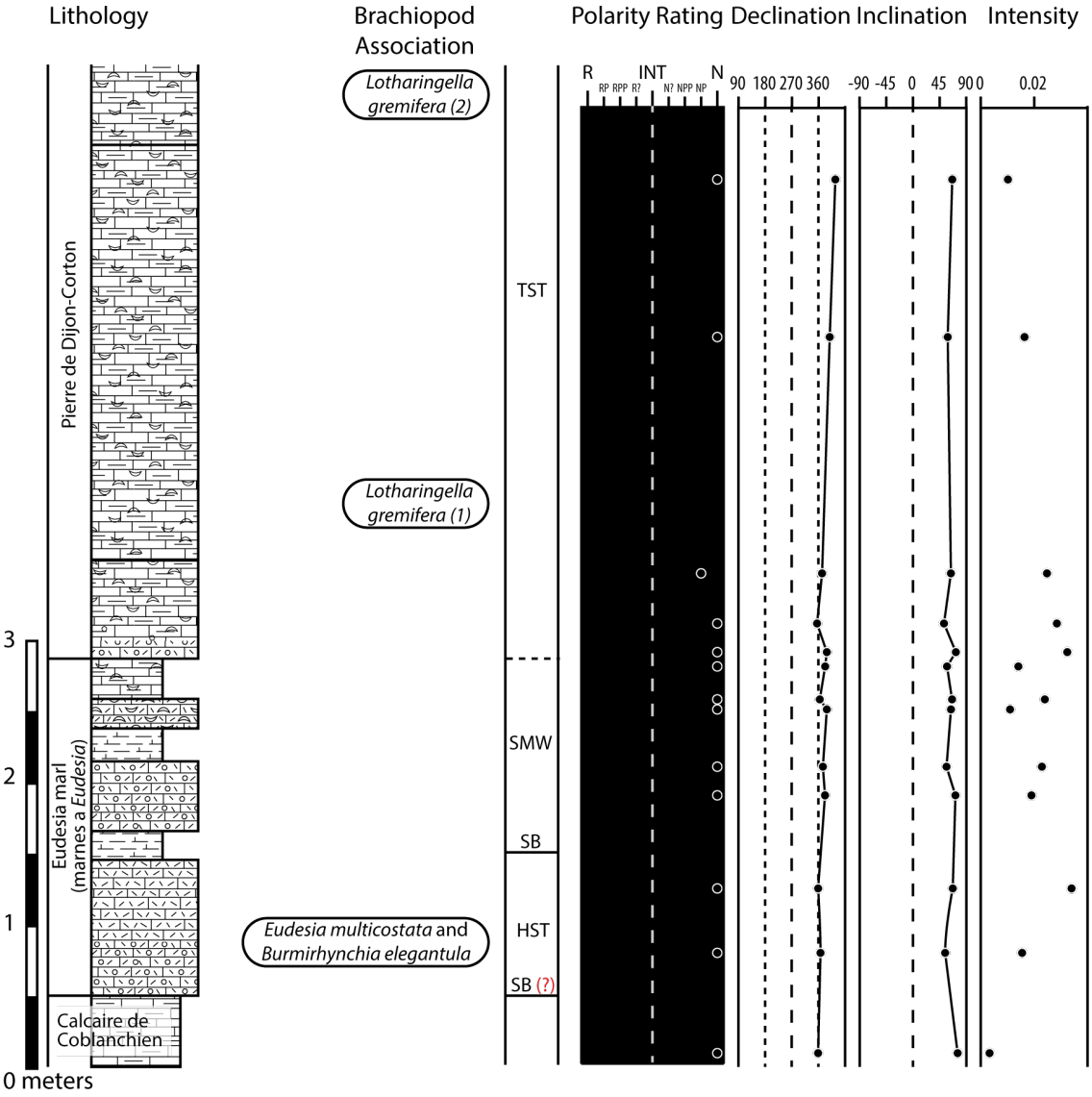

Figure 9: Paleomagnetic measurements from the outcrop alongside the Val Suzon valley are plotted by sample location alongside the lithostraigrahy of the outcrop.
The brachiopod associations and the sequence stratigraphic surfaces present in this outcrop are plotted at their stratigraphic locations, as interpreted by Garcia (1993). Polarity ranking, from highly ranked reversed (R) to highly ranked normal (N) with indeterminate samples falling along the middle (INT), is plotted over the interpreted magnetic sequence. The characteristic direction (declination and inclination) as well as intensity of the calculated best fit vectors for each sample are plotted, corresponding with the location on the outcrop from which the sample was collected. The normal vector calculated from the highly ranked (N & NP) samples is included in the table along with the produced VGP (latitude, longitude) and confidence levels (δp, δm).

4.1.7 Ladoix (LAD); lower Callovian

The magnetostratigraphic sampling in the large Ladoix Quarry near Montrachet spanned only the lower 13 meters of the approximately 20 meters of exposed Pierre de Ladoix formation. This formation overlies the Pierre de Dijon-Corton formation and terminates in a hardground overlain by a thin unit of Ferruginous oolites. The sampled section encompassed the third-order sequence Ca2, and the transgressive system tract for the Ca3 sequence (which were labeled Ca1bis and Ca2 in Garcia, 1993). Within the studied section, only markers for one ammonite zone (*Proplanulites koenigi* Zone) and one brachiopod association (*Kallirhynchia sp.*) were present, both within a marl bed in the lower portion of alternating sponge bioherms and marls of unit D (Figure 10).

The magnetostratigraphy delineated a reversed-polarity zone in the upper part of the highstand systems tract (unit D) of the Ca2 sequence within the Pierre de Dijon-Corton formation. Due to the lack of good clustering, the mean of the 3 high-quality reversed-polarity characteristic directions (194.9° declination, -43.1° inclination; α95: 57.3°, K: 17) is a poor antipode to the mean of the 10 high-quality normal-polarity characteristics directions (345.6° declination, 50.0° inclination; α95: 19.6°, K: 10). The two poles pass the reversal test of McFadden and McElhinny with an observed vector angle of 21.2° (γ_c: 39.6°) as intermediate because the large 95% confidence interval on the reversed polarity orientation. The combined paleomagnetic direction of 353.0° declination and 49.1° inclination (α95: 16.4°, K: 11) and the horizontal bedding requires no tilt-correction. This pole is not unique from the modern magnetic pole at the 95% confidence interval.

Figure 10: Paleomagnetic measurements from the Ladoix quarry are plotted by sample location alongside the lithostraigrahy and biostratigraphy of the outcrop.
The brachiopod associations, a point of dating for ammonite biostratigraphy and the sequence stratigraphic surfaces present in this outcrop are plotted at their stratigraphic locations, as interpreted by Garcia (1993). Polarity ranking, from highly ranked reversed (R) to highly ranked normal (N) with indeterminate samples falling along the middle (INT), is plotted over the interpreted magnetic sequence. The characteristic direction (declination and inclination) as well as intensity of the calculated best fit vectors for each sample are plotted, corresponding with the location on the outcrop from which the sample was collected. The orientations of the normal, reversed and combined vectors calculated from the highly ranked (R, N, RP, NP) samples are included in the table along with the produced VGP (latitude, longitude) and confidence levels (δp, δm).

Ladoix (LAD)

	Dec	Inc	α95	K	Intensity	Std.Dev (+/-)		R	N	Lat	Long	δp	δm	Paleolat
Normal	345.6	50.0	19.6	10.4	2.91E-02	4.15E-02	-1.71E-02	6.4	7	70.4	224.3	17.5	26.2	30.8
Reversed	194.9	-43.1	57.3	17.1	9.34E-02	3.60E-01	-7.42E-02	1.9	2	-65.1	-28.8	44.1	71.1	-25.1
Combined	353.0	49.1	16.4	10.9	3.77E-02	7.97E-02	-2.56E-02	8.3	9	72.2	205.0	14.3	21.6	30.0
Vector Comb.	8.7	45.4	-	-	6.05E-02	-	-	-	-	68.7	162.9	13.2	20.8	26.9
2nd Vector Comb.	204.9	-38.2	-	-	3.35E-02	-	-	-	-	-	-	-	-	-

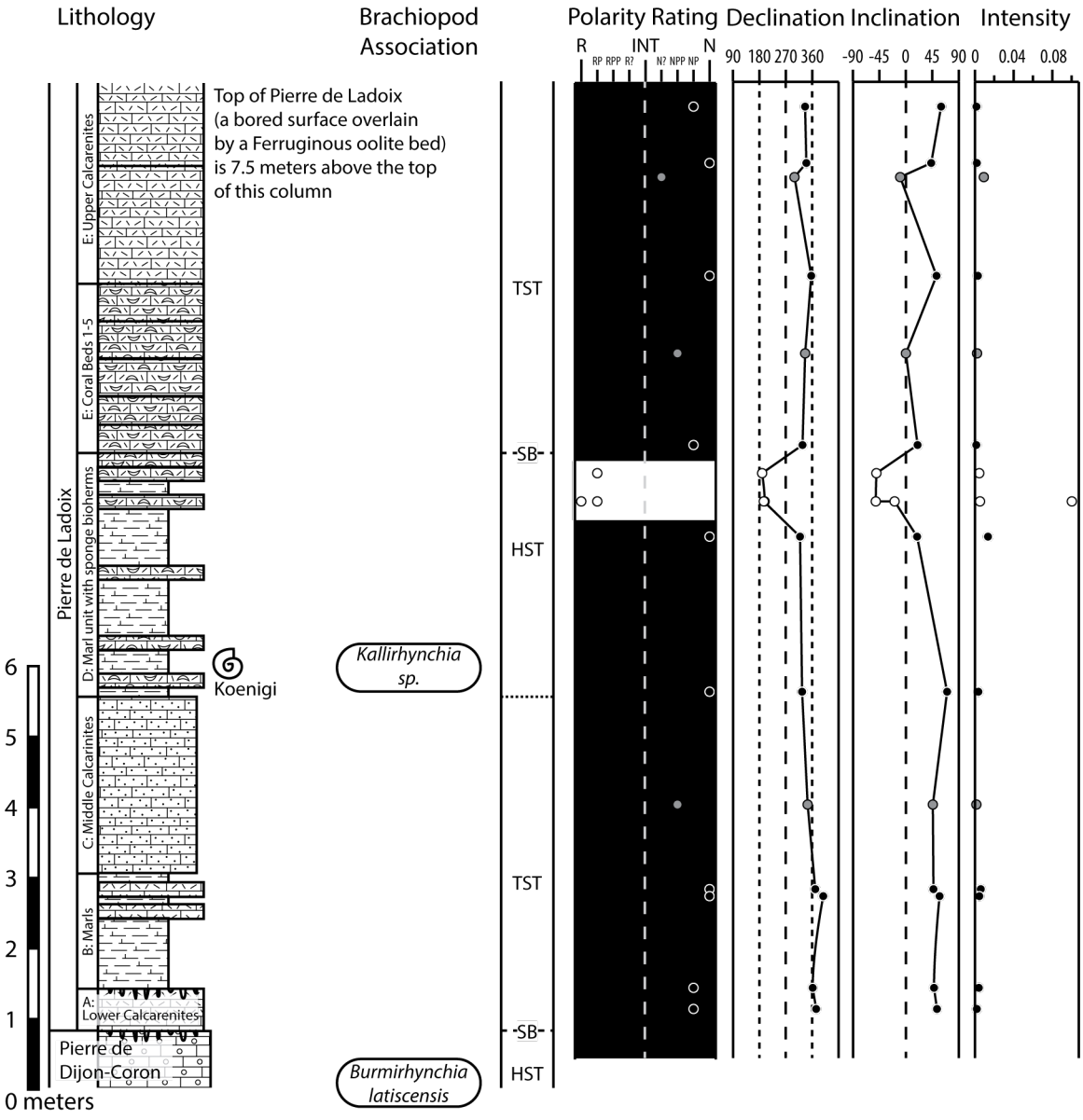

Figure 10

4.1.8 Veuxhaulles-sur-Aube (VSA); upper Callovian-lower Oxfordian

Even though there is just over 3 meters of condensed section dominated by iron oolite beds along this road cut near Veuxhaulles-sur-Aube, the abundant ammonites enable recognition of several ammonite zones, subzones and even some horizons and of discontinuities during its accumulation through the late Callovian through the middle Oxfordian (Collin, 1997; see Figure 11). This biostratigraphy enables a relatively precise correlation of these alternations of marls, mudstone to packstone limestone, and bioturbated bioclastic wackestone limestone beds. Nearly all of the samples from this ferruginous-oolite-bearing suite are from the more calcareous, hence more indurated, levels. Two samples were also taken from the dense purple-grey packstone to yellow mudstone of the underlying Calcaires à Rhynchonelles that terminates in a hardground hiatus spanning the entire middle Callovian.

The dense magnetostratigraphic sampling (20 levels) of this compact outcrop yielded only three horizons with relatively clear trends toward reversed polarity upon thermal demagnetization; plus two samples having questionable reversed polarity. The high-quality reversed-polarity samples are in two discrete levels in the *Collotia collotiformis* horizon and within the *Quenstedtoceras lamberti* subzone of uppermost Callovian and within the *Cardioceras cordatum* subzone of lower Oxfordian; each is separated by one or two samples that were interpreted as having normal-polarity characteristic directions. Even though these results from the highly discontinuous sedimentation of this condensed facies are inadequate for magnetostratigraphy, the observed indication of frequent polarity reversals in the uppermost Callovian is consistent with other sections.

The average of the two higher quality reversed-polarity characteristic directions is 186.5° declination and 39.8° inclination. The 15 relatively high-quality normal-polarity samples yield a mean direction of 14.2° declination and 66.5° inclination (α95: 5.4°, K: 59). A combined direction is calculated as 13.2° declination and 62.1° inclination (α95: 14.0°, K: 9). The combined orientation is indistinguishable from the modern magnetic pole at the 95% confidence interval, but the normal-polarity vector is unique at the 95% confidence interval.

Veuxhaulles-sur-Aube (VSA)

	Dec	Inc	α95	K	Intensity	Std.Dev (+/-)		R	N	Lat	Long	δp	δm	Paleolat
Normal	14.2	66.5	5.4	59.3	1.02E-01	1.97E-01	-6.73E-02	12.8	13.0	80.5	83.2	7.3	8.9	48.9
Reversed	186.5	39.8	41.2	0.0	3.70E-02	6.22E-02	-2.32E-02	2.0	0.0	-19.3	-1.5	29.7	49.5	22.6
Combined	**13.2**	**62.1**	**14.0**	**9.0**	**9.51E-02**	**1.86E-01**	**-6.29E-02**	**12.6**	**14.0**	**79.8**	**116.0**	**17.0**	**21.8**	**43.4**
Vector Comb.	11.0	45.4	-	-	4.92E-02	-	-	-	-	**67.3**	**158.6**	**11.3**	**17.8**	**26.9**
2nd Vector Comb.	30.9	83.6	-	-	5.91E-02	-	-	-	-	-	-	-	-	-

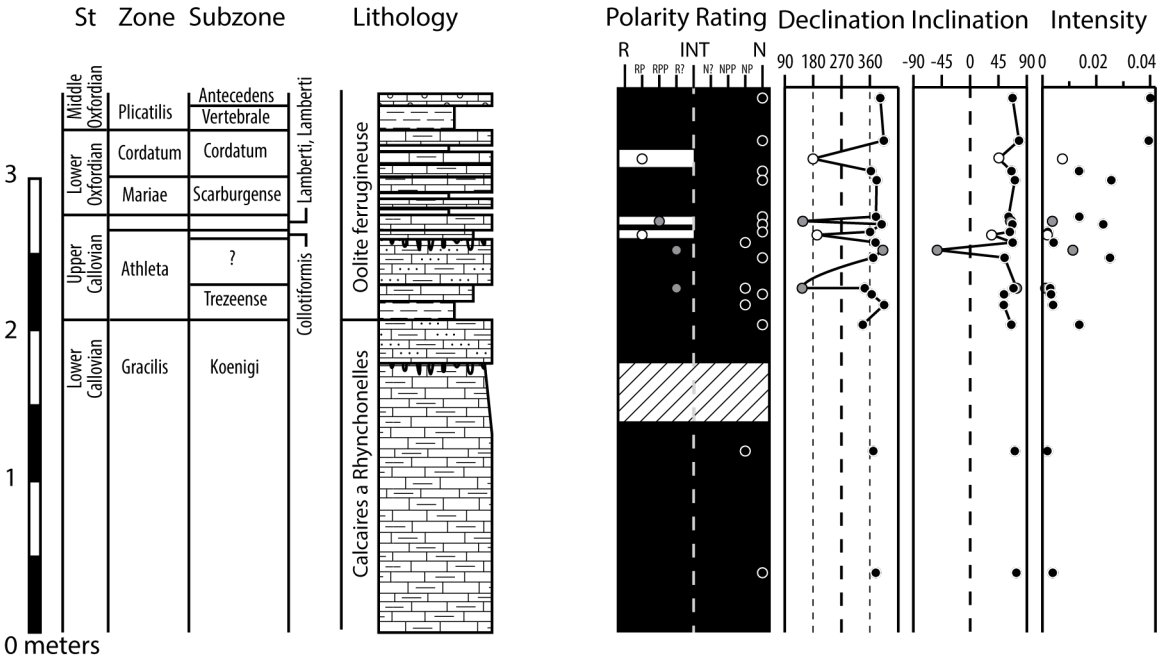

Figure 11: Paleomagnetic measurements from the Veuxhaulles-sur-Aube exposure are plotted by sample location alongside the lithostraigrahy and biostratigraphy of the outcrop. Ammonite biostratigraphic boundaries are placed according to the interpretation presented in Collin (1997). Polarity ranking, from highly ranked reversed (R) to highly ranked normal (N) with indeterminate samples falling along the middle (INT), is plotted over the interpreted magnetic sequence. The characteristic direction (declination and inclination) as well as intensity of the calculated best fit vectors for each sample are plotted, corresponding with the location on the outcrop from which the sample was collected. The orientations of the normal, reversed and combined vectors calculated from the highly ranked (R, N, RP, NP) samples are included in the table along with the produced VGP (latitude, longitude) and confidence levels (δp, δm).

4.1.9 Saulx-le-Duc (SLD); upper Callovian-lower Oxfordian

The upper part of this former limestone quarry outside of the village of Saulx-le-Duc, exposes a very condensed succession spanning portions of the upper Callovian to middle Oxfordian (Bonnot et al., 1992). The Pierre de Ladoix formation at the base of the outcrop is unconformably overlain by roughly half meter of biomicritic limestone beds alternating with marls (Figure 12). This is followed by a single compact bed of grey micritic limestone containing 0.5 millimeter limonite ooids (ferruginous oolites) and larger 6 millimeter brown clasts that has ammonite markers for the *Orionoides poculum* subzone of the *Quenstedtoceras lamberti* Zone,

which is the Tethyan equivalent to the Sub-Boreal *Quenstedtoceras henrici* subzone. The section ends in a condensed Oxfordian section of limestone rich in ferruginous oolites.

The 16 samples from this horizontally bedded, 1.5 m-thick, outcrop yield 9 samples of relatively high-quality normal-polarity characteristic directions (mean of 17.5° declination, 57.6° inclination; α95: 11.9, K: 29) and two samples of reversed-polarity characteristic directions (average of 196.1° declination, -47.4° inclination; α95: 57.3, K: 43). Both reversed-polarity horizons are in the ferruginous oolite formation within the *Quenstedtoceras mariae* zone of lowermost Oxfordian. The measured orientations passed the reversal test of McElheny and McFadden (1990) with an intermediate classification (γ_o/γ_c: 10.2°/23.3°). The combined mean direction has a 17.1° declination and 55.2° inclination (α95: 9.6°, K: 32), which is distinct from the modern magnetic pole at the 95% confidence interval. Samples from the basal portion of the outcrop yielded only low-quality characteristic directions of questionable polarity interpretation.

Saulx-le-Duc

	Dec	Inc	α95	K	Intensity	Std.Dev (+/-)		R	N	Lat	Long	δp	δm	Paleolat
Normal	17.5	57.6	11.9	29.4	3.18E-02	3.69E-02	-1.71E-02	6.3	6.5	74.2	124.7	12.8	17.4	38.2
Reversed	196.1	-47.4	57.3	43.0	1.59E-01	3.63E-01	-1.11E-01	2.0	2.0	-67.3	-34.2	48.3	74.4	-28.6
Combined	**17.1**	**55.2**	**9.6**	**32.0**	**4.65E-02**	**9.29E-02**	**-3.10E-02**	**8.3**	**8.5**	**72.7**	**131.7**	**9.7**	**13.6**	**35.7**
Vector Comb.	16.3	49.1	-	-	9.54E-02	-	-	-	-	**68.5**	**143.5**	**8.4**	**12.7**	**30.0**
2nd Vector Comb.	195.9	-44.9	-	-	6.41E-02	-	-	-	-	-	-	-	-	-

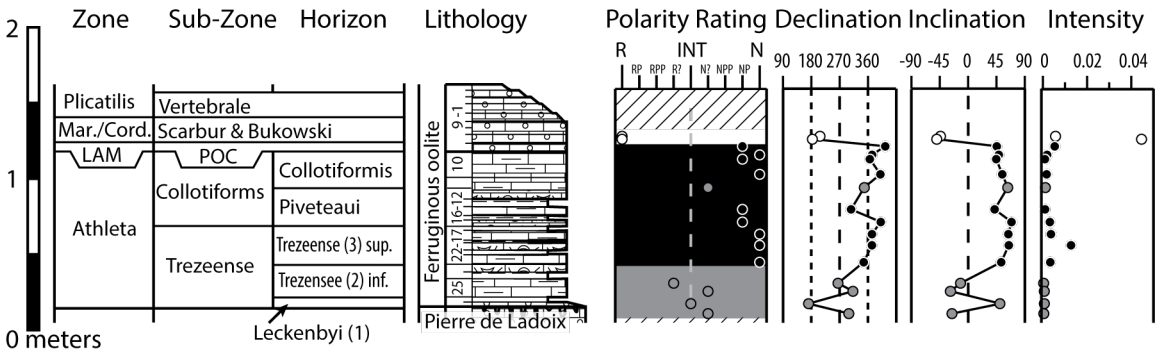

Figure 12: Paleomagnetic measurements from the Saulx-le-Duc exposure are plotted by sample location alongside the lithostraigrahy and biostratigraphy of the outcrop. Ammonite biostratigraphic boundaries are placed according to the interpretation presented in Bonnot et al. (1992). Abbreviations include the Lamberti (LAM), Mariae (Mar.), Cordatum (Cord.) zones and the Poculum (POM) subzone. Polarity ranking, from highly ranked reversed (R) to highly ranked normal (N) with indeterminate samples falling along the middle (INT), is plotted over the interpreted magnetic sequence. The characteristic direction (declination and inclination) as well as intensity of the calculated best fit vectors for each sample are plotted, corresponding with the location on the outcrop from which the sample was collected. The orientations of the normal, reversed and combined vectors calculated from the highly ranked (R, N, RP, NP) samples are included in the table along with the produced VGP (latitude, longitude) and confidence levels (δp, δm).

4.1.10 Talant: Cormbe Valton (CVT) and Corelles: La Cras (CRAS); upper Bathonian-lower Callovian

The two outcrops of Talant – Cormbe Valton and of Corelles – La Cras are short exposures in close proximity along the western edge of the Dijon city suburbs. CVT is a road cut in the Cormbe Valton valley just south of the Talant suburb. CRAS is within an old quarry just south of Lac Kir. Both sections contain a sequence that begins with upper Bathonian marls of the Calcaire de Comblanchien formation that are capped with a hardground, followed by the onset of the Marnes à Eudesia formation of Lower Callovian (Figures 13 & 14). The alternating marls and oolitic grainstones of the Marnes à Eudesia are interpreted as a lowstand systems tract that terminates in a transgressive surface. Both outcrops end with the cross-bedded grainstones of the Pierre de Dijon-Corton formation.

Only a pilot of four samples was made at the CRAS quarry from upper Marnes à Eudesia and a single sample from the lower part of the Pierre de Dijon Corton formation. All yielded normal-polarity characteristic directions (tilt-corrected mean of 359.2° declination, 60.7° inclination; α95: 14.4°, K: 53). The non tilt-corrected best-fit pole orientation is indistinguishable from the modern magnetic pole at the 95% confidence interval (2.1° declination, 63.3° inclination).

In contrast, the 8 samples from the Calcaires de Comblanchien, Marnes à Eudesia and lower part of the Pierre de Dijon-Corton formations in the CVT section are interpreted as reversed-polarity characteristic directions (mean of the 4 high-quality ones is 187.73° declination, -40.14° inclination; α95: 17.01, K: 38.52). A single sample is taken near the top of the Pierre de Dijon-Corton exposure at this location is interpreted as a high-quality normal-polarity characteristic direction (15.0° declination, 47.4° inclination); and the merged suite of high-quality characteristic directions has a tilt-corrected mean of 9.2° declination and 41.8° inclination (α95: 12.2°, K: 47). The non tilt-corrected pole is also indistinguishable from the modern magnetic pole at the 95% confidence interval (5.4° declination, 56.5° inclination).

Talant - Cormbe Valton (CTV)

	Dec	Inc	α95	K	Intensity	Std.Dev (+/-)		R	N	Lat	Long	δp	δm	Paleolat
Normal	15.0	47.4	0.0	0.0	4.30E-02	0.00E+00	0.00E+00	2.0	0.0	67.9	147.8	0.0	0.0	28.6
Reversed	187.7	-40.1	17.0	38.5	1.54E-02	3.09E-02	-1.03E-02	3.4	3.5	-64.8	-11.9	12.4	20.5	-22.9
Combined	**9.2**	**41.8**	**12.2**	**47.1**	**1.93E-02**	**3.62E-02**	**-1.26E-02**	**4.4**	**4.5**	**65.7**	**164.2**	**9.2**	**15.0**	**24.1**
Vector Comb.	12.9	45.6	-	-	2.91E-02	-	-	-	-	**67.3**	**153.9**	**9.9**	**15.6**	**27.0**
2nd Vector Comb.	19.9	51.2	-	-	1.40E-02	-	-	-	-	-	-	-	-	-

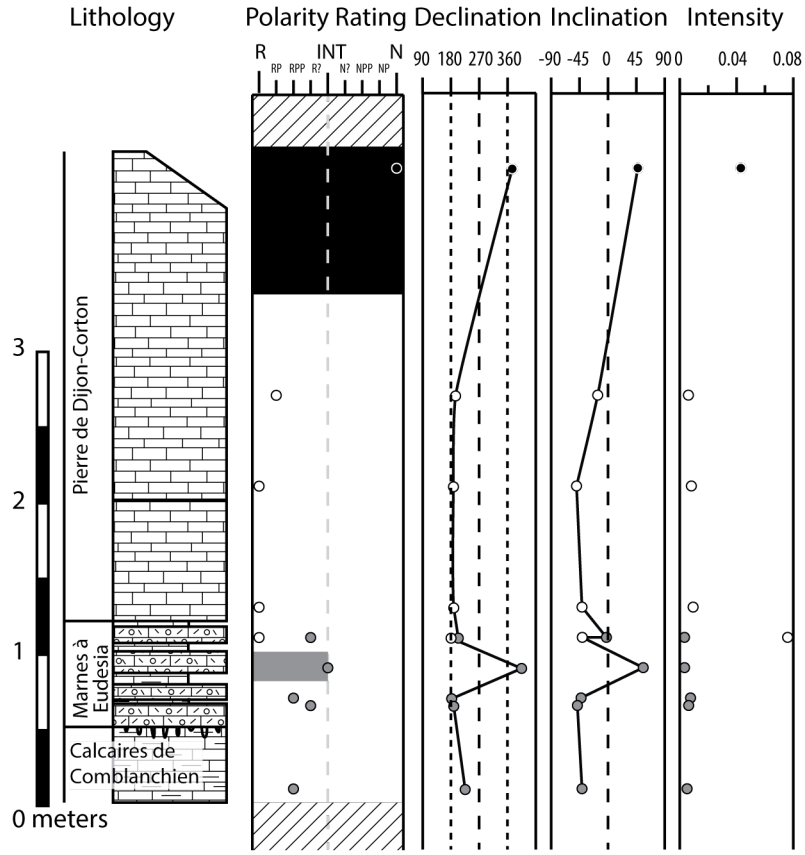

Figure 13: Paleomagnetic measurements from the Cormbe Valton exposure in Talant are plotted by sample location alongside the lithostraigrahy of the outcrop.
Polarity ranking, from highly ranked reversed (R) to highly ranked normal (N) with indeterminate samples falling along the middle (INT), is plotted over the interpreted magnetic sequence. The characteristic direction (declination and inclination) as well as intensity of the calculated best fit vectors for each sample are plotted, corresponding with the location on the outcrop from which the sample was collected. The orientations of the normal, reversed and combined vectors calculated from the highly ranked (R, N, RP, NP) samples are included in the table along with the produced VGP (latitude, longitude) and confidence levels (δp, δm).

Corelles - La Cras (CRAS)

	Dec	Inc	α95	K	Intensity	Std.Dev (+/-)		R	N	Lat	Long	δp	δm	Paleolat
Normal	359.2	60.7	14.4	53.1	1.87E-02	8.24E-03	-5.71E-03	3.5	3.5	84.4	191.2	16.8	22.0	41.7
Reversed	-	-	-	-	-	-	-	-	-	-	-	-	-	-
Combined	-	-	-	-	-	-	-	-	-	-	-	-	-	-
Vector Comb.	-	-	-	-	-	-	-	-	-	-	-	-	-	-
2nd Vector Comb.	-	-	-	-	-	-	-	-	-	-	-	-	-	-

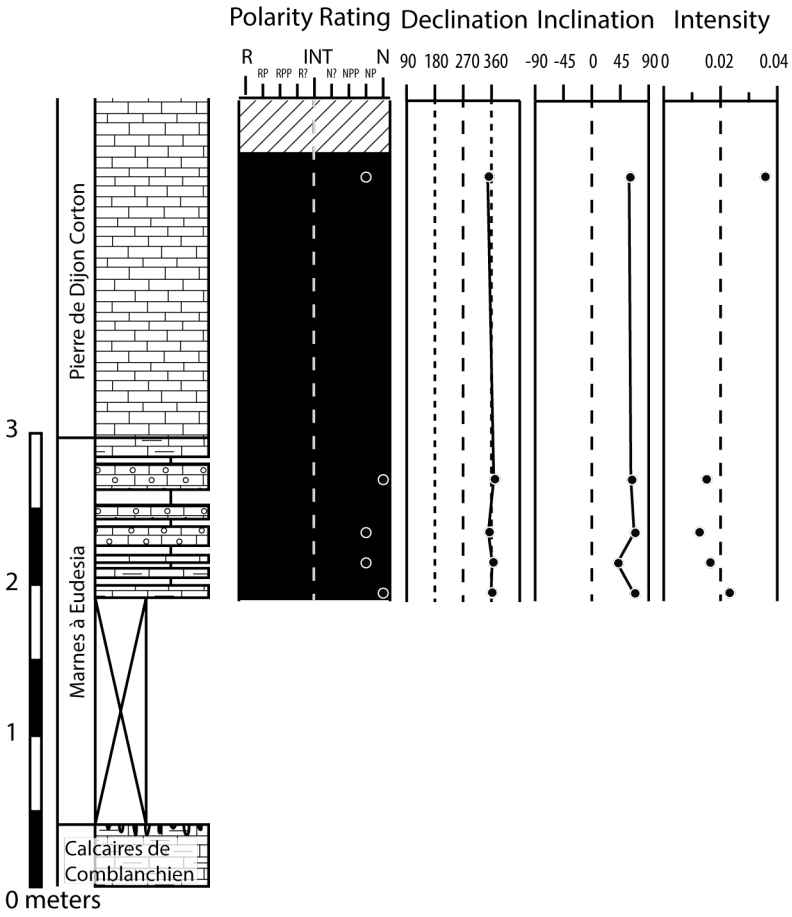

Figure 14: Paleomagnetic measurements from the Corelles – La Cras exposure are plotted by sample location alongside the lithostraigrahy of the outcrop.

Polarity ranking, from highly ranked reversed (R) to highly ranked normal (N) with indeterminate samples falling along the middle (INT), is plotted over the interpreted magnetic sequence. The characteristic direction (declination and inclination) as well as intensity of the calculated best fit vectors for each sample are plotted, corresponding with the location on the outcrop from which the sample was collected. The orientation of the normal vector calculated from the highly ranked (N & NP) samples is included in the table along with the produced VGP (latitude, longitude) and confidence levels (δp, δm).

4.2 French Composite Magnetostratigraphy

4.2.1 Paleomagnetic behavior

Previous magnetostratigraphy work in the region (e.g., Belkaaloul & Aïssaoui, 1997; Belkaaloul et al. 1995; Belkaaloul et al., 1997) demonstrated the potential of studies in the eastern Paris Basin. The shallow-shelf carbonates of the Burgundy platform and ramp was divided into three main facies types by Belkaaloul and Aïssaoui (1997): (1) oolitic grainstone grading into wackestone, (2) bioclastic packstone to grainstone, and (3) marly layers of reddish-brown mudstone and wackestones. Our study focused only on the first two types. Similar to other carbonates (Lowrie & Heller, 1982), the intensity of the remnant magnetization in these facies is typically very weak. Indeed, after the removal of the present-day and other secondary components, the remnant magnetization intensities in some samples can approach the noise levels of the cryogenic magnetometer.

Detailed rock-magnetic studies by Belkaaloul & Aïssaoui (1997) demonstrated that the natural remnant magnetization (NRM) has superimposed components from goethite, from authigenic magnetite minerals, and from primary magnetic minerals (biogenic single-domain magnetite/maghemite and multi-domain titanomagnetites/ titanomaghemites). However, the easy removal of goethite magnetization upon thermal demagnetization and the significant amount of single-domain magnetite grains allows these carbonates to be generally suitable for magnetic stratigraphy applications (Belkaaloul & Aïssaoui, 1997). The grey to bluish-gray appearance of fresh surfaces in many Burgundy platform limestone formations are typically associated with the preservation of magnetite and finely disseminated pyrite, whereas yellowish- to tannish-colored zones contain goethite as an oxidative replacement of pyrite from surficial weathering (Belkaaloul & Aïssaoui, 1997; Lowrie & Heller, 1982).

The thermal demagnetization procedures applied to our Callovian carbonate samples produced behaviors that are consistent with the previously interpreted paleomagnetic mineralogy from this region (Belkaaloul & Aïssaoui, 1997; Lowrie & Heller, 1982). The majority of the samples that yielded moderate- to high-quality remnant magnetization measurements had unblocking temperatures or removal of the majority of secondary magnetization in the range of 200-250°C. Belkaaloul and Aïssaoui (1997) observed that the secondary overprint produced by the authigenic magnetite displays a normal-polarity direction, therefore having the potential for erroneous interpretation that the magnetostratigraphy of some sections were entirely of normal

polarity. Incorporating multiple overlapping sections validated the reproducibility of the observed polarity sequence and reduced the influence of sections containing possible normally oriented secondary magnetic overprints. In addition, even when demagnetization procedures reveal a pattern of normal and reversed polarities, it is possible that the characteristic directions are still influenced by this normal-polarity secondary component, therefore the separated reversed-polarity and normal-polarity mean directions are not antipodal and the combined mean direction has a slight distortion toward post-Jurassic normal-polarity directions.

In most cases, the progressive heating steps typically caused the remnant magnetic intensity to continue to decrease while maintaining a consistent orientation through two to four heating steps, before weakening to low levels that were significantly affected by instrumentation background noise or experiencing spurious jump in intensity and/or susceptibility. This susceptibility surge and indications of viscous remnant magnetization (VRM) at temperatures at or above 360°C is likely the result of the conversion of pyrite to magnetite. These trends match the observations of Belkaaloul & Aïssaoui (1997), who interpreted that single-domain magnetite grains are the main contributor to remnant magnetization after initial heating steps. A low percentage of the samples displayed complex demagnetization behavior, which likely resulted from multiple generations and/or compositions of magnetic minerals; and these samples were rated as low to intermediate quality and excluded from computation of mean directions.

4.2.2 Composite magnetostratigraphy for Callovian of French sections

The composite sequence from our magnetic stratigraphy sections is mainly from the lower Callovian, and there are only three punctuated segments that span portions of the upper Callovian (Figure 3). The correlation of these lower Callovian sections is mainly based on brachiopod associations and interpreted third-order depositional sequences through the basin.

The lowest Callovian depositional sequence (Ca0) was interpreted as being predominantly normal polarity with only one outcrop indicating the presence of a reversed-polarity zone. The lower portion of the second depositional sequence (Ca1) contains two reversed-polarity zones, one within the lowstand system tract and the other in the transgressive system tract below the brachiopod association *Lotharingella gremifera (1)*. Two additional reversed-polarity zones near the maximum flooding surface of Ca1 are less well documented. Sequence Ca2 is dominated by a normal polarity, but is capped by a reversed-polarity zone. The

preserved deposits during depositional sequence Ca3 indicate normal polarity, with only a single reversed-polarity zone near its base.

There is an incomplete magnetostratigraphy spanning the Upper Callovian *Peltoceras athleta* and *Quenstedtoceras lamberti ammonite zones* and the basal Oxfordian *Quenstedtoceras mariae* zone from the condensed iron-oolite-rich sections at Veuxhaulles-sur-Aube and Saulx-le-Duc. These are dominated by normal polarity, but with poorly delimited brief reversed-polarity horizons suggested within the *Cardioceras scarburgense*, *Quenstedtoceras lamberti* and *Kosmoceras spinosum* ammonite subzones.

5 SOUTHEASTERN FRENCH GSSP CANDIDATE SECTIONS

Pilot magnetostratigraphic studies were conducted at the Callovian-Oxfordian stage Global Boundary Stratotype Secion and Point (GSSP) candidates in the Hautes-Alpes department in southeastern France. The Thuoux and Savournon sections, deposited in the Dauphinois basin, both exposes a more expanded stratigraphic boundary between the *Quenstedtoceras lamberti* Zone and the *Quenstedtoceras mariae* Zone in comparison to the other leading GSSP candidate at Redcliff Point in Weymouth, Dorset (UK) (Fortwengler et al., 2012; Meléndez, 2006, 2007). These outcrops, exposing the series of thick marly limestone and white, carbonate nodules of the Terres Noires formation, are comprehensively described by Fortwengler & Marchand (1994a, b, c, d) as cited by Fortwengler et al. (2012). Fortwengler et al. (1997) further discusses these candidates for the Callovian-Oxfordian boundary type section. The Thuoux section provided twelve samples over almost 30 meters, of which ten samples were thermally demagnetized and analyzed (Table 2A). From the Savournon section, 20 samples were collected near the top of the exposed anticline, from which a subset of 13 samples were thermally demagnetized and analyzed (Table 2B). A left lateral fault divides the samples into two subsets, with nine of the analyzed samples falling on one side of the fault (subset A) and four falling on the other (subset B). Thermal demagnetization of all the samples from these two locations produced normal-polarity orientation trends (Table 2).

The 13 samples from the Savournon section produced a least squares average characteristic direction with a 212.7° declination and 80.6° inclination (α95: 6.3°, K: 86) for the geographic orientations of the samples. Tilt-correcting the samples produces a least squares average characteristic direction with a 319.6° declination and 47.3° inclination (α95: 13.8°, K: 17). The increase in the dispersion of pole orientations is clearly visible between figure 15a and figure 15b were the tilt correct data contains a 95% confidence interval that is 7.3° larger than that of the non-tilt corrected orientations. These samples failed the fold test of Graham (1949) indicating that the measured polarity orientations from this section contain a component of remnant magnetization imparted on the rock after deformation occurred. This indicates that the magnetostratigraphic sequence suggesting a normally dominated polarity sequence for the

Quenstedtoceras lamberti Zone and Subzone through the *Quenstedtoceras mariae* Zone, *Scarburgiceras praecordatum* Subsone in this section is unreliable.

The 10 samples from the Thuoux section produced a least squares average characteristic direction with a 10.1° declination and 48.9° inclination (α95: 10.0°, K: 31.9) for non-tilt corrected sample orientations with a 306.2° declination and 37.1° inclination (α95: 9.83°, K: 32.71) when the samples were corrected for bedding orientation. The best-fit orientation at the 95% confidence interval matches the modern magnetic pole (Figure 16), indicating the magnetic orientation produced from the Thuoux section is indicative of a modern overprint and does not provide a reliable signal for magnetic stratigraphy.

Table 2: Characteristic magnetic directions of samples at Thuoux (THX) and Savournon (SAV)

Table 2A

	Sample	Meters	Label	GDec	GInc	TDec	Tinc	Intensity	Error	N
SAV	A 1.2	0	N?	172.6	54.6	271.8	65.2	2.97E-02	10.2	8
SAV	A 2.1	2.6	N?	279.3	78.8	314.5	55.9	5.46E-02	9.2	5
SAV	A 3	9.5	NP	257.9	58.3	289.8	22.8	2.27E-02	13.0	8
SAV	A 5.1	14.7	NP	165.3	84.1	316.3	47.3	4.23E-02	7.7	5
SAV	A 5.2	14.7	NP	225.8	77.1	297.8	53.9	3.81E-02	8.2	8
SAV	A 5.3	14.7	N	211.1	81.2	308.3	44.3	4.11E-02	7.4	6
SAV	A 5.4	14.7	N	214.5	68.4	290.4	44.1	4.65E-02	7.7	5
SAV	A 7	20.7	N?	329.5	49.5	326.2	1.9	7.19E-02	13.6	5
SAV	A 8	25.7	N	242.4	78.7	305.9	38.7	4.14E-02	2.4	5
SAV	B 1	0	N	10.2	85.8	352.8	39.0	3.25E-02	2.5	3
SAV	B 3	0	N	170.8	77.7	351.0	55.3	2.97E-02	3.2	3
SAV	B 5	0	N	225.6	76.3	333.6	49.7	3.08E-02	2.2	3
SAV	B 7	0	NP	182.9	83.0	348.8	49.8	5.30E-02	6.4	3

Table 2B

	Sample	Meters	Label	GDec	GInc	TDec	Tinc	Intensity	Error	N
THX	1	0	N	48.0	62.0	278.2	51.0	3.11E-02	3.3	7
THX	2	3.7	INT	287.1	4.6	303.3	-46.4	8.48E-02	1.8	3
THX	3	5.2	N	21.8	36.5	321.8	43.2	2.82E-02	6.9	7
THX	4	7.2	N	357.5	50.7	301.8	27.7	6.49E-02	3.6	9
THX	5	9.3	N	6.6	37.9	319.5	33.1	9.04E-02	4.7	5
THX	6	12.8	N	5.8	57.7	300.2	43.3	2.30E-02	7.4	9
THX	7	14.8	N	1.8	54.6	298.1	31.8	1.16E-01	2.7	4
THX	8	16.4	N	7.4	33.7	322.5	31.1	8.57E-02	5.4	7
THX	10	20.8	NPP	25.1	29.3	333.8	45.2	1.45E-02	14.6	5
THX	12	29.8	N	0.4	51.5	301.5	30.0	8.88E-02	5.6	6

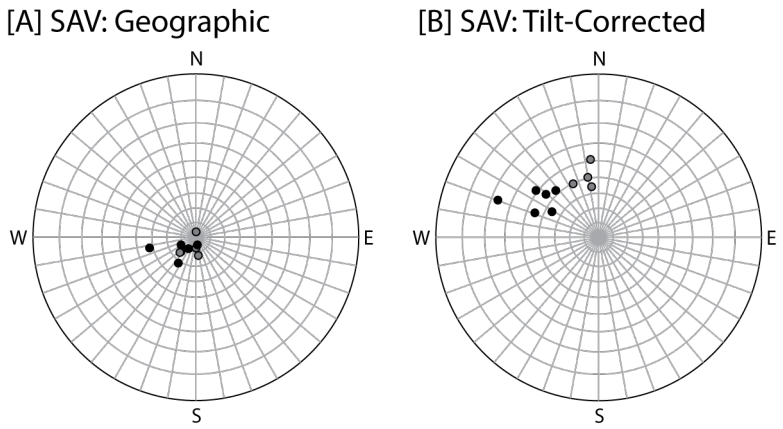

Figure 15: Distribution of sample orientations for Savournon (SAV) both non-tilt-corrected (A) and tilt-corrected (B) plotted on a stereographic equal-angle plot.

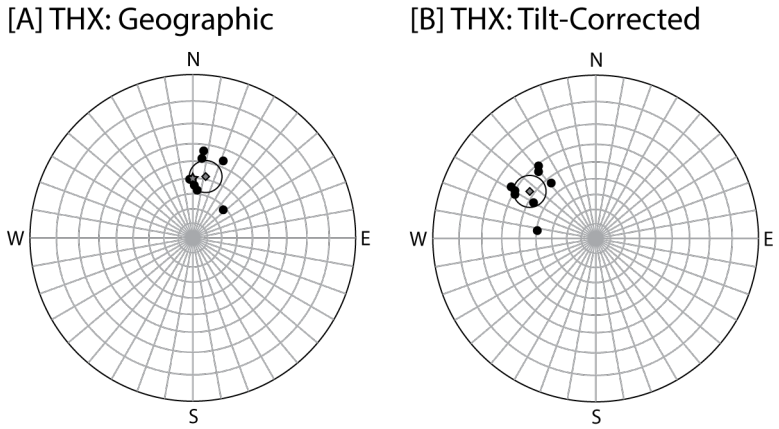

Figure 16: Distribution of sample orientations for Thuoux (THX) both non tilt-corrected (A) and tilt-corrected (B) plotted on a stereographic equal-angle plot. The non tilt-corrected plot contains a star at the modern paleomagnetic pole declination and inclination in southern France.

6 ENGLISH CALLOVIAN SECTIONS

The English Middle Jurassic sediments were deposited in shallow waters (<100 meter depth) north of the Paris Basin between several islands of variable size within the southern end of an epicontinental seaway located between the Scandinavian and Laurentian margins, (Barron et al., 2012; Beccaletto et al., 2011; Cope, 2006; Bradshaw et al., 1992; Ziegler, 1992). This approximately north-south oriented seaway was formed during the Triassic rifting and crustal thinning associated with the breakup of Pangaea, and continued to subside through the end of the Cretaceous until the initiation of crustal separation in the Arctic North Atlantic Rift Zone (Barton & Wood, 1984; Cope, 2006; Ziegler, 1975, 1988; Ziegler & Dézes, 2006). This epicontinental seaway connected the Tethys Sea with the Arctic Sea, thereby allowing for partial mixing of Boreal and Tethyan faunal assemblages and influencing sedimentary patterns (Barron et al., 2012; Cope, 2006; Ziegler, 1992). This seaway covered the majority of Britain through the Early Jurassic, but a significant fall in sea level near the end of the Middle Jurassic compounded with domal upwarping and coeval volcanicity in the North Sea Basin produced a variety of depositional environments (Bradshaw et al., 1992; Cox, 2002; Underhill & Partington, 1993). Therefore, intervals of both carbonate and clastic sedimentation are widespread during the late Bathonian through Callovian (Cope, 2006; Cox, 2002).

Deposition within this shallow seaway reflects a variation of depositional environments (including shallow marine, fluvial, deltaic, salt marsh and coastal lagoon) that were influenced by the paleolatitude (between 30° and 40° N), the warm CO_2-rich greenhouse climate, and the proximity to land (Cope, 2006; Cox, 2002). The Middle Jurassic in England is typically dominated by fine-grained siliciclastic facies with episodes of sandy influx interrupted by extensive oolite shoals and infrequent reef coral growth (Cope, 2006). The deposition rate of carbonate sediments during the Middle Jurassic is markedly higher compared to the successions during the Early or the Late Jurassic (Cox, 2002).

At the regional scale, the upper-Middle Jurassic stratigraphy consists of a progression of backstepping sequences culminating with the most distal offshore facies during the late Callovian to earliest Oxfordian depending on location (Hesselbo, 2008; Jacquin et al., 1998; Norris & Hallam, 1995). This second-order depositional cycle begins at the base of the Upper Bathonian

(*Morrisiceras morrisi/Procerites hodsoni* ammonite zone boundary) (Jacquin et al., 1998). This basal unconformity also marks the transition from overall progradation to overall retrogradation in the larger-scale North Sea cycle (Jacquin et al., 1998). The onset of this depositional cycle above a basal unconformity was variable in the regional basins, with the commencement in the British portion of the seaway at the Bt5 flooding surface of latest Bathonian (*Clidoniceras discus* Zone), in contrast to the onset at the earlier Bt4 flooding surface in the Paris Basin (*Prohecticoveras retrocostatum* Zone) (Jacquin et al., 1998; Jacquin & Gracianski, 1998a).

The strata of the studied region across the East Midlands (Peterborough/ Cambridgeshire) to the northern part of the South West and South East regions of England (Gloucestershire and Oxfordshire) (Figure 1) was deposited along the East Midlands Shelf and Cotswold Shelf (Bradshaw et al., 1992; Cox et al., 2002b; Sumbler et al., 2002). The units of the lower Middle Jurassic are dominated by ooidal, peloidal and variably shelly limestone lithologies (Cox et al., 2002b; Sumbler et al., 2002). The latest Bathonian transgression is the initiation of the Great Oolite Group that culminates in the succession of the White Limestone, Forest Marble and Cornbrash formations within the study area (Cope, 2006; Jacquin et al., 1998; Sumbler, 1984). The White Limestone formation consists of the Shipton, Ardley, Signet and Baldon members. The Signet member is laterally related to the Baldon member (Sumbler, 1984, 1991) and was not sampled in our study. In some places, these members are divided by gastropod-rich limestone beds, generally developed as hardgrounds, and were named after the within-contained dominant species; where *Aphanoptyxis excavata* is capping the Shipton member and *Aphanoptyxis bladonensis* caps the Ardley member (Sumbler, 1984, 1991). Regionally, the White Limestone formation typically consists of bioturbated white- to cream-colored wackestones and packstones containing minor sporadic seams of clay and marls, and occasionally in shades of grey and buff (Barron et al., 2012; Sumbler, 1984, 1991). These lithologies that are typical of back-barrier facies are interpreted to have formed in association with increasing productivity produced by the relative sea-level rise (Hesselbo, 2008).

Unconformably overlying the White Limestone is the Forest Marble formation of latest Bathonian (Sumbler, 1991). This facies change represents the progressive eustatic sea-level rise through the early Callovian that replaced the shallow-shelf facies with the deposition of marine clastic lithologies (Cox et al., 2002b; Sumbler et al., 2002). Within these units, ammonites are typically abundant, which allows for high-resolution correlation of biostratigraphy at the zone and subzone level with occasional biohorizon-level markers allowing finer-scale resolution (Cope, 2006). The surrounding emergent areas to the north (Mid North Sea High and Pennine Landmass),

east (Anglo-Brabant Landmass) and west (Welsh Landmass) were persistent source areas that provided a clastic sediment input that enhanced the contributions from major rivers systems of the Scandinavian and Laurentian continents to the east and west (Barron et al., 2012; Bradshaw et al., 1992; Cope, 2006).

The Forest Marble formation varies in thickness from about 5 meters in Oxfordshire to over 25 meters in Dorset. This formation generally has an upward transition from limestone-dominated beds to a clay-dominated facies (Baron et al., 2012; Sumbler, 1984, 1991). This progression of lime-sand shoals with channel-fills and banks to low-energy marine conditions indicates an increasing water depth (Barron et al., 2012; Hesselbo, 2008; Klein, 1965; Sumbler, 1984). Limestones of the Forest Marble formation are typically cross-bedded, contain variable quantities of oolites, and are blue-grey to buff colored on fresh surfaces, but weather to a brownish color with a flaggy texture (Barron et al., 2012; Sumbler, 1984). The clays of the Forest Marble formation are generally unbedded, often contain oolites and shell fragments, and are grey to greenish grey on fresh surfaces that weather to an orange-brown color (Sumbler, 1984).

Capping the Great Oolite Group is the Cornbrash Formation (Barron et al., 2012; Chidlaw & Campbell, 1988). The Lower Cornbrash member varies from very pale colored bioclastic micrite to nodular limestones (Cox & Page, 2002; Page, 1989; Sumbler et al., 2002). The Upper Cornbrash member consists of intermixed beds dominated by sandy limestone, calcareous sand, and calcareous limestone (Barron et al., 2012; Cox & Page, 2002; Page, 1989; Sumbler et al., 2002; Wright, 1977). The erosional unconformity separating these Lower and Upper Cornbrash members across most of the region corresponds to the boundary between the Bathonian and the Callovian (Bradshaw et al., 1992; Page, 1989).

The Callovian through Kimmeridgian Ancholme Group begins with the Kellaways Formation of lower Callovian and the Oxford Clay Formation of upper Callovian through lower Oxfordian (Baron et al., 2012; Cope, 2006). The Kellaways Formation is comprised of the lower Kellaways Clay member and the upper Kellaways Sand member (Cope, 2006; Page, 1989; Sumbler et al., 2002). The Kellaways Clay of silty to sandy, medium-grey mudstones passes upwards and northwards into the Kellaways Sand of pale grey sands and silts and calcareous cement with occasional clay bands (Baron et al., 2012; Cope, 2006; Page, 1989). The contact between these silty sandstones of the Kellaways Formation and the overlying mudstones of the Oxford Clay Formation is a sharp but conformable boundary (Baron et al., 2012; Cox et al., 1992; Cox et al., 2002b).

The Oxford Clay Formation consists of the Peterborough and Stewartby Members of Callovian and the Weymouth member of lower Oxfordian (Baron et al., 2012; Cox et al., 1992). The Peterborough Member, dominated by laterally persistent beds of organic-rich, brownish-grey, fissile silty claystone and with minor grey-colored beds, is interpreted as deposits from a shallow-marine environment with high productivity (Cope, 2006; Cox et al., 1992; Cox et al., 2002b; Hudson & Martill, 1994; MacQuaker, 1994). The Peterborough Member typically grades upward into the Stewartby Member of thinly interbedded pale- to medium-grey calcareous mudstones (Cope, 2006; Cox et al., 1992; Hudson & Martill, 1994). This slightly silty, blocky mudstone tends to be more calcareous, less fossiliferous, and thicker-bedded than the underlying Peterborough Member (Cox et al., 1992; Hudson & Martill, 1994; Norris & Hallam, 1995). A thin limestone band, termed the Lamberti Limestone from the abundance of *Quenstedtoceras lamberti* ammonites, is near the top of the Stewartby Member in the South Midlands (Cope, 2006; Hollingworth & Wignall, 1992). The transition to the Oxfordian-aged Weymouth member is placed where the pale-grey, blocky, smooth-textured calcareous mudstone supersedes the facies of the Stewartby Member (Cox et al., 1992; Norris & Hallam, 1995). This transition is interpreted as a second-order maximum flooding surface within the overall transgressive systems tract of the North Sea Cycle, although the placement of the maximum transgression varies from uppermost Callovian (*Quenstedtoceras lamberti* Subzone) in marginal areas to lowest Oxfordian (lower *Cardioceras scarburgense* Subzone) in more proximal sections (eg. Yorkshire) (Jacquin et al., 1998b; Norris & Hallam, 1995; Partington et al., 1993).

6.1 English Outcrops

The four magnetostratigraphy sections with a total of 162 samples from 40 meters are from the Cotswold and East Midland Shelves of England (Cox, 2002; Cox et al., 2002b; Sumbler et al., 2002) (Figure 1). In approximate stratigraphic order from lowest to highest, these are (1) the outcrop at Shipton-on-Cherwell Cement Works (SC) located north of Oxford, in Oxfordshire, (2) Shorncote Quarry (SK) near the southern boarder of Gloucestershire, (3) the thick King's Dyke Clay Pit (KD) next to the Peterborough edge of Cambridgeshire, and (4) Dix Pit at Stanton Harcourt (SH) located west of Oxford in Oxfordshire. These four ammonite-zoned sections span approximately two thirds of the Callovian, including its upper and lower Stage boundaries.

6.1.1 Shipton-on-Cherwell Cement Works (SC); middle-upper Bathonian

The outcrop at the Shipton-on-Cherwell Cement Works Quarry in Oxfordshire exposes the lower White Limestone Formation through Forest Marble and lower Cornbrash formations (Figure 17). This outcrop has been extensively studied (e.g., Arkell, 1931; Richardson et al., 1946; Allen and Kaye, 1972; Palmer, 1979; Page, 1989; Sumbler, 1984; Sumbler et al., 2002). Faunal studies and regional correlations have assigned ammonite zones from *Tulites subcontractus* through the *Macrocephalites herveyi* to the strata (e.g., Page, 1989; Sumbler et al., 2002), although the dating for the White Limestone and Forest Marble formations relies predominantly on regional correlation (e.g. Wyatt, 1996). Ammonites provide direct zone and subzone assignments within the Cornbrash (Sumbler et al., 2002).

A pilot study of five cores within the White Limestone yielded one low-quality reversed-polarity horizon within the *Tulites subcontractus* Zone of the Shipton Member, one indeterminate level within the *Morrisicera morrisi* Zone in that Shipton Member, and three low-quality normal-polarity levels within the *Cadomites bremeri* Zone of the Ardley member.

Detailed sampling of the Forest Marble Formation indicated mainly normal polarity (6 high-quality and 2 low-quality characteristic directions) with two low-quality single-sample horizons interpreted as reversed polarity.

The overlying Lower Cornbrash member of the Cornbrash Formation (*Clydoniceras discus, Clydoniceras discus*) was densely sampled and resolved a normal-polarity zone sandwiched between of two reversed-polarity zones, although many of the reversed-polarity samples yielded low-quality characteristic directions. The four relatively high-quality reversed-polarity characteristic directions are poorly clustered with a mean of 190.8° declination and -38.2° inclination (α95: 44.2°, K: 14) which is not antipodal to the mean from the 15 high-quality normal-polarity characteristic directions (358.0° declination, 59.3° inclination; α95: 12.8°, K: 12). The combined direction is 1.2° declination and 55.7° inclination (α95: 11.8°, K: 12). The normal-polarity and reversed-polarity vectors pass the reversal test of McFadden and McElhinny (1990) with an intermediate classification (γ_o/γ_c: 22.6°/30.3°) and the non tilt-corrected combined best fit orientation (359.2° declination and 54.3° inclination) is distinct from the modern magnetic pole at the 95% confidence interval.

Figure 17: Magnetiostratigraphy of the Shipton-on-Cherwell Cement Works (SC, Oxfordshire) alongside the outcrop lithology and biostratigraphy.
The precise location of zonal and subzonal boundaries are placed utilizing descriptions in Page, (1989) and Wyatt (2002) with further corroboration from studies by Allen and Kaye (1973), Arkell (1931), Chidlaw & Campbell (1988), Douglas and Arkell (1928, 1932, 1935), Palmer (1979), and Sumbler (1984). Polarity ranking, from highly ranked reversed (R) to highly ranked normal (N) with indeterminate samples falling along the middle (INT), is plotted over the interpreted magnetic sequence. The characteristic direction (declination and inclination) as well as intensity of the calculated best fit vectors for each sample are plotted, corresponding with the location on the outcrop from which the sample was collected. The orientations of the normal, reversed and combined vectors calculated from the highly ranked (R, N, RP, NP) samples are included in the table along with the produced VGP (latitude, longitude) and confidence levels (δp, δm).

Shipton-on-Cherwell Cement Works, Oxfordshire

	Dec	Inc	α95	K	Intensity	Std.Dev (+/-)		R	N	Lat	Long	δp	δm	Paleolat
Normal	358.0	59.3	12.8	12.5	2.05E-02	1.34E-02	-8.10E-03	11.1	12.0	78.1	546.0	14.4	19.2	40.1
Reversed	190.8	-38.3	44.2	14.1	2.21E-02	1.54E-02	-9.07E-03	2.4	2.5	-58.5	339.2	31.1	52.4	-21.5
Combined	1.2	55.7	11.8	11.8	2.08E-02	1.34E-02	-8.15E-03	13.4	14.5	74.3	535.1	12.1	16.9	36.3
Vector Comb.	6.0	48.5	-	-	2.09E-02	-	-	-	-	67.1	525.1	10.2	15.5	29.5
2nd Vector Comb.	208.6	27.3	-	-	4.25E-03	-	-	-	-	-	-	-	-	-

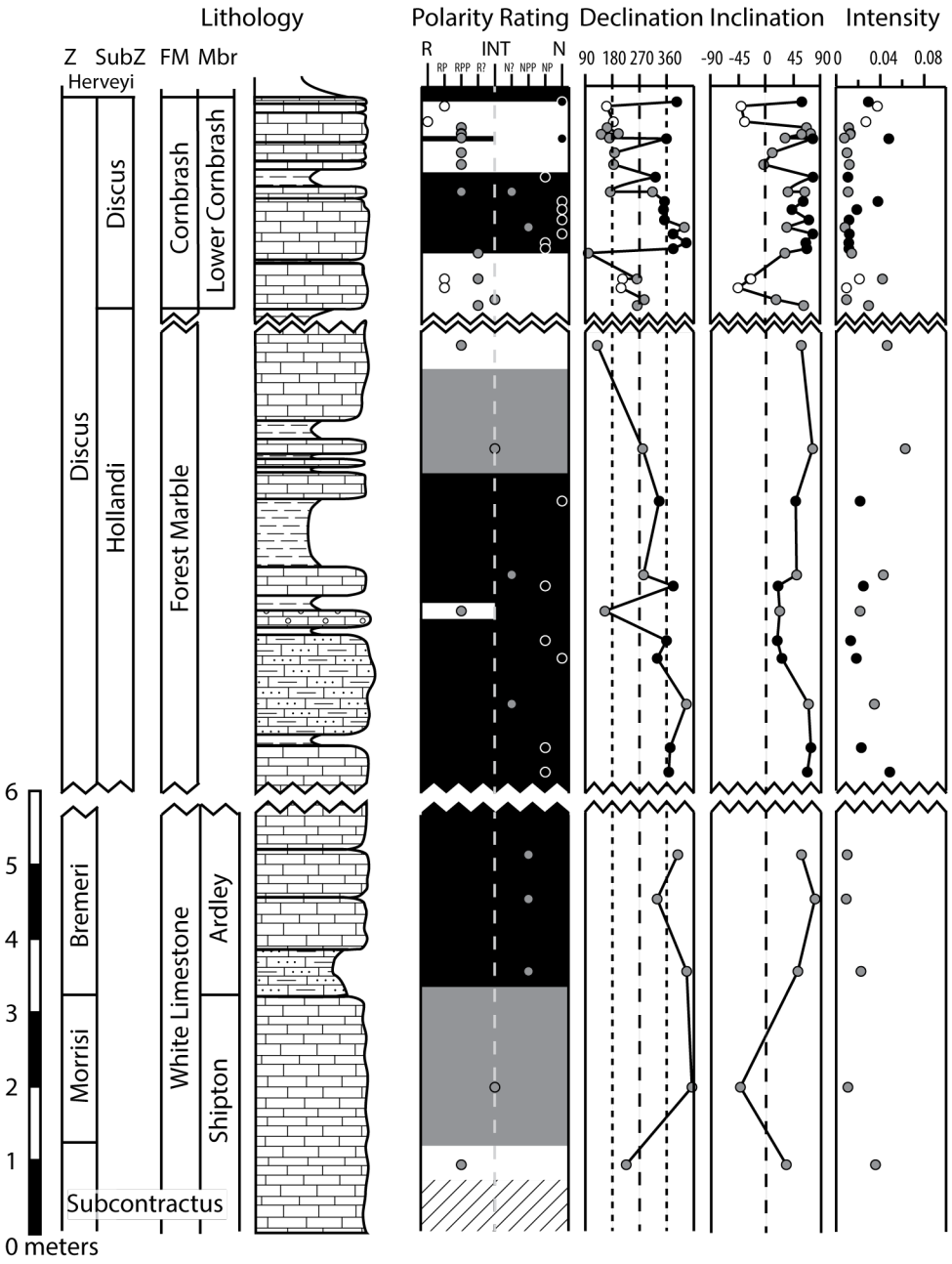

Figure 17

6.1.2 Shorncote Quarry (SK); lower Callovian

The Shorncote Quarry exposes the upper Cornbrash formation through the Kellaways Sand (Figure 18). However, the soft Kellaways Clay of at least 2 meters of medium light grey claystone with aragonitic ammonites is a poorly exposed and its single paleomagnetic sample yielded only a very poor characteristic direction interpreted as normal polarity.

Four samples from the Upper Cornbrash member of the Cornbrash formation (either the *Kepplerites keppleri* or *Macrocephalites terebratus* Subzone of the *Macrocephalites herveyi* Zone of Early Callovian) had poor magnetic behavior with a possible interpretation of reversed polarity. The Kellaways Sand in the upper portion of the outcrop is over 3 meters of calcareous sandstone beds of bluish-to-greenish-tinted light to medium grey that weather to a tan-yellow shade. Thin clay beds periodically interrupt these sandstones, but all the magnetostratigraphy samples are from the sandstone beds. Regional correlation ties the sampled interval to the *Kepplerites galilaei* Subzone of the *Proplanulites koenigi* Zone and the bottom of the *Sigaloceras calloviense* Subzone and Zone. The lower three-fourths of this interval yielded a reversed polarity zone (7 high-quality and 5 low-quality characteristic directions with a mean of 197.2° declination, -48.4° inclination; α95: 12.3°, K: 39), with a single horizon containing a high-quality normal-polarity direction. The upper quarter of the exposure is normal polarity (3 high-quality, 1 poor-quality, and 1 indeterminate characteristic directions). The mean of all high-quality normal-polarity characteristic directions is 1.9° declination, 41.4° inclination (α95: 43.4°, K: 15), and the combined mean of all high-quality characteristic directions is 11.8° declination and 46.3° inclination (α95: 11.4, K: 27). The normal-polarity and reversed-polarity vectors pass the reversal test of McFadden and McElhinny (1990) with an intermediate classification (γ_o/γ_c: 12.9°/24.5°) and the non tilt-corrected combined best fit orientation (12.9° declination and 43.6° inclination) is unique from the modern magnetic pole at the 95% confidence interval.

Shorncote Quarry, Ashton Keynes, Wilts

	Dec	Inc	α95	K	Intensity	Std.Dev (+/-)		R	N	Lat	Long	δp	δm	Paleolat
Normal	1.9	41.4	43.4	14.6	2.59E-02	9.38E-03	-6.89E-03	2.4	2.5	62.0	534.3	32.3	52.9	23.8
Reversed	197.2	-48.4	12.3	39.5	3.61E-02	7.79E-02	-2.47E-02	4.9	5.0	-64.3	321.6	10.6	16.2	-29.4
Combined	11.8	46.3	11.4	26.5	3.23E-02	5.13E-02	-1.98E-02	7.3	7.5	64.4	513.3	9.4	14.6	27.7
Vector Comb.	10.3	45.7	-	-	3.08E-02	-	-	-	-	64.2	516.4	9.3	14.5	27.1
2nd Vector Comb.	242.0	-53.6	-	-	6.12E-03	-	-	-	-	-	-	-	-	-

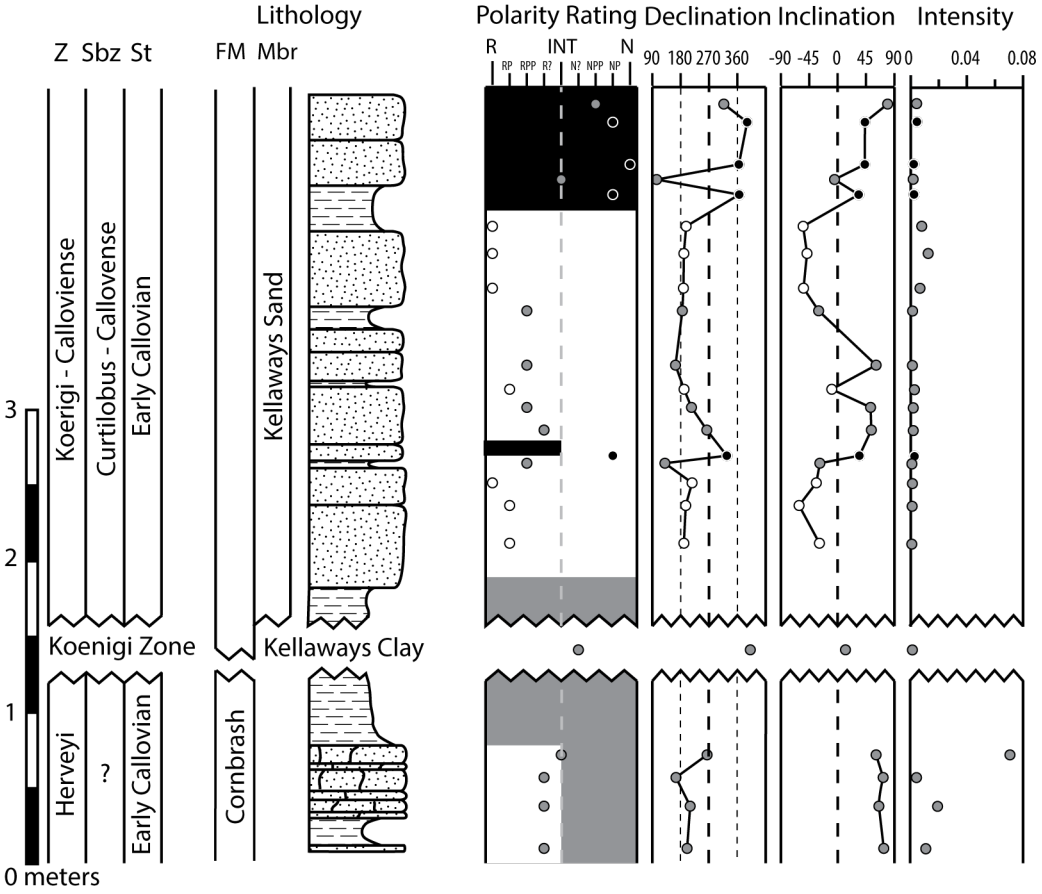

Figure 18: Magnetiostratigraphy of the Shorncote Quarry (SK, Ashton Keynes, Wilts) alongside the outcrop lithology and biostratigraphy.

Location of zonal and subzonal boundaries are placed utilizing descriptions in Hollingworth and Wignall (1992), Hudson and Martill (1994) and Page (1989) with further corroboration from studies by Cave and Cox (1975), Chidlaw & Campbell (1988) and Douglas and Arkell (1928, 1932, 1935). Polarity ranking, from highly ranked reversed (R) to highly ranked normal (N) with indeterminate samples falling along the middle (INT), is plotted over the interpreted magnetic sequence. The characteristic direction (declination and inclination) as well as intensity of the calculated best fit vectors for each sample are plotted, corresponding with the location on the outcrop from which the sample was collected. Normal, reversed and combined vectors calculated from the highly ranked (R, N, RP, NP) samples are included in the table along with the produced VGP (latitude, longitude) and confidence levels (δp, δm).

6.1.3 King's Dyke Clay Pit (KD); lower-upper Callovian

The King's Dyke Clay Pit, Whittlesey, Cambridgeshire, exposes over 25 meters of Middle Callovian from the top of the Kellaways Sand Member of Kellaways Formation through the entire of the Peterborough and into the Stewartby members of the Oxford Clay Formation (Figure 19). Previous work has established ammonite zone and subzone correlations for this quarry site (e.g., Callomon, 1955; Cox et al., 2002b; Hudson & Martil, 1994). A total of 58 samples were analyzed, with denser sampling within the more condensed strata of the upper Kellaways and basal Oxford Clay interval.

The 7 paleomagnetic samples from the upper 56 cm of the Kellaways Formation (*Sigaloceras calloviense* Subzone and Zone) indicated a possible normal-polarity horizon (one high-quality characteristic direction) between two bands of poor-quality reversed-polarity to indeterminate characteristic directions. The upper reversed-polarity interval continues into the lower of two overlying light grey to olive-brown shaley clay beds representing the *Kosmoceras endodatum* Subzone of the *Sigaloceras calloviense* Zone.

All samples from the overlying *Kosmoceras jason* and *Erymnoceras coronatum* zones of Middle Callovian yielded normal polarity. The *Kosmoceras jason* Zone interval is condensed into approximately 1 meter, but the alternating shale beds and *Graphyaea* and *Grammatodon* shell-beds have detailed ammonite subzones and yielded relatively high-quality characteristic directions. The *Kosmoceras medea* Subzone spans Peterborough beds 3 through 9 and the *Kosmoceras jason* Zone and Subzone is beds 10 through 13.

Of the 16 samples taken from beds within the *Kosmoceras obductum* and *Kosmoceras grossouvrei* Subzones of the relatively expanded *Erymnoceras coronatum* Zone, all but two were of high quality normal-polarity orientations.

The upper Peterborough Member beds of the *Kosmoceras phaeinum* Subzone of the *Peltoceras athleta* Zone yielded a pair of reversed-polarity intervals represented by low-quality

characteristic directions (2 for the lower one; 4 for the upper one), but the extent of these reversed-polarity zones is uncertain due to adjacent intervals yielding indeterminate samples or having inadequate sampling (Figure 19). The lower part of the Stewartby Member in this *Kosmoceras phaeinum* Subzone is normal polarity, based on four high-quality and one low-quality characteristic directions.

The 32 high-quality normal-polarity characteristic directions have a mean of 358.6° declination, 47.8° inclination (α95: 8.3°, K: 15). The single high-quality reversed-polarity samples has a characteristic direction is 210.5° declination, -65.2° inclination, and is not antipodal

to the normal-polarity mean direction falling outside the normal 95% confidence interval and failing the McFadden & McElhiney (1990) reversal test (γ_o/γ_c: 24.2°/22.5°). The combined direction is 359.1° declination and 48.3° inclination (α95: 8.2°, K: 15). The combined direction is unique from the modern magnetic pole at the 95% confidence interval.

Kings Dyke Clay Pit, Cambridgeshire

	Dec	Inc	α95	K	Intensity	Std.Dev (+/-)		R	N	Lat	Long	δp	δm	Paleolat
Normal	358.6	47.8	8.3	14.7	2.49E-02	1.42E-02	-9.03E-03	21.0	22.5	66.3	542.8	7.0	10.8	28.9
Reversed	210.5	-65.2	0.0	100.0	4.00E-02	4.00E-02	-3.99E-08	1.0	0.0	-69.8	273.0	0.0	0.0	-47.2
Combined	359.1	48.3	8.2	14.6	2.51E-02	1.43E-02	-9.13E-03	21.5	23.0	66.7	541.9	7.0	10.7	29.3
Vector Comb.	14.6	59.5	-	-	3.17E-02	-	-	-	-	74.2	494.9	9.2	12.3	40.3
2nd Vector Comb.	284.1	-62.7	-	-	1.00E-02	-	-	-	-	-	-	-	-	-

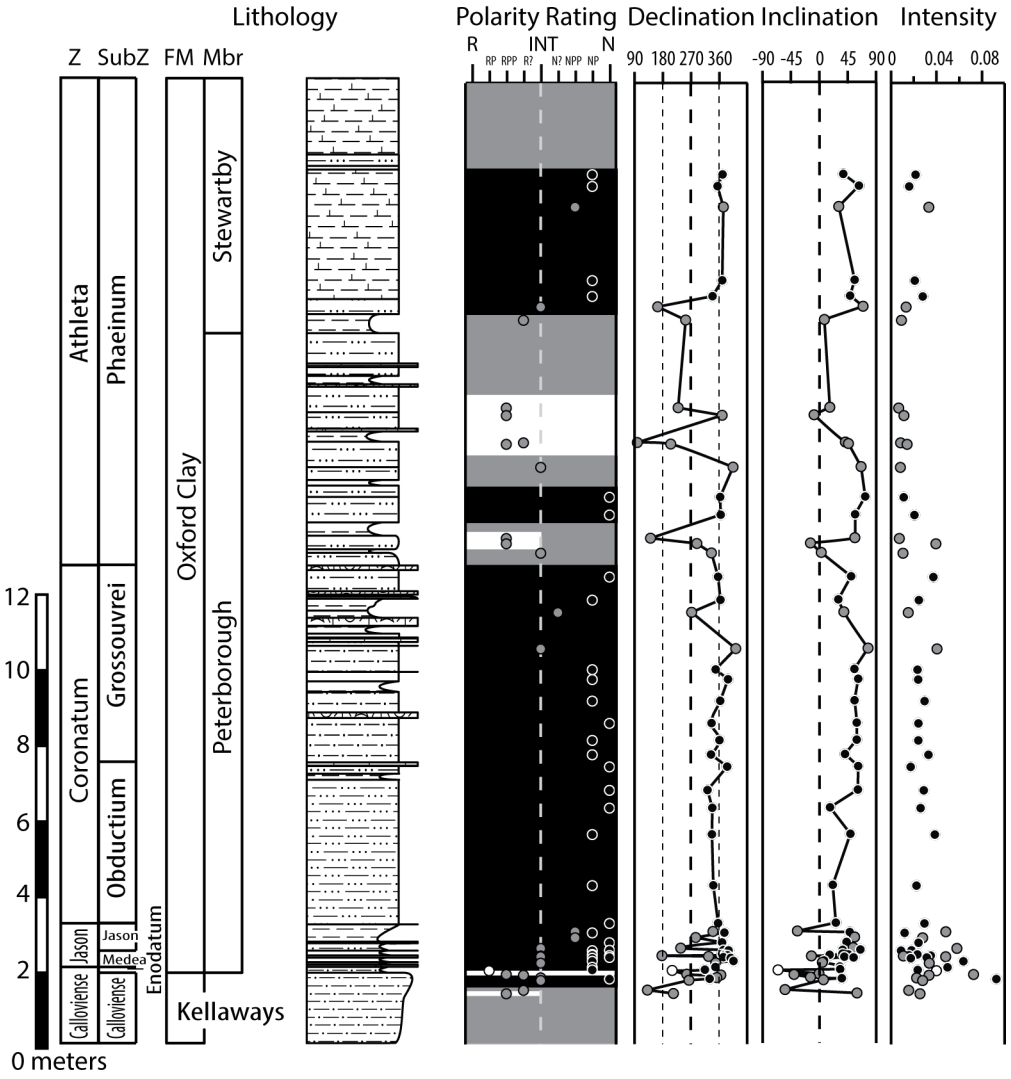

Figure 19: Magnetiostratigraphy of the Kings Dyke pit (KD, Cambridgeshire) alongside the outcrop lithology and biostratigraphy.

The precise location of zonal and subzonal boundaries are placed utilizing descriptions in Hudston and Martill (1994) and Page (2002) with further corroboration from studies by Anderson (1994), Cox et al. (1992), Kenig (1994), Macquaker (1994) and Norry et al. (1994). Polarity ranking, from highly ranked reversed (R) to highly ranked normal (N) with indeterminate samples falling along the middle (INT), is plotted over the interpreted magnetic sequence. The characteristic direction (declination and inclination) as well as intensity of the calculated best fit vectors for each sample are plotted, corresponding with the location on the outcrop from which the sample was collected. The orientations of the normal, reversed and combined vectors calculated from the highly ranked (R, N, RP, NP) samples are included in the table along with the produced VGP (latitude, longitude) and confidence levels (δp, δm).

6.1.4 Dix Pit, Stanton Harcourt (SH); upper Callovian-lower Oxfordian

We densely sampled the Callovian/Oxfordian boundary interval from the middle to upper Oxfordian Clay Formation in Dix Pit next to Stanton Harcourt in Oxfordshire. Regional lithologic correlations and studies of the nearby Stanton Harcourt Quarry provide biostratigraphic correlation of ammonites to the zone level (e.g. Cox et al., 2002b; Hollingworth & Wignall, 1992; Norris & Hallam, 1995). A total of 37 samples were collected from this 4-meter exposure that spans the upper *Peltoceras athleta* Zone to the lower *Quenstedtoceras mariae* Zone (Figure 20).

Even though many of the samples yielded low-quality characteristic directions, a succession of 3 normal-polarity zones separated by intervals of mixed reversed-polarity and indeterminate characteristic directions was established. The upper reversed-polarity-dominated interval within the *Quenstedtoceras lamberti* Zone may contain two normal-polarity horizons. However, the condensed nature of the uppermost Callovian of Dix Pit indicates that this reversal frequency is possibly a minimum for this time span.

The three higher-quality reversed-polarity characteristic directions have a very poor cluster with a mean of 154.7° declination and -9.5° inclination (α95: 57.3, K: 8.6). The larger suite of high-quality normal-polarity characteristic directions has a mean of 14.4° declination and 45.5° inclination (α95: 15.0°. K: 17). This outcrop has a γ_o/γ_c of 49.5°/34.0°, failing the reversal test of McFadden and McElhinny (1990). The reduced precision for the combined mean direction (3.4° declination, 39.2° inclination; α95: 19.4, K: 8) reflects the lack of antipodal reversed-polarity directions. The both the normal-polarity and the combined direction orientations are distinct from the modern magnetic pole at the 95% confidence interval.

Dix Pit, Stanton harcourt, Oxfordshire (SH)

	Dec	Inc	α95	K	Intensity	Std.Dev (+/-)		R	N	Lat	Long	δp	δm	Paleolat
Normal	14.4	45.5	15.0	17.2	8.27E-02	1.73E-01	-5.59E-02	6.7	7.0	62.9	509.4	12.1	19.1	27.0
Reversed	154.7	-9.5	57.3	8.6	3.24E-02	6.17E-03	-5.18E-03	1.9	2.0	-38.5	391.6	29.3	57.9	-4.8
Combined	3.4	39.2	19.4	8.0	4.43E-02	3.05E-02	-1.81E-02	8.0	9.0	60.3	532.2	13.8	23.1	22.2
Vector Comb.	355.2	32.8	-	-	3.68E-02	-	-	-	-	55.8	545.8	12.4	21.9	17.9
2nd Vector Comb.	80.0	52.4	-	-	1.84E-02	-	-	-	-	-	-	-	-	-

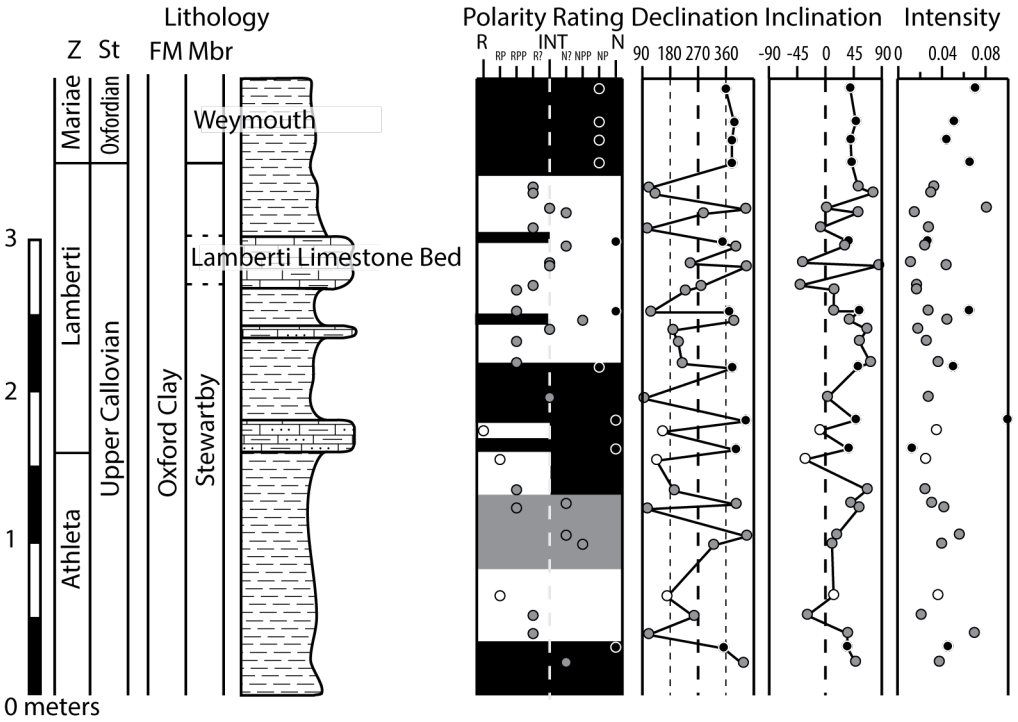

Figure 20: Magnetiostratigraphy of Stanton Harcourt (SH) alongside the outcrop lithology and biostratigraphy.

The precise location of zonal boundaries are placed utilizing descriptions by Hollingworth and Wignall (1992), Norris and Hallam (1995) and Page (2004) with further corroboration from the lithological studies of Cox et al., (1992) and Kenig et al., (1994). Polarity ranking, from highly ranked reversed (R) to highly ranked normal (N) with indeterminate samples falling along the middle (INT), is plotted over the interpreted magnetic sequence. The characteristic direction (declination and inclination) as well as intensity of the calculated best fit vectors for each sample are plotted, corresponding with the location on the outcrop from which the sample was collected. The orientations of the normal, reversed and combined vectors calculated from the highly ranked (R, N, RP, NP) samples are included in the table along with the produced VGP (latitude, longitude) and confidence levels (δp, δm).

6.1.5 Paleomagnetic behavior

During the Callovian, the shallow shelf seas that were partially influenced by warmer waters from the Tethyan realm received two major packages of sediment: the Great Oolite Group and the Ancholme Group. These units contain a variety of rock types, especially mudstone, shale, calcareous silt to sandstone, and bioclastic packstone to grainstone limestone. The sediment type influences the NRM and the behavior of the paleomagnetic samples during thermal demagnetization. The common ferromagnetic minerals present in sedimentary rock include magnetite, maghemite, titanomagnetite, pyrrhotite, hematite and goethite with unblocking temperatures ranging from 80 to 580°C (magnetite: 580°C, maghemite: ~350°C, titanomagnetite x=0.3: 350°C, titanomagnetite x=0.1: 150°C, pyrrhotite: 325°C, hematite: 675°C and goethite: 80-120°C (McElhinny & McFadden, 2000; Lowrie, 1990; O'Reilly, 1984). After unblocking and removal of the secondary magnetic overprint, continued heating can cause some of these minerals or other iron-bearing minerals to dehydrate and transform. Examples include conversion of goethite to hematite (above 300°C), from maghemite to hematite (above 300°C) and the conversion of pyrite to pyrrhotite and magnetite (at ~500 and ~800°C) (Lowrie & Heller, 1982).

The lowest units in our study are dominated by shallow-water limestone of the White Limestone and Forest Marble formations. The thermal demagnetization procedure applied to the yellowish grey bioclastic packstones of the Shipton Member initially partly removed a normal-polarity overprint to unblock some intervals of reversed-polarity; but also yielded low intensities and a large jump in susceptibility and error at the 270°C temperature step. Thermal demagnetization of the Ardley Member, very light grey with light yellow discoloration bioclastic packstone, showed very similar behavior with a consistent and dramatic jump in susceptibility at the 240°C step. Likewise, the Forest Marble Formation yielded characteristic directions between 200 and 270°C with rapid susceptibility increase in three quarters of the samples at 270°C.

Paleomagnetic samples from the overlying Cornbrash and Kellways formations had a similar behavior during thermal demagnetization. The lower beds of the Lower Cornbrash typically provided characteristic directions between 240 and 330°C. The samples taken from the upper Cornbrash turned red upon reaching the 270°C heating step and did not provide reliable orientations. The calcareous sandstone of the Kellaways Sand had an unblocking temperature range of 240-330°C.

The overlying shale of the Oxford Clay's Peterborough Member and mudstones of the Stewartby Member typically yielded characteristic directions between 240 and 300°C, followed

by a susceptibility jump at 330 or 360°C. The lowest samples collected from the Weymouth Member had susceptibility spikes beginning at 270°C.

The similar temperature range for unblocking and the interpretation of characteristic directions (between about 200° and 300°C) terminating in a surge in susceptibility (generally at 270° or 300°C) for these various units indicates a similar magnetic mineral assemblage across the lithologies. We tentatively attribute the demagnetization of goethite-carried secondary overprints followed by the dewatering and mineralogical decomposition of goethite to new viscous magnetic phases as contributing to these demagnetization behaviors, but with magnetite as the primary carrier of characteristic magnetization.

6.1.6 Composite magnetostratigraphy for Callovian of English sections

The magnetic stratigraphy composite from these four main English sections covers over two thirds of the Callovian timespan (Figure 21). Whereas the French composite is most detailed in the lower Callovian, the English composite enables establishment of the main polarity signature for the Middle Callovian (*Kosmoceras medea* Subzone) to lowermost Oxfordian (*Cardioceras scarburgense* Subzone). The Middle Callovian is dominated by an uninterrupted normal polarity. The Upper Callovian has several reversals within a dominance in the reversed polarity orientation. The composite sequence indicates a normal-polarity zone in the basal lower Oxfordian.

The Lower Callovian of these English sections contains four discontinuous segments of coverage: (1) a portion of the *Sigaloceras calloviense* Subzone, (2) the *Sigaloceras calloviense* Subzone through the *Kepplerites curtilobus* Subzone, (3) a poorly resolved signal in the *Macrocephalites terebratus* Subzone, and (4) the boundary between the Callovian *Kepplerites keppleri* Subzone and the Bathonian *Clydoniceras discus* Subzone. Sampling also covers a brief period in the *Clydoniveras hollandi* Subzone and across the *Wagnericeras fortecostatum* Subzone through the base of the *Morrisiceras morrisi* Subzone. There are indications that the Lower Callovian is dominated by reversed polarity, but with relatively brief normal-polarity levels. The lowermost Callovian and uppermost Bathonian have a signal of rapid reversals.

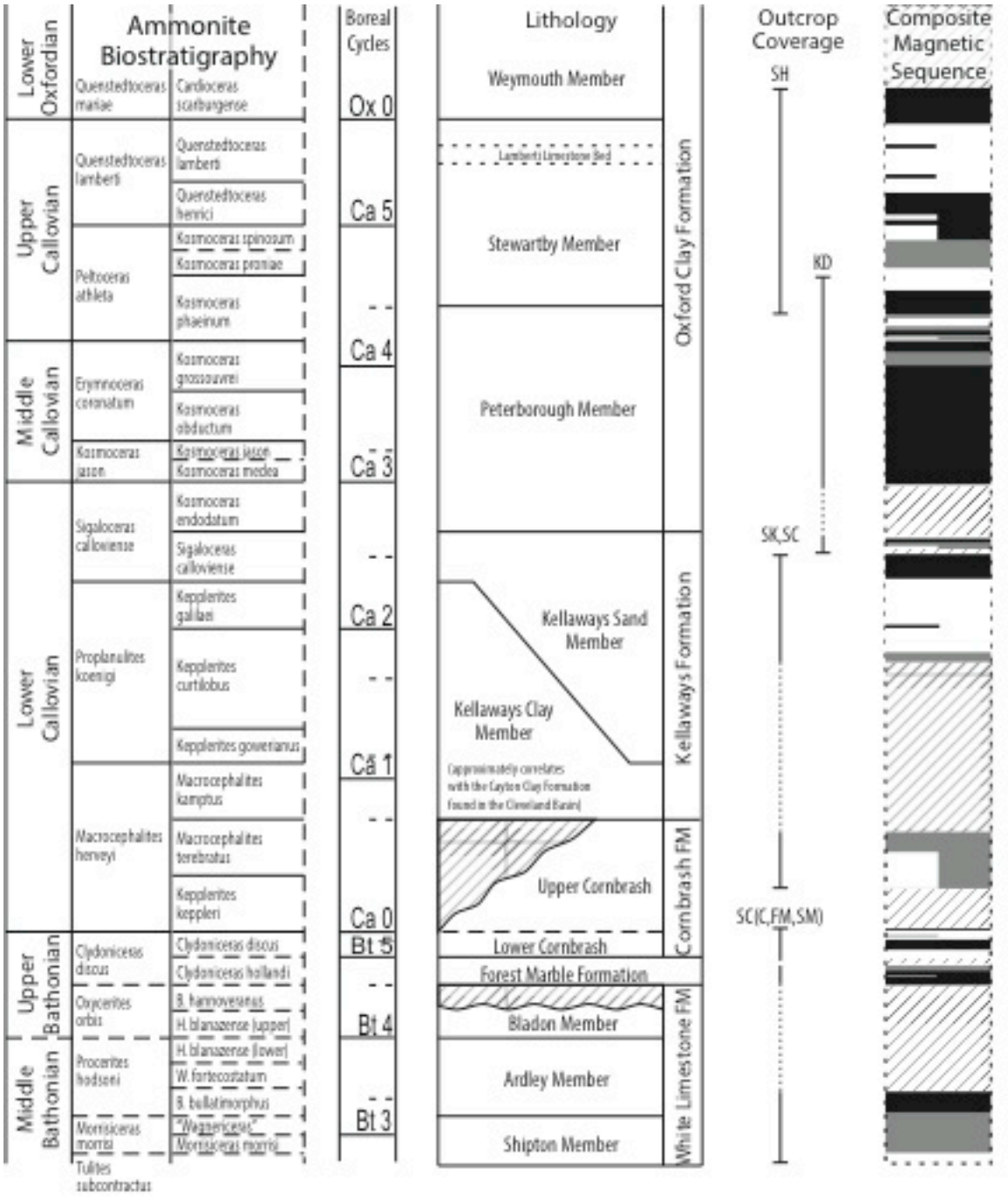

Figure 21: A composite magnetostratigraphic sequence constructed from the English Callovian outcrops is plotted against Sub-Boreal ammonite biostratigraphy and Boreal third order cycles as scaled by Hardenbol et al. (1998) and the GTS2012 (Ogg & Hinnov, 2012). The spans represented in the English outcrops are indicated next to the interpreted composite sequence.

7 ISLE OF SKYE (SCOTLAND) CALLOVIAN; LOWER CALLOVIAN-LOWER OXFORDIAN

The inter-tidal shoreline of Staffin Bay along the eastern edge of the Trotternish peninsula on the Isle of Skye in Scotland exposes well-studied Middle to Upper Jurassic rocks (e.g., Anderson and Dunham, 1966; Cox et al., 2002a; Duff, 1980; Morton and Hudson, 1995; Sykes, 1975; Sykes and Callomon, 1979). During the late Middle Jurassic, this region was located within the Hebrides Basin between the Hebrides Platform and Scottish Landmass. This was a northward extension of the same seaway that contained our sampling sites in England (Bradshaw et al., 1992). The Callovian and Oxfordian units at Staffin Bay consist of two coarsening-upward formations that overly the Great Estuarine Group of Harris and Hudson (1980; Barron et al., 2012). The deposition of these packages of clays and siltstones occurred during part of a continued sea-level rise that is also observed in other regions (Bradshaw et al., 1992). The depositional facies progresses through a coastal lagoonal setting for the Upper Ostrea Member of the Staffin Bay Formation, an open-marine influenced sand bar that transgressed across the lagoon (Belemnite Sands member), and an open-marine mudstones of the Staffin Shale Formation (Barron et al., 2012; Hudson, 1963a, b; Hudson et al., 1995; Riding and Thomas, 1997).

The base of our studied section is constructed of the five beds that comprise the Upper Ostrea Member of the Staffin Bay Formation (Cox and Sumbler, 2002; Morton and Hudson, 1995; Riding, 1992) (Figures 22, 23 and 24). This member is dominated by dark grey, fissile mudstones and dated with dinoflagellates as coeval with the *Macrocephalites herveyi* ammonite Zone of lowermost Callovian, (Barron et al., 2012; Cox et al., 2002a; Riding, 1992; Ridding & Thomas, 1997); therefore it is coeval with the Upper Cornbrash Member of the Cornbrash Formation of southern and central England. (Riding, 1992). The overlying Belemnite Sand Member contains rare ammonites that indicate the *Proplanulites koenigi* ammonite Zone of the Lower Callovian (Cox et al., 2002a). The Dunans Shale and Dunans Clay members of the Staffin Shale Formation are dated by ammonite and palynomorphs studies as Middle Callovian through Lower Oxfordian (Cox et al., 2002a; Morton & Hudson, 1995; Riding & Thomas, 1997). Samples collected from the *Quenstedtoceras lamberti* and *Quenstedtoveras mariae* zones were reanalyzed to find results

consistent with that of Ogg et al. (2010). The uninterrupted upward continuation of this section, including the Oxfordian-Kimmeridgian GSSP candidate, provides a reversed-polarity dominated magnetostratigraphic sequence as established by Ogg et al., (2010) and Przybylski et al. (2010a; Wierzbowski et al., 2006).

We applied thermal demagnetization to 71 samples collected through the 40 meters of Callovian into lower Oxfordian. The resulting polarity pattern is dominated by normal-polarity or indeterminate characteristic directions in the Lower and Middle Callovian and by reversed polarity in the Upper Callovian and Lower Oxfordian (Figure 22).

However, only 27 of these interpreted characteristic directions were ranked as high-quality (N, R, NP and RP) and utilized for the analysis of mean directions. Even though these have a poor clustering, the mean normal-polarity vector (9.7° declination, 33.4° inclination; α95: 26.1°, K: 8) is antipodal to the reversed vector (212.7° declination, -35.8° inclination; α95: 13.4, K: 12). The combined mean direction is 25.1° declination and 35.5° inclination (α95: 11.9°, K: 9). This is substantially different from the 17.0° declination and 45.0° inclination (α95: 6.6°, K: 10.7) produced by the great circle mean of the overlying sections (Przybylski et al., 2010a).

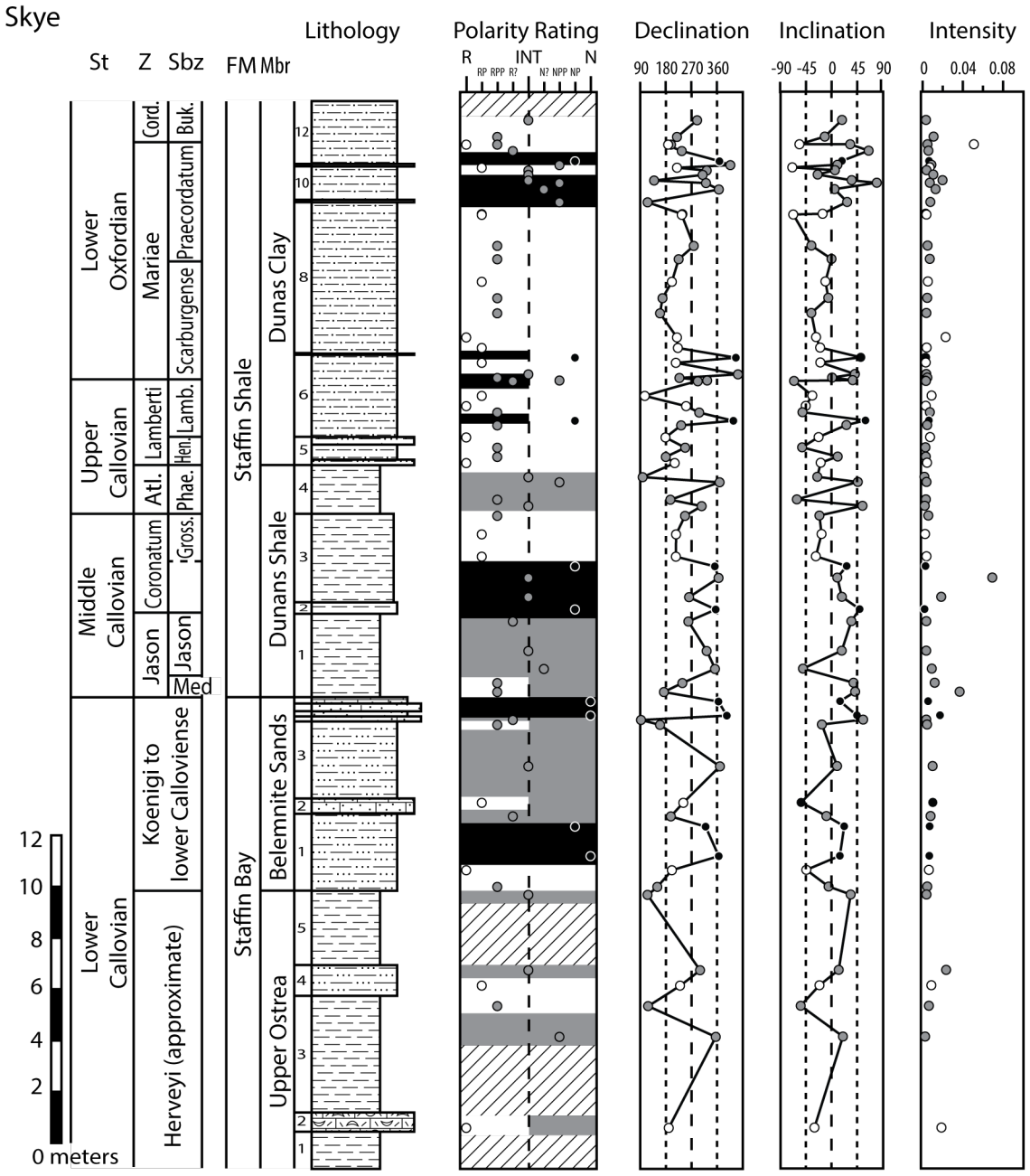

Figure 22: Magnetiostratigraphy of Callvian aged units from Staffin Bay (Isle of Skye, Scotland) alongside outcrop lithology and biostratigraphy.
Precise location of zonal and subzonal boundaries are placed utilizing descriptions in Cox et al. (2002a) and Sykes (1975) with further corroboration from Hudson (1963a, b), Hudson et al., (1995), Morton and Hudson (1995), Riding (1992) and Riding and Thomas (1997). Ammonite abbreviations include Medea (Med.), Grossouvrei (Gross.), Phaeinum (Phae.), Henrici (Hen.), LAmberti (Lamb.), Cordatum (Cord.) and Bukowskii (Buk.). Polarity ranking is plotted over the interpreted magnetic sequence. Characteristic direction (declination and inclination) and intensity of the best fit vectors for each sample are plotted, corresponding with the location on the outcrop from which the sample was collected.

Skye

	Dec	Inc	α95	K	Intensity	Std.Dev (+/-)		R	N	Lat	Long	δp	δm	Paleolat
Normal	9.7	33.4	26.1	7.6	5.54E-02	5.52E-02	-2.76E-02	5.3	6.0	50.0	159.4	16.9	29.7	18.3
Reversed	212.7	-35.8	13.4	11.5	7.03E-02	1.06E-01	-4.23E-02	11.1	12.0	-45.3	-52.4	9.0	15.5	-19.8
Combined	25.1	35.5	11.9	9.4	6.49E-02	8.68E-02	-3.71E-02	16.2	18.0	47.8	137.4	8.0	13.8	19.6
Vector Comb.	22.4	35.3	-	-	6.20E-02	-	-	-	-	48.5	501.0	8.0	13.8	19.5
2nd Vector Comb.	263.9	-24.6	-	-	1.27E-02	-	-	-	-	-	-	-	-	-

Figure 23: The normal, reversed and combined vectors calculated from the highly ranked (R, N, RP, NP) samples along with VGP (latitude, longitude) and confidence levels (δp, δm).

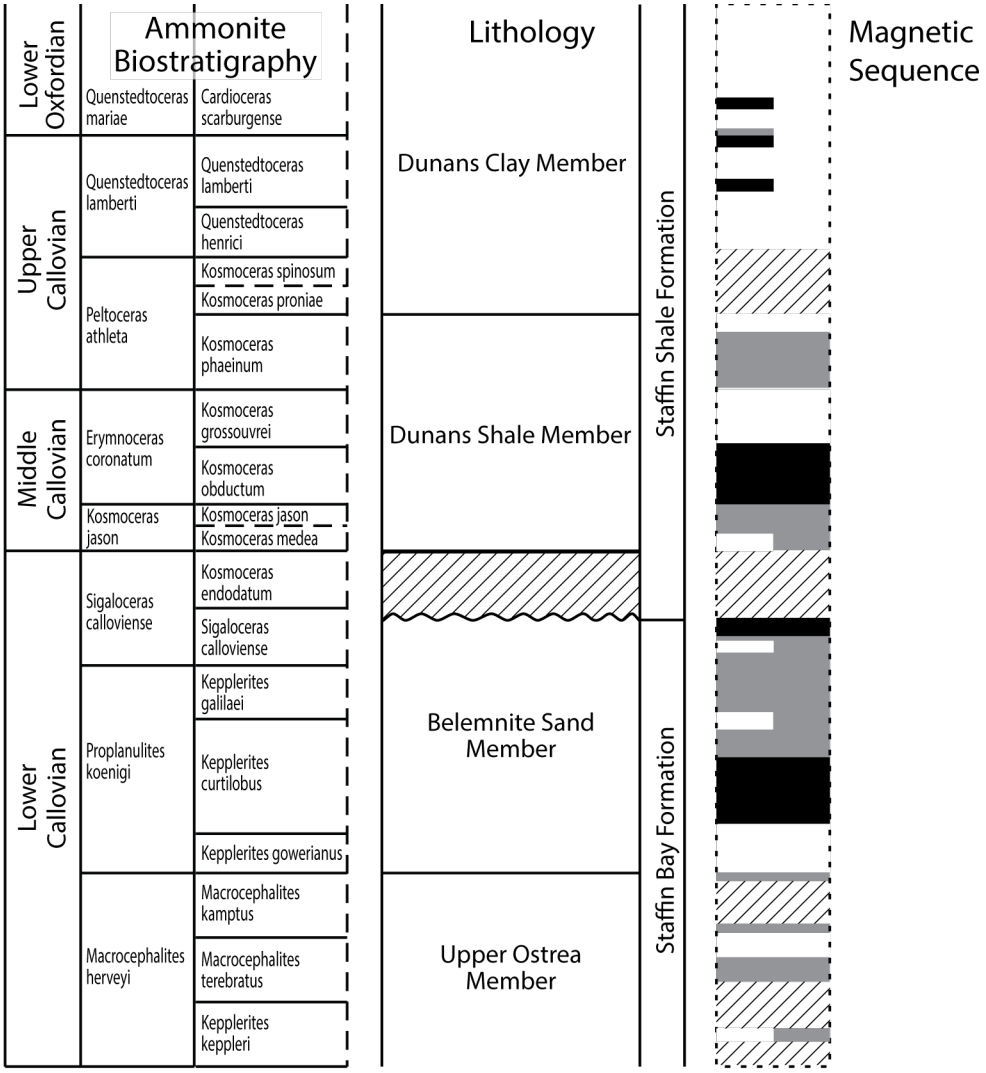

Figure 24: The Staffin Bay Callovian interpreted magnetic sequence scaled to a standard ammonite biostratigraphy.

8 SWABIA JURA (SOUTHERN GERMANY) CALLOVIAN; UPPER BATHONIAN-LOWER CALLOVIAN

The Jurassic formations in the Swabian Alb of southern Germany were deposited within Central European Basin System bordering the Tethyan sea and were connected by an epicontinental seaway to the Paris Basin in the west (Pieńkowski et al., 2008). The middle Jurassic succession is traditionally called Bauner Jura in reference to its dominant coloration in the outcrop. The Callovian portion consists of the Ornatenton Formation mudstones that contain two condensed iron-oolitic members, a basal Macrocephalen-Oolith and a higher Anceps-Oolith members (Beher et al., 2010; Pieńkowski et al., 2008). The Macrocephalen-Oolith unit marks the Bathonian-Callovian boundary and overlies the dark claystones of the Dentalienton Formation of Bathonian (Beher et al., 2010; Pieńkowski et al., 2008). A small excavation into the ammonite-rich Macrocephalen-Oolith within a forest region near the village of Albstadt-Pfeffingen is a candidate for the Global Boundary Stratotype Section and Point (GSSP) of the Callovian Stage (Callomon & Dietl, 2000; Dietl, 1994; Mönning, 2012). The studies of this excavation and other nearby Bathonian-Callovian boundary sections have provided ammonite faunal horizons (e.g., *suspensum, orbis, hochstetteri, keppleri, quenstedti, suevecum* and *toricelli*; Figure 25) based on collections of hundreds of ammonite specimens that contain the indicator species (Callomon & Dietl, 2000; Dietl, 1994; Pieńkowski et al., 2008). These faunal horizons have been correlated to those in England for high-resolution correlation of the basal Callovian boundary (Callomon & Dietl, 2000). In addition to high-resolution ammonite biostratigraphy, this section has been analyzed for strontium isotope stratigraphy, palynology and other faunal assemblages including ostracods and foraminifera (Beher, 2010; Callomon & Dietl, 2000; Franz and Knott, 2012).

In coordination with Dr. Gerd Dietl (Staatliches Museum für Naturkunde, Stuttgart), this section of iron-oolite-rich sandy claystone was re-excavated and densely sampled (ca. 3-cm spacing; Figures 25 and 26), before being again covered to discourage fossil collectors.

Thermal demagnetization was applied to the 37 samples collected from 1.2 meters of the 2 meter thick exposure. These samples underwent thermal demagnetization in 25-40°C temperature steps between 250° and 480°C, with susceptibility measured at every step taken.

Samples showed a strong initial magnetization (~10 mA/m) that rapidly declined by 80-95% of initial NRM upon heating to 300-350°C. Characteristic directions were typically computed from the interval between 350° and 450°C, producing an average intensity of 0.9 mA/m. With a few exceptions, samples heated beyond 430°C experienced a significant susceptibility increase and a likely associated reddening in color. The magnetic behavior of these samples indicates magnetite and hematite as the dominant magnetization carriers, with goethite contributing a rapidly removed (by 150°C) NRM component. Further description of the magnetic behavior and interpretation is available in the unpublished report to the Callovian GSSP working group (Appendix A).

The reinterpretations of the magnetostratigraphy of this set of compact strata indicated several reversals in the lowest Callovian. The 18 high–quality normal-polarity characteristic directions (of 22 total) are tightly clustered with a mean of 4.6° declination, 64.6° inclination (α95: 3.8°, K: 102). Only 3 of the 13 reversed-polarity samples were rated high–quality, producing a mean of 182.7° declination and -37.9° inclination (α95: 19.5°, K: 12). The combined orientation has a best-fit mean of 5.5° declination and 63.21° inclination (α95: 5.67°, K: 33.25) for the tilt-corrected data. The non tilt-corrected combined orientation (5.5° declination, 63.2° inclination) is indistinguishable from the modern magnetic pole at the 95% confidence interval despite the non tilt-corrected normal-polarity orientation (6.2° declination, 66.5° inclination) being unique at the same confidence level.

Swabia

	Dec	Inc	α95	K	Intensity	Std.Dev (+/-)		R	N	Lat	Long	δp	δm	Paleolat
Normal	4.6	64.6	3.8	101.5	8.78E-01	1.24E+00	-5.14E-01	14.9	15.0	86.3	129.2	4.9	6.1	46.5
Reversed	182.7	-37.9	48.0	12.2	1.07E+00	9.85E-01	-5.12E-01	2.4	2.5	-62.8	3.5	33.5	56.7	-21.3
Combined	4.2	61.0	6.1	34.3	9.03E-01	1.20E+00	-5.15E-01	17.0	17.5	83.0	162.7	7.1	9.3	42.0
Vector Comb.	3.3	50.0	-	-	9.46E-01	-	-	-	-	72.2	179.8	5.4	8.1	30.8
2nd Vector Comb.	181.1	16.5	-	-	2.42E-01	-	-	-	-	-	-	-	-	-

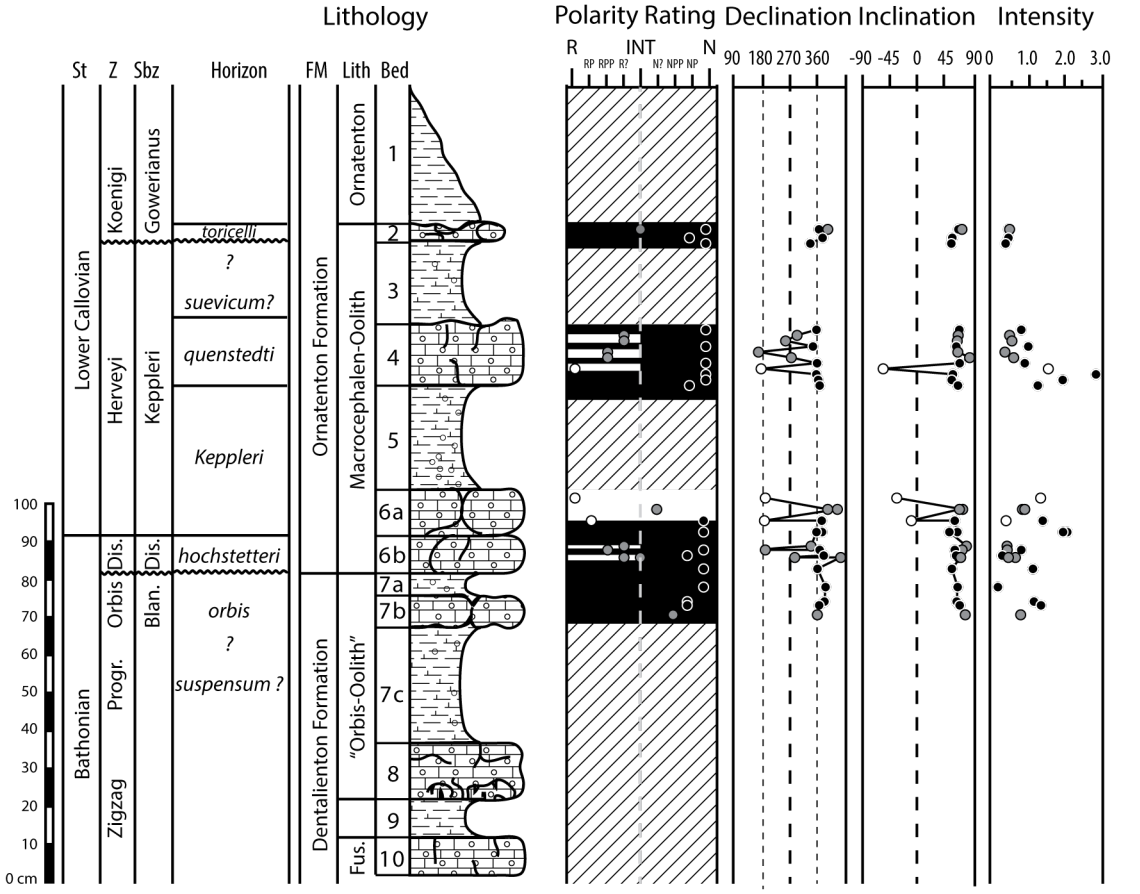

Figure 25: Magnetiostratigraphy of the proposed Callovian GSSP site at Albstadt-Pfeffingen in the Swabian Alb alongside the outcrop lithology and biostratigraphy.
Zonal and subzonal boundaries placed after Callomon and Dietl (2000) with continued work by Beher et al. (2010) and Franz and Knott (2012). Polarity ranking, from highly ranked reversed (R) to highly ranked (N) with indeterminate samples falling along the middle (INT), is plotted over the interpreted magnetic sequence. The characteristic direction (declination and inclination) as well as intensity of the calculated best fit vectors for each sample are plotted, corresponding with the location on the outcrop from which the sample was collected. The orientations of the normal, reversed and combined vectors calculated from the highly ranked (R, N, RP, NP) samples are included in the table along with the produced VGP (latitude, longitude) and confidence levels (δp, δm).

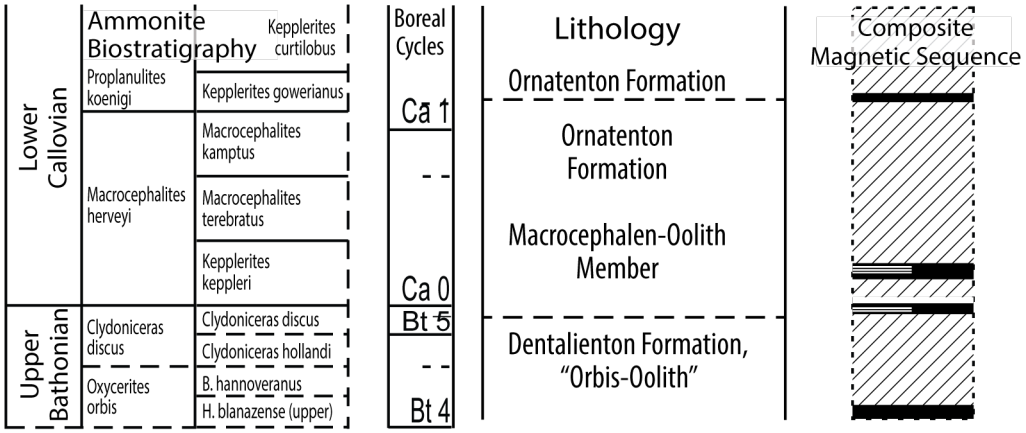

Figure 26: The interpreted magnetic sequence of the Albstadt-Pfeffingen outcrop of the Swabian Alb scaled to standard sub boreal ammonite biostratigraphy.

9 MAGNETIC POLARITY COMPOSITE AND CORRELATION

9.1 Composite polarity sequence from our sections

The suite of magnetostratigraphy sections from England, France and Germany are generally consistent within the biostratigraphic constraints, thereby enabling a composite polarity scale that spans nearly the entire Callovian (Figure 27). The third-order depositional sequences interpreted in the lower Callovian outcrops of France by Garcia (1993) assisted in assigning ammonite zones and subzones from the sequence-biostratigraphy compilation by Jacquin et al. (1998). The general pattern is dominated by normal-polarity. Three intervals with relatively close-spaced reversed-polarity zones occur at (1) basal Callovian, (2) upper Lower Callovian, and (3) the majority of the Upper Callovian.

The base of the Callovian at the boundary interval between the *Clydoniceras discus* Zone and the *Macrocephalites herveyi* Zone is marked by a set of very close-spaced reversals recorded in both Swabia and England. There are a few narrow reversed-polarity intervals in the overlying basal Callovian in the *Macrocephalites herveyi* Zone and basal *Proplanulites koenigi* Zone, but these are less well resolved and there is a sampling gap within part of the *Kepplerites keppleri* Subzone.

There is a relatively wide reversed-polarity zone in the *Kepplerites galilaei* and the top half of *Kepplerites curtilobus* subzones of the *Proplanulites koenigi* Zone; however, the record of this reversed-polarity zone is inconsistent between England and France. Here our composite favors the English record with its suite of high-quality characteristic directions over the relatively poorer data that had been interpreted as low-quality "normal-polarity" samples from France that may have residual secondary overprints and less precise biostratigraphic control.

The very base of the Middle Callovian is a narrow reversed-polarity zone in England, Skye and France. This is followed by a thick interval of normal-polarity that spans nearly the two ammonite zones of Middle Callovian.

The Upper Callovian (*Quenstedtoceras lamberti* and *Peltoceras athleta* Zones) is characterized by nearly six reversed-polarity intervals and relatively lesser normal-polarity zones. The Callovian-Oxfordian boundary falls within a normal-polarity band.

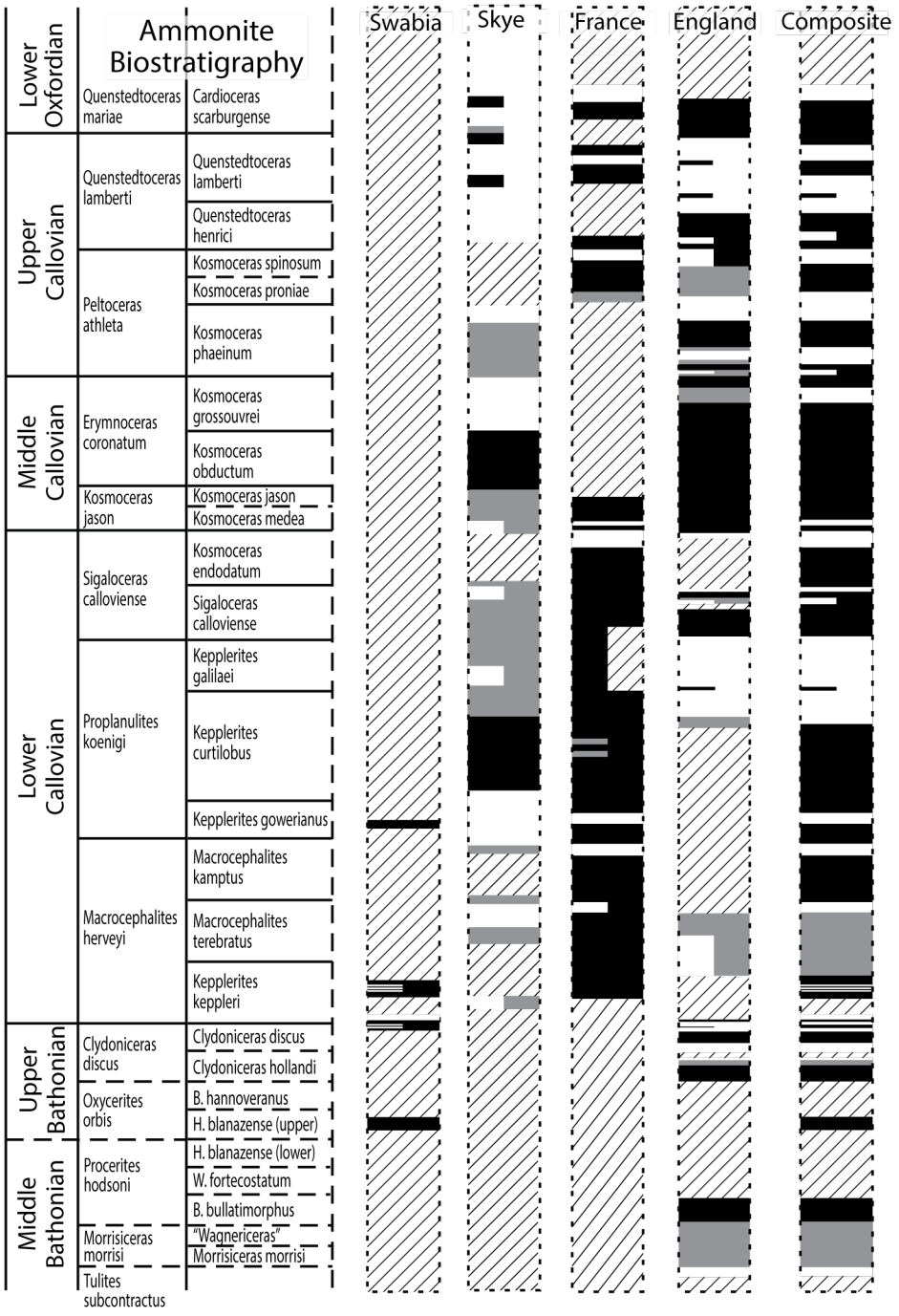

Figure 27: Four regional magnetostratigraphic studies and the interpreted Callovian composite scaled to the standard sub boreal ammonite biostratigraphy.

9.2 Our Composite Polarity Sequence alongside previous biostratigraphic-zoned studies of Callovian magnetostratigraphy

Previous magnetostratigraphy studies with partial ammonite or other biostratigraphic control in sections from Poland (Ogg et al., 1991), Britain (Ogg et al., 2010), France (Belkaaloul et al., 1995, 1997) and Russia Guzhikov et al. (2010) intermittently cover a large portion of the Callovian stage. The majority of these magnetostratigraphy studies corroborate the findings of our study (Figure 28). The composite sequence at the upper boundary of the Callovian produced a good match to the sequence identified by Ogg et al. (2010) at East Hammond Cliff (HCO) in Dorset, which is a candidate for the basal Oxfordian GSSP. There is partial agreement with the condensed sequences of upper Callovian in Skye (Ogg et al., 2010) and in the Krakow Uplands in Poland (OCZL, OCZS and OCP sections of Ogg et al., 1991) that were interpreted as being dominated by reversed polarity direction; disagreement arose from a lower number of resolved the number of normal-polarity bands in comparison to our present composite sequence. The long normal-polarity zone spanning the *Erymnoceras coronatum* and *Kosmoceras jason* ammonite zones is also apparent in the previous studies, particularly in the CMCZ and CMCB sections of the Krakow Uplands (Ogg et al., 1991) and in the Narcisse and Cyrano cores from France (Belkaaloul et al., 1995, 1997). The lower boundary of the Callovian in our composite section is consistent with the Prosek section in the Nizhni Novgord Region, Russia (Guzhikov et al., 2010), and that Russian study had also correlated their results to an earlier informal report on our Swabian magnetostratigraphy.

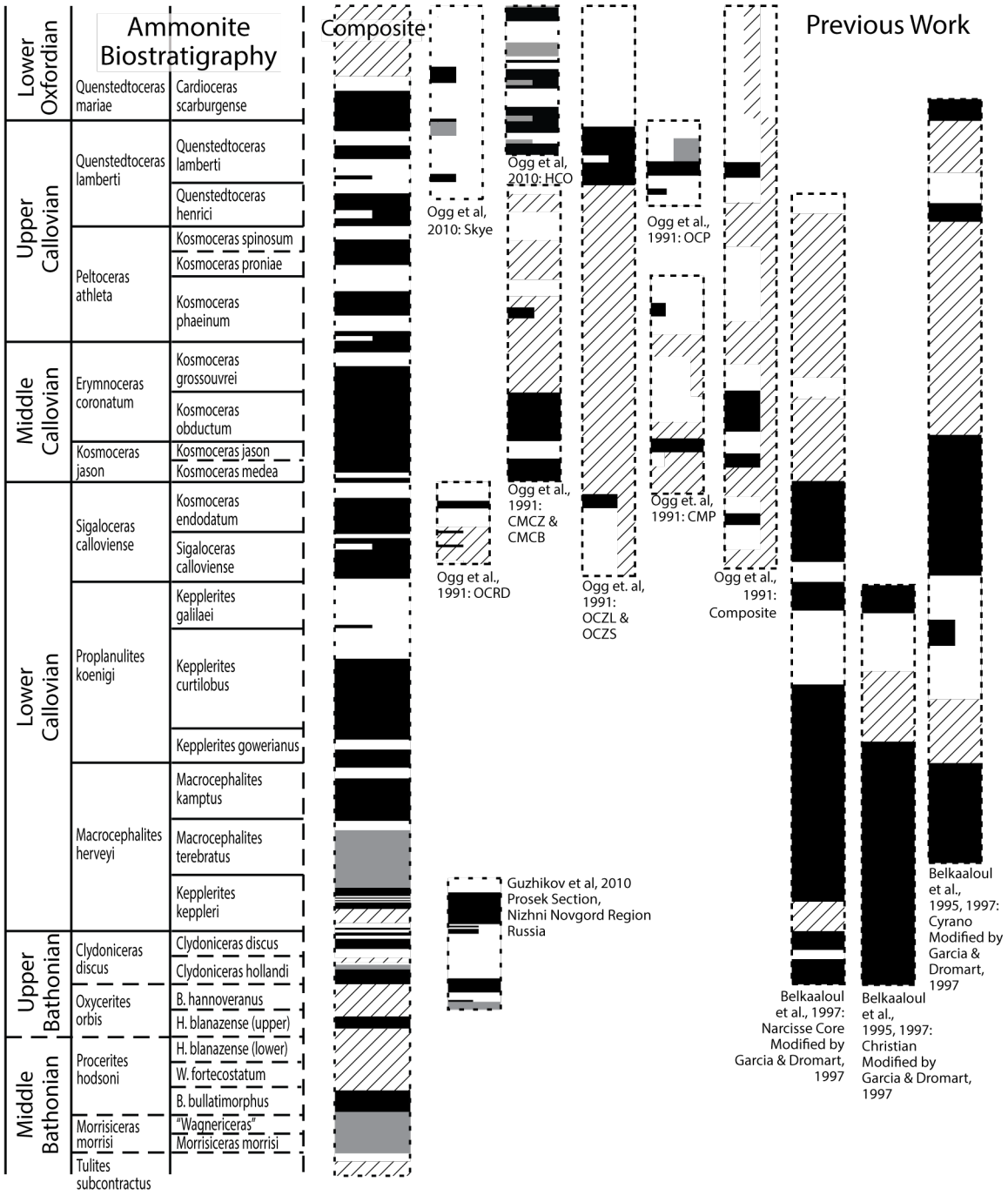

Figure 28: The magnetostratigraphic sequence of the Callovian as interpreted within this study plotted alongside previous work from Ogg et al. (1991), Guzhikov et al. (2010), Belkaaloul et al. (1995, 1997) and Garcia and Dromart (1997).

9.3 Our Composite Polarity Sequence and the pre-M29 marine magnetic anomaly model

The progressive correlation of magnetostratigraphy with the marine magnetic polarity reversal patterns has been conducted using the Upper Jurassic Tithonian and Kimmeridgian Chrons M19-M25 (e.g., Ogg et al., 1984; Gradstein et al., 2004; Speranza et al., 2005) and gradually into older strata through the Oxfordian that enabled matching to Chrons M25-M37n (e.g., Ogg et al., 2010; Przybylsi et al., 2010a, 2010b). The pre-M29 marine magnetic anomalies have low amplitudes, short-wavelength features that are mitigated at the sea surface level. To document such anomalies, high-resolution, deep-tow marine magnetic surveys have been conducted (Tominaga et al., 2010; 2008; Tivey et al., 2006; Sager et al., 1998). Two interpretation models – one is based on the near-bottom signal (5.5 km) and the other uses an upward continued mid-water depth (3 km) signal – are established through the anomaly named Chron M44 (Tivey et al., 2006; Tominaga et al., 2008). The polarity block models at both levels are displayed in Figure 29. The deep-tow and the mid-water profiles likely represent the highest and lowest end-member models regarding the number of reversals, respectively (e.g., Ogg et al., 2010; Tominaga et al., 2008). The main method to validate and improve either model or a hybrid between the two versions is to obtain a magnetostratigraphic record of the Earth's field reversals from sedimentary successions.

An estimate for the relative durations and ages of the pre-M29 marine magnetic polarity reversal sequence is made by applying a constant spreading rate with two radiometric-dated basalt core samples from two ODP sites (e.g., Sager et al., 1998; Tominaga et al., 2008): (1) 155.3 ± 3.4 Ma at Chron M26r from basalts assigned as near the Oxfordian/Kimmeridgian boundary interval in ODP Site 765 (Ludden, 1992) and (2) 167.7 ± 1.4 Ma at Chron M42 from basalts assigned as approximately upper Bajocian or lower Bathonian in ODP Site 801 (Koppers et al., 2003; Tominaga et al., 2008). An assumption of a constant spreading rate is probably adequate to produce a good approximation of relative durations of normal- and reversed-polarity blocks in the models through the short time interval spanned by the Callovian stage. When combined with Oxfordian magnetostratigraphic studies (e.g., Ogg et al., 2010; Przybylsi et al., 2010a, 2010b), these biostratigraphic constraints and dates from ODP sites indicate that the Callovian interval should span the interval assigned as marine magnetic polarity reversal sequence from M37 to either M39 or M40. Calibration of this pre-M29 marine magnetic polarity reversal sequence also requires either distinctive "fingerprints" of extra-long polarity chrons/zones and/or a partial adjustment of the magnetostratigraphic sequences to overcome the distortions from a variable sediment accumulation rate and depositional sequences. Unfortunately,

unlike in the Oxfordian-Kimmeridgian, there are not yet detailed cycle-stratigraphic scaling to aid in this effort. However, the observation in those younger strata that many of the depositional sequences correspond to responses to the 405 kyr long-eccentricity-induced orbital-climate Milankovitch signal suggests that the third-order depositional sequences in the Callovian (Garcia, 1993; Jacquin et al., 1998) may provide a similar equal-interval estimate. Smaller parasequences within these third order cycles or variable transgressive versus regressive accumulation rates were not taken into account.

The initial correlation of the Callovian magnetostratigraphy with the marine magnetic polarity reversal record was based on generalized features of each pattern; and then followed with a partial correlation of individual polarity zones with the interpreted chrons of the both deep-tow and upward continued models. The initial correlation utilized the general features of the Callovian composite sequence plus its upward extension through the Oxfordian (Ogg et al., 2010; Przybylski et al., 2010a, 2010b) and its potential downward extension into the Bathonian and Bajocian (Steiner et al., 1987). This trend of the main features and polarity-bias shows that the normal-polarity-dominated Callovian is consistent with the interpreted dominance of normal polarity in Chrons M37 through the middle of Chron M39. Above and below this interval, the interpreted anomalies are dominated by reversed polarity (Chron/anomalies M33-M36, and older M39 through younger M42) that is consistent with the general reversed-polarity biases of the lower Oxfordian and of the lowermost Callovian through Bathonian (Figure 29).

This general match is followed by the more distinctive correlations of relatively longer polarity intervals (e.g., the relatively thickest reversed-polarity zone of upper Lower Callovian with the longest interpreted reversed-polarity anomaly at the young end of Chron M39), then to progressively finer-scale correlations.

The youngest reversed-to-normal-polarity change is tied to the reversal just above the Oxfordian-Callovian boundary that Ogg et al. (2010) had also correlated to the young end of Chron M37. This places the Oxfordian-Callovian boundary within the normal-polarity Chron M37n.1n. A very narrow reversed-polarity block near the top of the *Quenstedtoceras lamberti* Zone in both this study and in the section used by Ogg et al. (2010) is apparently not resolved in either deep-tow or mid-water magnetic polarity reversal model. The reversed-polarity dominance of the *Quenstedtoceras lamberti* Zone (Figures 27 and 29) corresponds to Chron M37r.

The triplet of narrow reversed-polarity blocks of M38n.1r through M38n.3r (upper half of M38) correspond to a dual or partial-resolved trio of reversed-polarity zones that comprise the *Peltoceras athleta* Zone and uppermost *Erymnoceras coronatum* Zone. As indicated earlier, the

relatively long/thick normal-polarity zone spanning the *Kosmoceras jason* through *Erymnoceras coronatum* zones corresponds to the widest normal-polarity sub-chron of mid-M38.

There is a considerable difference between the two methods of marine anomaly signal interpretation for the older part of Chron M38 and upper half of Chron M39 in the bottom deep-tow versus mid-depth projection versions. The magnetostratigraphy of the Lower Callovian suggests that the actual relative durations of normal- and reversed-polarity chrons would be a partial intermediate, such that the oldest portion of M38 is best modeled by the bottom deep-tow interpretation, whereas upper Chron M39 consists of the relatively long reversed-polarity in the mid-depth projection interpretation that is coeval with the relatively major reversed-polarity of the upper *Proplanulites koenigi* ammonite Zone.

The relatively frequent reversals observed in the lowermost Callovian and uppermost Bathonian with adjustment for minor sampling gaps resulting from sedimentation hiatuses fit the general pattern in the lower half of Chron M39 in either model. This suggests that the Callovian-Bathonian Boundary is tentatively within subchron M39n.5r.

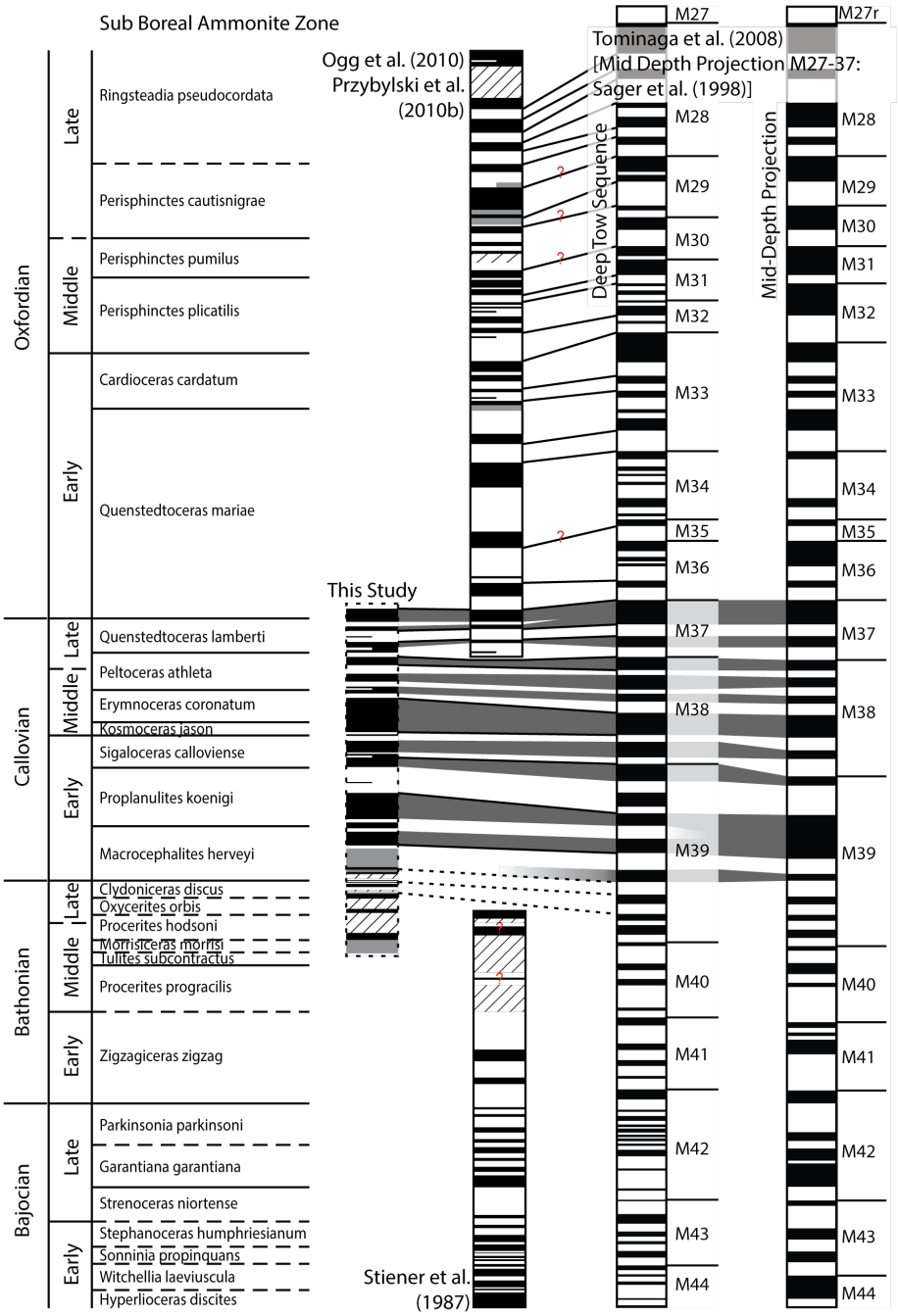

Figure 29: Our composite magnetostratigraphic sequence plotted next to the deep tow and mid depth Pre-M25 marine magnetic reversal sequence of Tominaga et al. (2008) with the mid-depth project anomalies M27-M37 filled in from Sager et al (1998).

The spacing of anomalies for the marine magnetic sequence is done assuming a constant spreading rate, consistent with the distance model of Tominaga et al. (2008). The placement against the ammonite biostratigraphy is congruent with the GTS2012 (Ogg, 2012). The composite magnetostratigraphic sequence of Ogg et al. (2010), Przybylski et al. (2010b) and Steiner et al. (1987) provide the surrounding magnetostratigraphic interpretations.

10 PALEOMAGNETIC POLES AND PALEOLATITUDE

The calculation of mean characteristic paleomagnetic direction, paleomagnetic pole and paleolatitude were calculated from the high-rated (R, N, RP and NP) samples in the normal, reversed and combined directions, each with their respective uncertainties, utilizing a method modified from Fisher (1953). Samples with less reliable orientations, rated as NP and RP, were half weighted compared to samples with R and N ratings. Samples falling outside two standard deviations from the calculated mean were omitted as outliers. The vector sum of the normal and reversed pole was calculated for comparison with the combined calculated pole orientation, providing a less distorted mean characteristic in the cases where the relative number of normal- and reversed-polarity samples differed significantly with a lingering residual overprint component. The intensities of each mean direction vector were obtained by calculating the logarithmic average of the characteristic direction intensities from the incorporated samples. The limitations resulting from the low sample size yielded by the majority of outcrops were overcome by treating the samples as regional datasets (table 3). Combining the high-rated samples from England and France respectively allowed for a statistical test on significance, the reversal test of McFadden and McElhinny (1990), to be conducted (table 4). This test requires more than five samples for each polarity in order to evaluate the critical angle (γ_c) between two Fisher mean directions at a defined confidence level (5% significance utilized in this study). When the observed angle between the normal vector and the antipode of the reversed vector (γ_o) is within the critical angle (γ_c) the hypothesis of a common mean cannot be rejected. When this is the case, further classification scheme is applied, designating 'A' when $\gamma_c \leq 5°$, 'B' if $5° < \gamma_c \leq 10°$, 'C' if $10 < \gamma_c \leq 20°$ and ‘indeterminate’ if $\gamma_c > 20°$ (McFadden & McElhinny, 1990). If the test fails, and γ_o falls outside of γ_c, the hypothesis of a shared mean between the two vectors is rejected at the 95% confidence level.

Table 3: Mean composite orientation and the array of poles from which they were calculated.

	Weighted least squares analysis							Mean virtual geomagnetic pole				
	Dec (°)	Inc (°)	Intensity (A/m)	α95 (°)	K	R	N	Lat (°N)	Long (°E)	δp (°)	δm (°)	Paleo Lat (°)
England Composite												
Normal	0.9	50.6	2.63E-02	6.1	13.5	41.3	44.5	69.3	176.6	5.5	8.2	31.34
Reversed	184.9	-37.8	3.08E-02	16.7	9.4	9.1	10	-59.0	349.9	11.6	19.7	-21.19
Combined	1.8	48.3	2.71E-02	5.8	12.2	50.1	54.5	67.3	174.8	5.0	7.6	29.32
V. Comb	3.3	43.7	2.83E-02	-	-	-	-	63.4	172	4.5	7.2	25.55
French Composite												
Normal	8.1	60.4	2.76E-02	2.4	40.1	84.4	86.5	81.6	138.8	2.8	3.7	41.32
Reversed	189.8	-46.1	4.19E-02	5.7	94.8	7.9	8	-68.5	-19.8	4.7	7.3	-27.47
Combined	8.3	59.2	2.86E-02	2.4	38.5	92.1	94.5	80.4	143.4	2.7	3.6	39.94
V. Comb	9.3	51.8	3.45E-02	-	-	-	-	73.4	156.4	2.2	3.2	32.41
Skye (Single Location)												
Normal	9.7	33.4	5.54E-02	26	7.6	5.3	6	50.0	159.4	16.9	29.7	18.25
Reversed	212.7	-35.8	7.03E-02	13	12	11.1	12	-45.3	-52.4	9.0	15.5	-19.8
Combined	25.1	35.5	6.49E-02	12	9.4	16.2	18	47.8	137.4	8.0	13.8	19.61
V. Comb	22.4	35.3	6.20E-02	-	-	-	-	48.5	141.0	8.0	13.8	19.46
Swabia (Single Location)												
Normal	4.6	64.6	8.78E-01	3.8	101.5	14.9	15	86.3	129.2	4.9	6.1	46.45
Reversed	182.7	-37.9	1.07E+00	48.0	12.2	2.4	2.5	-62.8	3.5	33.5	56.7	-21.29
Combined	4.2	61.0	9.03E-01	6.1	34.3	17.0	17.5	83.0	162.7	7.1	9.3	42.04
V. Comb	3.3	50.0	9.46E-01	-	-	-	-	72.2	179.8	5.4	8.1	30.75

England: Skye: France: Swabia:

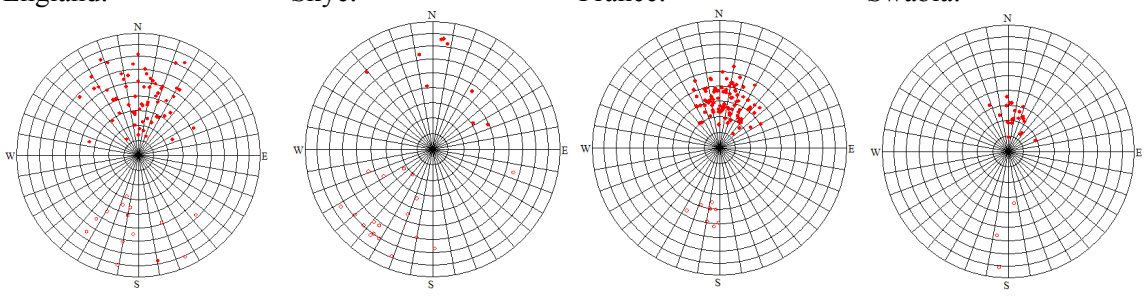

Table 4: Reversal test of McFadden and McElhinny (1990) applied to the four regions

	yo (°)	yc (°)	Test
England Composite	13.13	14.78	Pass "C"
Swabia Single Location	28.60	11.29	Fail
French Composite	14.29	8.11	Fail
Skye Single Location	19.00	24.78	Pass "INDETERMINATE"

The set of mean directions yielded by the English composite, the French composite and the Swabian outcrop, displayed in table 3 shows the mean orientation produced when considering stable orientations obtained during thermal demagnetization behaviors. The English region yielded a combined VGP of 67.3°N, 174.8°E (α95: 5.8°) and passed the reversal test of McFadden and McElhinny (1990) with a $\gamma_o/\ \gamma_c$ ratio of 13.1°/14.8° and a 'C' classification. The French region provided a combined VGP of 80.4°N, 143.4°E (α95: 2.38°) but it failed the reversal test with a $\gamma_o/\ \gamma_c$ ratio of 14.3°/8.1°. The Skye virtual geomagnetic pole worked out to be located at 47.7°N, 137.4°E passing the McFadden and McElhinny (1990) reversal test ($\gamma_o/\ \gamma_c$ of 19.0°/24.8°) but was classified as 'indeterminate' due to a critical angle greater than 20 degrees. The Swabian VGP is located at 5.47°N, 63.21°E (α95: 5.67°) and also failed the McFadden and McElhinny (1990) reversal test with a $\gamma_o/\ \gamma_c$ ratio of 28.6°/13.5°. This failure of the reversal test may indicate a partial or complete overprint component in some samples that was not adequately removed during thermal demagnetization, partially biasing the paleomagnetic pole orientation.

The combined pole orientations for these three outcrops ranged in latitude and longitude from the 48°N to 82°N and from 137°E to 175°E, respectively. The angle between the combined French and Swabian pole passes the common mean test of McFadden and McElhinny (1990) (γ_o/γ_c of 2.57°/5.75°) with a 'B' classification. The English pole on the other hand demonstrates a γ_o of 11.4° and 11.5° with the Swabian and French vectors, respectively. These angles cause the failure of the test and indicate that the difference between these samples is not due to sampling error, but rather is likely the result of a partial bias by an overprinted component. All observed angles produced between the composite vector for the outcrop in Scotland and the composite vectors from England, France and Swabia exceeded the critical angle (21.5°/12.0°, 28.0°/12.6° and 26.1°/7.5° respectively for γ_o/γ_c).

The examination of the angle between the normally oriented vectors shows an observed angle of 16.1° between the English composite orientation and the Swabian outcrop orientation, 10.6° between the English and French composite orientations and 6.1° between the French composite orientation and the Swabian outcrop orientation. All of these are larger than their respective critical angle and a 95% confidence level (9.4°, 5.5° and 5.4° respectively), causing them to fail the common mean test. The normally oriented vector from the outcrop in Scotland only passed the common mean test of McFadden and McElhinny (1990) when compared with the pole from England (18.4°/18.6° for γ_o/γ_c), earning it a 'C' classification. The reverse oriented pole from the Isle of Skye outcrop didn't pass any reversal test with any of the outcrops from the other three locations. The comparison of the reversed vectors between the other three outcrops all pass

the common mean test of McFadden and McElhinny (1990) with an angle of 6.7° between the mean pole orientations from the English composite and Swabian outcrop (γ_c=25.2°), 9.1° between the mean pole orientations of the French and English composites (γ_c=18.2°) and 15.1° between the Swabian outcrop mean pole orientation and that from the French composite (γ_c=15.4°). The consistency of the reversed-oriented poles from the three different regions suggests that the secondary overprint bias is affecting measurements in the normal direction more.

Tentative paleolatitude analysis places the English study region at 29°N, the French study region at 40.1°N, the outcrop on the Isle of Skye at 19.1°N and the Swabian outcrop at 40°N. These measurements indicate that the paleolatitudes are located further south from their modern location by 19°, 11°, 38° and 4° respectively. Because the normal-polarity orientations for England, France and Swabia are likely biasing these measurements closer to the modern latitude, the measured shift in paleolatitude between the Callovian and now for these sections should be considered a low-end estimate.

11 CONCLUSIONS

Magnetostratigraphic results compiled from outcrops in Scotland, France, Germany and England produced a nearly continuous, high-resolution, polarity pattern for the Callovian (upper Middle Jurassic). Significance tests indicate the need for caution when examining paleomagnetic pole orientations with probable overprint of a secondary magnetization or declination shallowing. The paleopoles calculated for the Callovian from the four study regions vary by up to 28°, including pole orientations of 48°N, 137°E (Skye), 80.4°N, 137.4°E (French Composite), 81.8°N, 171.1°E (Swabia) and 67.3°N, 174.8°E (English Composite).

The correlation of the established composite pattern with the marine magnetic anomaly patter further confirms the presence of the Jurassic 'low amplitude zone' with a succession of numerous short-duration polarity zones rather than a Jurassic Quiet Zone. The dominant polarity trend and the observed reversal frequencies of the composite sequence matches the main polarity features of the marine magnetic anomaly sequence described by the provisional correlation presented. This correlation places the Oxfordian-Callovian boundary within Chron M37n.1n and the Callovian-Bathonian correlation tentatively placed in Chron M39n.5r.

This composite polarity pattern enables the association of ammonite subzones with the marine magnetic anomalies M37 through M39 and improves the detail within this portion of the polarity model. The tentative spacing of the ammonite zone and subzones based on a constant spreading rate of the marine magnetic anomaly model of Tominaga et al (2008) and the five Callovian cycles of Hardenbol et al (1998) hold up to further testing within this study.

LIST OF REFERENCES

LIST OF REFERENCES

Allen, J. R. L., & Kaye, P. (1973). Sedimentary facies of the Forest Marble (Bathonian), Shipton-on-Cherwell Quarry, Oxfordshire. *Geological Magazine, 110*(2), 153-163.

Anderson, F. W., & Dunham, K. C. (1966). *The Geology of Northern Skye*: *Memoir of the Geological Survey of the United Kingdom.* London: Her Majesty's Stationery Office.

Anderson, T. F., Popp, B. N., Williams, A. C., Ho, L. Z., & Hudson, J. D. (1994). The stable isotopic records of fossils from the Peterborough Member, Oxford Clay Formation (Jurassic), UK: palaeoenvironmental implications. *Journal of the Geological Society*, *151*(1), 125-138. doi: 10.1144/gsjgs.151.1.0125

Arkell, W. J. (1931). The upper Great Oolite, Bradford Beds and Forest Marble of south Oxfordshire, and the succession of gastropod faunas in the Great Oolite. *Quarterly Journal of the Geological Society*, *87*(1-4), 563-629.

Arkell, W. J. (1956). *Jurassic Geology of the World*. (pp. 806) Edinburgh: Oliver & Boyd.

Barron, A., Lott, G., & Riding, J. (2012). *Stratigraphical framework for the Middle Jurassic strata of Great Britain and the adjoining continental shelf* (Geology and Landscape Programme: Research Report RR/11/06). Keyworth, Nottingham: British Geological Survey.

Barton, P. & Wood, R. (1984). Tectonic evolution of the North Sea basin: crustal stretching and subsidence. *Geophysical Journal of the Royal Astronomical Society, 79*(3), 987–1022. doi:10.1111/j.1365-246X.1984.tb02880.x

Beccaletto, L., Hanot, F., Serrano, O., & Marc, S. (2011). Overview of the subsurface structural pattern of the Paris Basin (France): Insights from the reprocessing and interpretation of regional seismic lines. *Marine and Petroleum Geology*, *28*(4), 861–879. doi:10.1016/j.marpetgeo.2010.11.006Beher, E., Brand, E., & Franz, M. (2010). Bathonian and Lower Callovian ostracods of Albstadt-Pfeffingen (Middle Jurassic, Baden-Württemberg , Germany). *Palaeodiversity*, *3*, 43–57.

Belkaaloul, N. K., & Aïssaoui, D. M. (1997). Nature and origin of magnetic minerals within the Middle Jurassic shallow-water carbonate rocks of the Paris Basin, France: implications for magnetostratigraphic dating. *Geophysical Journal International*, *130*(2), 411–421. doi:10.1111/j.1365-246X.1997.tb05657.x

Belkaaloul, K. N., Aïssaoui, D. M., Rebelle, M., & Sambet, G. (1995). Magnetostratigraphic correlations of the Jurassic carbonates from the Paris Basin: implications for petroleum exploration. *Geological Society, London, Special Publications*, *98*(1), 173–186. doi:10.1144/GSL.SP.1995.098.01.10

Belkaaloul, K. N., Aïssaoui, D. M., Rebelle, M., & Sambet, G. (1997). Resolving sedimentological uncertainties using magnetostratigraphic correlation: An example from the Middle Jurassic of Burgundy, France. *Journal of Sedimentary Research*, *67*(4), 676–685. doi:10.1306/D4268612-2B26-11D7-8648000102C1865D

Bonnot, A., Marchand, D., & Garcia, J. P. (1992). Le contact Dogger-Malm en Côte d'Or (France)–II. La coupe type de Saulx-le-Duc–Interprétation biostratigraphique. *Bulletin Scientifique de Bourgogne*, *45*, 53-65.

Bradshaw, M. J., Cope, J. C. W., Cripps, D. W., Donovan, D. T., Howarth, M. K., Rawson, P. F., … Wimbledon, W. A. (1992). Jurassic. *In* J. C. W. Cope, J. K. Ingham & P. F. Rawson (Eds.) *Atlas of Palaeogeography and Lithofacies: Geological Society Memoir #13* (pp. 107-129) Bath, UK: The Geological Society Publishing House. doi:10.1144/GSL.MEM.1992.013.01.12

Brigaud, B., Durlet, C., Deconinck, J.-F., Vincent, B., Pucéat, E., Thierry, J., & Trouiller, A. (2009). Facies and climate/environmental changes recorded on a carbonate ramp: A sedimentological and geochemical approach on Middle Jurassic carbonates (Paris Basin, France). *Sedimentary Geology*, *222*(3-4), 181–206. doi:10.1016/j.sedgeo.2009.09.005

Brunet, M.-F., & Le Pichon, X. (1982). Subsidence of the Paris Basin. *Journal of Geophysical Research*, *87*(B10), 8547 -8560. doi:10.1029/JB087iB10p08547

Callomon, J. (1955). The Ammonite Succession in the Lower Oxford Clay and Kellaways Beds at Kidlington, Oxfordshire, and the Zones of the Callovian Stage. *Philosophical Transactions of the Royal Society of the Royal Society of London. Series B, Biological*, *239*(664), 215–264.

Callomon, J.H. & Dietl, G. (2000) On the proposed Basal Boundary Stratotype (GSSP) of the Middle Jurassic Callovian Stage. *In* R. L. Hall & P. L. Smith (Eds.). Advances in Jurassic Research 2000. Proceedings of the 5th International Symposium on the Jurassic System: *GeoResearch Forum, 6* (41-54) Totton, Hampshire: Trans Tech Publications Ltd.

Cande, S. C., & Kent, D. V. (1992a). A New Geomagnetic Polarity Time Scale for the Late Cretaceous and Cenozoic. *Journal of Geophysical Research*, *97*(B10), 13917–13951. doi:10.1029/92JB01202

Cande, S. C., & Kent, D. V. (1992b). Ultrahigh Resolution Marine Magnetic Anomaly Profiles: A Record of Continuous Paleointensity Variations? *Journal of geophysical research*, *97*(B11), 15075–15083.

Cande, S. C., & Kent, D. V. (1995). Revised calibration of the geomagnetic polarity timescale for the Late. *Journal of Geophysical Research*, *100*(B4), 6093–6095.

Cave, R., & Cox, B. M. (1975). The Kellaways Beds of the are between Chippenham and Malmesbury, Wiltshire. In *Bulletin of the Geological Survey of Great Britain, No.54* (pp. 41–46). London: Her Majesty's Stationery Office.

Channell, J. E. T., T.J., B., & Grandesso, P. (1987). Biostratigraphic correlation of Mesozoic polarity chrons CM1 to CM23 at Capriolo and Xausa (Southern Alps, Italy). *Earth and Planetary Science Letters*, *85*(1-3), 203–221. doi:10.1016/0012-821X(87)90032-X

Chidlaw, N. & Campbell, M. J. A. (1988). Sedimentation patterns in the Cornbrash Limestone Formation of the Cotswold Hills. *Proceedings of the Geologists' Association*, *99*(1), 27–42. doi:10.1016/S0016-7878(88)80025-7

Coe, A. L., & Weedon, G. P. (2006). Jurassic cyclostratigraphy: recent advances, implications and problems. *Volumina Jurassica*, *4*(4), 156–157.

Collin, P.-Y. (1997). *Paléoenvironnements des series condensées: contrôle de la repartition et de la preservation des depots sur la plate-forme bourguignonne au Callovo-Oxfordien* (Doctoral dissertation). Centre des Sciences da la Terre, University of Burgundy.

Collin, P.-Y., & Courville, P. (2006). Sedimentation and palaeogeography of the eastern part of the Paris Basin (France) at the Middle–Upper Jurassic boundary. *Comptes Rendus Geoscience*, *338*(12-13), 824–833. doi:10.1016/j.crte.2006.07.011

Cope, J. C. W. (2006). Jurassic: The returning seas *In* Brenchley, P. J. & Rawson, P. F. (Eds.), *The Geology of England and Wales*. The Geological Society, London, 325-363.

Cox, A., Doell, R. R., & Dalrymple, G. B. (1963). Geomagnetic polarity epochs and Pleistocene geochronometry. *Nature*, *198*(4885), 1049-1051. doi: 10.1038/1981049a0

Cox, B. M. (2002). General introduction to the Aalenian to Callovian stratigraphy of Great Britain. *In* B. M. Cox & M. G. Sumbler (Eds.) *British Middle Jurassic Stratigraphy: Geological Conservation Review Series, #26*. (pp. 1-11) Peterborough: Joint Nature Conservation Committee.

Cox, B. M., Hudson, J. D., & Martill, D. M. (1992). Lithostratigraphic nomenclature of the Oxford Clay (Jurassic). *Proceedings of the Geologists' Association*, *103*(4), 343–345. doi:10.1016/S0016-7878(08)80130-7

Cox, B. M. & Page, K. N. (2002). The Middle Jurassic stratigraphy of Wessex. *In* B. M. Cox & M. G. Sumbler (Eds.) *British Middle Jurassic Stratigraphy: Geological Conservation Review Series, #26*. (pp. 13-111) Peterborough: Joint Nature Conservation Committee.

Cox, B. M., Page, K. N. & Morton, N. (2002a). The Middle Jurassic stratigraphy of Scotland. *In* B. M. Cox & M. G. Sumbler (Eds.) *British Middle Jurassic Stratigraphy: Geological Conservation Review Series, #26*. (pp. 365-426) Peterborough: Joint Nature Conservation Committee.

Cox, B. M., Sumbler, M. G., Wyatt, R. J. & Page, K. N (2002b). The Middle Jurassic stratigraphy of the East Midlands. *In* B. M. Cox & M. G. Sumbler (Eds.) *British Middle Jurassic Stratigraphy: Geological Conservation Review Series, #26*. (pp. 229-312) Peterborough: Joint Nature Conservation Committee.

Delance, J. H., Garcia, J.-P., & Laurin, B. (1993). Succession et remplacements de communautés à brachiopodes en régime de sédimentation discontinue (Jurassique Moyen, Bourgogne, France). *Palaeogeography, palaeoclimatology, palaeoecology, 100*(1), 169-182.

Dietl, G. (1994). Der hochstetteri-Horizont - ein Ammonitenfaunen-Horizont (Discus-Zone, Ober-Bathonium, Dogger) aus dem Schwäbischen Jura. *Stuttgarter Beiträge zur Naturkunde - Serie B (Geologie und Paläontologie)*, *202*, 1–39.

Douglas, J. A., & Arkell, W. J. (1928). The stratigraphical distribution of the Cornbrash: I. The south-western area. *Quarterly Journal of the Geological Society, 84*(1-4), 117-NP.

Douglas, J. A., & Arkell, W. J. (1932). The stratigraphical distribution of the Cornbrash: II. The north-eastern area. *Quarterly Journal of the Geological Society, 88*(1-4), 112-170.

Douglas, J. A., & Arkell, W. J. (1935). On a New Section of Fossiliferous Upper Cornbrash of North-Eastern Facies at Enslow Bridge, near Oxford. *Quarterly Journal of the Geological Society, 91*(1-4), 318-322.

Dromart, G., Garcia, J.-P., Gaumet, F., Picard, S., Rousseau, M., Atrops, F., … Sheppard, S. M. F. (2003). Perturbation of the Carbon Cycle at the Middle/Late Jurassic Transition: geological and geochemical evidence. *American Journal of Science*, *303*(October), 667–707.

Duff, K. L. (1980). Callovian correlation chart. *In* Cope, J. C. W. *A Correlation of Jurassic rocks in the British Isles: part two: Middle and Upper Jurassic*. Geological Society of London Special Report #15. (pp. 45–60) London: Blackwell Scientific Publications.

Fisher, R. (1953). Dispersion on a sphere. *Proceedings of the Royal Society A Mathematical Physical and Engineering Sciences*, *217*(1130), 295–305. doi:10.1098/rspa.1953.0064

Fortwengler, D., & Marchand, D. (1994a). Nouvelles unités biochronologiques de la zone à Mariae (Oxfordien inférieur). *Geobios*, *27*, 203-209.

Fortwengler, D., & Marchand, D. (1994b). The Callovian-Oxfordian Boundary in the Basin of South of France. *In*: Atrops, F. (Ed.) *4th Oxfordian and Kimmeridgian Working Groups Meeting: Field guide book and Abstracts.* (pp. 24-26) Lyon, France.

Fortwengler, D., & Marchand, D. (1994c). The Savournon section: Upper Callovian (Lamberti zone) to Lower Oxfordian (Mariae zone) under "Terres Noires" facies. *In*: Atrops, F. (Ed.) *4th Oxfordian and Kimmeridgian Working Groups Meeting: Field guide book and Abstracts.* (pp. 95-99) Lyon, France.

Fortwengler, D., & Marchand, D. (1994d). The Thuoux section: Callovian-Oxfordian boundary (Lamberti to Mariae zone) under "Terres Noires" facies. *In*: Atrops, F. (Ed.) *4th Oxfordian and Kimmeridgian Working Groups Meeting: Field guide book and Abstracts.* (pp. 103-106) Lyon, France.

Fortwengler, D., Marchand, D., & Bonnot, A. (1997). Les coupes de Thuoux et de Savournon (SE de la France) et la limite Callovien-Oxfordien. *Geobios*,*30*(4), 519-540.

Fortwengler, D., Marchand, D., Bonnot, A., Jardat, R., & Raynaud, D. (2012). Proposal for the Thuoux section as a candidate for the GSSP of the base of the Oxfordian stage. *Carnets de Geologie [Notebooks on Geology] 2012/06*(CG2012_A06), 117-136.

Franz, M., & Knott, S. D. (2012). Foraminifera from the Callovian GSSP candidate section of AlbstadtPfeffingen (Middle Jurassic, Southern Germany). *Neues Jahrbuch für Geologie und Paläontologie - Abhandlungen*, *264*(3), 263–282. doi:10.1127/0077-7749/2012/0240

Garcia, J.-P. (1993). *Les variations du niveau marin sur le bassin de Paris au bathonien-callovien. Impacts sur les communautés benthiques et sur l'évolution des ornithellidés (Terebratellidina)*. (Doctoral dissertation). Mémoires Géologique de Universite of Dijon.

Garcia, J.-P., & Dromart, G. (1997). The validity of two biostratigraphic approaches in sequence stratigraphic correlations: brachiopod zones and marker-beds in the Jurassic. *Sedimentary Geology*, *114*(1-4), 55–79. doi:10.1016/S0037-0738(97)00072-9

Garcia, J.-P., Laurin, B., & Sambet, G. (1996). Les associations de brachiopodes du Jurassique moyen du bassin de Paris; une echelle biochronologique ponctuee de niveaux-reperes pour la contrainte des correlations sequentielles a haute resolution. *Bulletin de la Société géologique de France*, *167*(3), 435-451.

Gaumet, T., Garcia, J.-P., Dromart, G. and Sambet G. (1996). Faciès, géométrie et profils de dépôt de la bordure de la plate-forme bourguignonne au Bathonien–Callovien. *Bulletin de la Societe Geologique de France, 167*(3), 409-421.

Golonka, J., & Ford, D. (2000). Pangean (Late Carboniferous–Middle Jurassic) paleoenvironment and lithofacies. *Palaeogeography, Palaeoclimatology, Palaeoecology*, *161*(1-2), 1–34. doi:10.1016/S0031-0182(00)00115-2

Gradstein, F. M., Ogg, J. G., & Smith, A. G. (Eds.). (2004). *A Geologic Time Scale 2004*. New York: Cambridge University Press.

Graham, J. W. (1949). The stability and significance of magnetism in sedimentary rocks. *Journal of Geophysical Research*, *54*(2), 131-167.

Guillocheau, F., Robin, C., Allemand, P., Bourquin, S., Brault, N., Dromart, G., … Grandjean, G. (2000). Meso-Cenozoic geodynamic evolution of the Paris Basin: 3D stratigraphic constraints. *Geodinamica Acta*, *13*(4), 189-245.

Guzhikov, A. Y., Pimenov, M. V., Malenkina, S. Y., Manikin, a. G., & Astarkin, S. V. (2010). Paleomagnetic, petromagnetic, and terrigenous—Mineralogical studies of Upper Bathonian—Lower Callovian sediments in the Prosek section, Nizhni Novgorod region. *Stratigraphy and Geological Correlation*, *18*(1), 42–62. doi:10.1134/S0869593810010041

Hallam, A. (1978). Eustatic cycles in the Jurassic. *Palaeogeography, Palaeoclimatology, Palaeoecology*, *23*, 1–32. doi:10.1016/0031-0182(78)90079-2

Hallam, A. (2001). A review of the broad pattern of Jurassic sea-level changes and their possible causes in the light of current knowledge. *Palaeogeography, Palaeoclimatology, Palaeoecology*, *167*(1-2), 23–37. doi:10.1016/S0031-0182(00)00229-7

Hardenbol, J., Thierry, J., Farley, M. B., Jacquin, T., de Graciansky, P.-C., Vail, P. R., (1998). Jurassic Sequence Chronostratigraphy: Mesozoic and Cenozoic sequence chronostratigraphic framework of European basins. *In* P.-C. de Graciansky, J. Hardenbol, T. Jacquin, P. R. Vail, (Eds.), *Mesozoic-Cenozoic Sequence Stratigraphy of European Basins. SEPM Special Publication 60*. (Chart 6) Tulsa, OK: Society for Sedimentary Geology.

Harris, J. P., & Hudson, J. D. (1980). Lithostratigraphy of the Great Estuarine Group (Middle Jurassic), Inner Hebrides. *Scottish Journal of Geology*, *16*(2-3), 231-250. doi: 10.1144/sjg16020231

Heirtzler, J. R., Dickson, G. O., Herron, E. M., Pitman, W. C., & Le Pichon, X. (1968). Marine Magnetic Anomalies, Geomagnetic Field Reversals, and Motions of the Ocean Floor and Continents. *Journal of Geophysical Research*, *73*(6), 2119–2136. doi:10.1029/JB073i006p02119

Hesselbo, S. P. (2008). Sequence stratigraphy and inferred relative sea-level change from the onshore British Jurassic. *Proceedings of the Geologists' Association*, *119*(1), 19–34. doi:10.1016/S0016-7878(59)80069-9

Hollingworth, N. T. J., & Wignall, P. B. (1992). The Callovian-Oxfordian boundary in Oxfordshire and Wiltshire based on two new temporary sections. *Proceedings of the Geologists' Association*, *103*(1), 15–30. doi:10.1016/S0016-7878(08)80195-2

Hudson, J. D. (1963a). The recognition of salinity-controlled mollusc assemblages in the Great Estuarine Series (Middle Jurassic) of the Inner Hebrides. *Palaeontology*, *6*(2), 318-326.

Hudson, J. D. (1963). The ecology and stratigraphical distribution of the invertebrate fauna of the Great Estuarine Series. *Palaeontology*, *6*(2), 327-348.

Hudson, J. D., Clements, R. G., Riding, J. B., Wakefield, M. I. & Walton, W. (1995). Jurassic Paleosalinities and Brackish-Water Communities: A Case Study. *PALAIOS*, *10*(5), 392-407.

Hudson, J. D., & Martill, D. M. (1994). The Peterborough Member (Callovian, Middle Jurassic) of the Oxford Clay Formation at Peterborough, UK. *Journal of the Geological Society, London*, *151*(1), 113–124. doi:10.1144/gsjgs.151.1.0113

Jacquin, T., Dardeau, G., Durlet, C., Graciansky, P.-C. & Hantzpergue, P. (1998). The North Sea Cycle: an overview of 2nd-order transgressive/regressive facies cycles in Western Europe. *In* P.-C. de Graciansky, J. Hardenbol, T. Jacquin, & P. R. Vail (Eds.), *Mesozoic and Cenozoic Sequence Stratigraphy of European Basins, SEPM Special Publication #60* (pp. 445–466). Tulsa, OK: Society for Sedimentary Geology.

Jacquin, T. & Graciansky, P.-C. (1998a). Major transgressive/regressive cycles: the stratigraphic signature of European basin. *In* P.-C. de Graciansky, J. Hardenbol, T. Jacquin, & P. R. Vail (Eds.), *Mesozoic and Cenozoic Sequence Stratigraphy of European Basins, SEPM Special Publication #60* (pp. 15-30). Tulsa, OK: Society for Sedimentary Geology.

Jacquin, T. & Graciansky, P.-C. (1998b). Transgressive/regressive (second order) facies cycles: the effect of tectono-eustasy. *In* P.-C. de Graciansky, J. Hardenbol, T. Jacquin, & P. R. Vail (Eds.), *Mesozoic and Cenozoic Sequence Stratigraphy of European Basins, SEPM Special Publication #60* (pp. 31-42). Society for Sedimentary Geology: Tulsa, OK.

Kenig, F., Hayes, J. M., Popp, B. N., & Summons, R. E. (1994). Isotopic biogeochemistry of the Oxford Clay Formation (Jurassic), UK. *Journal of the Geological Society*, *151*(1), 139–152. doi:10.1144/gsjgs.151.1.0139

Kirschvink, J. L. (1980). The least-squares line and plane and the analysis of palaeomagnetic data. *Geophysical Journal International*, *62*(3), 699–718. doi:10.1111/j.1365-246X.1980.tb02601.x

Klein, G. de V. (1965). Dynamic significance of primary structures in the Middle Jurassic Great Oolite Series, Southern England. *In* G. V. Middleton (Ed) *Primary Sedimentary Structures and Their Hydrodynamic Interpretation: Special Publication #12* (pp. 173-191) Tulsa, OK: Society of Economic Paleontologists and Mineralogists. doi:10.2110/pec.65.08.0173

Koppers, A. a. P., Staudigel, H., & Duncan, R. (2003). High-resolution 40 Ar/ 39 Ar dating of the oldest oceanic basement basalts in the western Pacific basin. *Geochemistry Geophysics Geosystems*, *4*(11). doi:10.1029/2003GC000574

LaBrecque, J., Kent, D. V, & Cande, S. C. (1977). Revised magnetic polarity time scale for the Late Cretaceous and Cenozoic time. *Geology*, *5*(6), 330–335. doi:10.1130/0091-7613(1977)5<330:rmptsf>2.0.co;2

Larson, R. L., & Hilde, T. W. C. (1975). A Revised Time Scale of Magnetic Reversals for the Early Cretaceous and Late Jurassic. *Journal of Geophysical Research*, *80*(17), 2586–2594. doi:10.1029/JB080i017p02586

Lowrie, W. (1990). Identification of Ferromagnetic Minerals in a Rock by Coercivity and Unblocking Temperature Properties. *Geophysical Research Letters*, *17*(2), 159–162. doi:10.1029/GL017i002p00159/full

Lowrie, W., & Heller, F. (1982). Magnetic Properties of Marine Limestones. *Reviews of Geophysics and Space Physics*, *20*(2), 171–192.

Ludden, J.N., 1992. Radiometric age determinations for basement from Sites 765 and 766, Argo Abyssal Plain and northwestern Australian margin. *In* Gradstein, F.M., Ludden, J.N., et al., *Proceedings of the Ocean Drilling Program, Scientific Results, 123* (pp. 557-559) College Station, TX: Ocean Drilling Program. doi:10.2973/odp.proc.sr.123.162.1992

Macquaker, J. H. S. (1994). A lithofacies study of the Peterborough Member, Oxford Clay Formation (Jurassic), UK: an example of sediment bypass in a mudstone succession. *Journal of the Geological Society*, *151*(1), 161–172. doi:10.1144/gsjgs.151.1.0161

Marchand, D., & Thierry, J. (1997). Enregistrement des variations morphologiques et de la composition des peuplements d'ammonites durant le cycle regressif/transgressif de 2e ordre Bathonien inferieur-Oxfordien inferieur en Europe occidentale. *Bulletin de la Société géologique de France*, *168*(2), 121-132.

McElhinny, M. W., & McFadden, P. L. (2000). *Paleomagnetism: continents and oceans*: *Vol 73. International Geophysical Series.* San Diego, CA: Academic Press.

McFadden, P. L., & McElhinny, M. W. (1990). Classification of the reversal test in palaeomagnetism. *Geophysical Journal International*, *103*(3), 725–729. doi:10.1111/j.1365-246X.1990.tb05683.x

Meléndez, G. (2006). Report of the Oxfordian Working Group. *International Subcommission on Jurassic Stratigraphy, Newsletter*, *33*. 16-19.

Meléndez, G. (2007). Report of the Oxfordian Working Group. *International Subcommission on Jurassic Stratigraphy, Newsletter*, *34*(2), 17.

Mönnig, E. (2012). Report of the Callovian Working Group. *Volumina Jurassica*,*10*(10), 109-112.

Morton, N., & Hudson, J. D. (1995). Field guide to the Jurassic of the Isles of Raasay and Skye, Inner Hebrides, NW Scotland. *Field geology of the British Jurassic*, *209*, 280.

Norris, M. S., & Hallam, A. (1995). Facies variations across the Middle-Upper Jurassic boundary in Western Europe and the relationship to sea-level changes. *Palaeogeography, Palaeoclimatology, Palaeoecology*, *116*(3-4), 189–245. doi:10.1016/0031-0182(94)00096-Q

Norry, M. J., Dunham, A. C., & Hudson, J. D. (1994). Mineralogy and geochemistry of the Peterborough Member , Oxford Clay Formation , Jurassic , UK: element fractionation during mudrock sedimentation. *Journal of the Geological Society, London*, *151*(1), 195–207.

Ogg, J. G. (1988). Early Cretaceous and Tithonian Magnetostratigraphy of the Glacia Margin (Ocean Drilling Program Let 103). *Early Cretaceous and Tithonian magnetostratigraphy of the Galicia Margin (Ocean Drilling Program Leg 103)*, *103*, 659–682.

Ogg, J. G. (2012). Geomagnetic Polarity Time Scale. *In* Gradstein, F. M., Ogg, J. G., Schmitz, M. & Ogg, G. (Eds.). *The Geologic Time Scale 2012* (pp. 85-113) Oxford, UK: Elsevier.

Ogg, J. G. & Hinnov, L. (2012). Jurassic. *In* Gradstein, F. M., Ogg, J. G., Schmitz, M. & Ogg, G. (Eds.). *The Geologic Time Scale 2012* (pp. 731-792) Oxford, UK: Elsevier.

Ogg, J. G., Steiner, M. B., Oloriz, F., & Tavera, J. M. (1984). Jurassic magnetostratigraphy, 1. Kimmeridgian-Tithonian of Sierra Gorda and Carcabuey, southern Spain. *Earth and Planetary Science Letters*, *71*(1), 147-162. doi:10.1016/0012-821X(84)90061-X

Ogg, J. G., Steiner, M. B., Wieczorek, J., & Hoffmann, M. (1991). Jurassic magnetostratigraphy, 4. Early Callovian through Middle Oxfordian of the Krakow Uplands (Poland). *Earth and Planetary Science Letters*, *104*(2-4), 488–504. doi:10.1016/0012-821X(91)90224-6

Ogg, J. G., Coe, A. L., Przybylski, P. A., & Wright, J. K. (2010). Oxfordian magnetostratigraphy of Britain and its correlation to Tethyan regions and Pacific marine magnetic anomalies. *Earth and Planetary Science Letters*, *289*(3-4), 433–448. doi:10.1016/j.epsl.2009.11.031

Opdyke, N. D., Glass, B., Hays, J. D., & Foster, J. (1966). Paleomagnetic study of Antarctic deep-sea cores. *Science*, *154*(3747), 349-357.

O'Reilly, W. (1984). *Rock and Mineral Magnetism*. Glasgow: Blackie.

Page, K. N. (1989). A stratigraphical revision for the English Lower Callovian. *Proceedings of the Geologists' Association*, *100*(3), 363–382. doi:10.1016/S0016-7878(89)80055-0

Page, K. N. (2002). Peterborough Brickpits, Cambridgeshire (TL 165 940, TF 210 025, TF 248 978) *In* B.M. Cox & M.G. Sumbler (Eds.) *British Middle Jurassic Stratigraphy* (pp. 266-273) Peterborough, UK: Joint Nature Conservation Committee.

Page, K. N. (2004). Callovian-Oxfordian boundary in Britain: A review of key sections and their correlation with the proposed Global Stratotype Section and Point for the Oxfordian. *Rivista Italiana di Paleontologia e Stratigrafia*, *110*(1), 201–208.

Palmer, T. J. (1979). The Hampen Marly and White Limestone formations: Florida-type carbonate lagoons in the Jurassic of central England.*Palaeontology*, *22*(1), 189-228.

Partington, M. A., Copestake, P., Mitchener, B. C., & Underhill, J. R. (1993). Biostratigraphic calibration of genetic stratigraphic sequences in the Jurassic–lowermost Cretaceous (Hettangian to Ryazanian) of the North Sea and adjacent areas. *In* J. R. Parker (Ed.) *Petroleum Geology of Northwest Europe: Proceedings of the 4th Conference* (pp. 371-386) Bath, UK: The Geological Society Publishing House. doi:10.1144/0040371

Perrodon, A. & Zabek, J. (1990) Chapter 32: Paris Basin. *In* M. W. Leighton, D. R. Kolata, D. F. Oltz & J. J. Eidel (Eds.), *Interior Cratonic Basins: AAPG Memoir 51* (pp. 633-679) Tulsa, OK: The American Association of Petroleum Geologists

Pieńkowski, G., Schudack, M. E., Bosák, P., Enay, R., Feldman-Olszewska, A., Golonka, J., … Wong, T. E. (2008). Jurassic *In* McCann, T (Ed.), *The Geology of Central Europe, Volume 2: Mesozoic and Cenozoic* (pp. 823-922) Bath, UK: Geological Society of London.

Pringle, M.S., and Duncan, R.A., 1995. Radiometric ages of basement lavas recovered at Loen, Wodejebato, MIT, and Takuyo-Daisan Guyots, northwestern Pacific Ocean. *In* Haggerty, J.A., Premoli Silva, I., Rack, F., and McNutt, M.K. (Eds.), *Proceedings of the Ocean Drilling Program, Scientific Results*, *144* (pp. 547-557) College Station, TX: Ocean Drilling Program. doi:10.2973/odp.proc.sr.144.033.1995

Pomerol, C. (1978). Evolution paléogéographique et structurale du Bassin de Paris, du Précambrien à l'actuel, en relation avec les régions avoisinantes. *Geologie en Mijnbouw*, *57*(4), 533-543.

Przybylski, P. A., Ogg, J. G., Wierzbowski, A., Coe, A. L., Hounslow, M. W., Wright, J. K., … Settles, E. (2010a). Magnetostratigraphic correlation of the Oxfordian–Kimmeridgian boundary. *Earth and Planetary Science Letters*, *289*(1-2), 256–272. doi:10.1016/j.epsl.2009.11.014

Przybylski, P. A., Glowniak, E., Ogg, J. G., Ziólkowski, P., Sidorczuk, M., Gutowski, J., & Lewandowski, M. (2010b). Oxfordian magnetostratigraphy of Poland and its correlation to Sub-Mediterranean ammonite zones and marine magnetic anomalies. *Earth and Planetary Science Letters*, *289*(3-4), 417–432. doi:10.1016/j.epsl.2009.11.030

Richardson, L., Arkell, W. J., Dines, H. G., & Morison, C. G. T. (1946). *Geology of the Country Around Witney: Memoir of the Geological Survey of the United Kingdom*. London: Her Majesty's Stationery Office.

Riding, J. B. (1992) On the age of the upper Ostrea Member, Staffin Bay Formation (Middle Jurassic) of North-west Skye. *Scottish Journal of Geology, 28*(2), 155-158. doi:10.1144/sjg28020155

Riding, J. B., & Thomas, J. E. (1997). Marine palynomorphs from the Staffin Bay and Staffin Shale formations (Middle-Upper Jurassic) of the Trotternish Peninsula, NW Skye. *Scottish Journal of Geology*, *33*(1), 59-74. doi: 10.1144/sjg33010059

Robin, C., Guillocheau, F., Allemand, P., Bourquin, S., Dromart, G., Gaulier, J.-M., & Prijac, C. (2000). Echelles de temps et d'espace du controle tectonique d'un bassin flexural intracratonique; le bassin de Paris. *Bulletin de la Société Géologique de France*, *171*(2), 181–196. doi:10.2113/171.2.181

Sager, W. W., Weiss, C. J., Tivey, M. A., & Johnson, H. P. (1998). Geomagnetic polarity reversal model of deep-tow profiles from the Pacific Jurassic Quiet Zone. *Journal of Geophysical Research*, *103*(B3), 5269–5486. doi:10.1029/97JB03404

Speranza, F., Satolli, S., Mattioli, E., & Calamita, F. (2005). Magnetic stratigraphy of Kimmeridgian-Aptian sections from Umbria-Marche (Italy): New details on the M polarity sequence. *Journal of Geophysical Research*, *110*(B12), B12109–B12138. doi:10.1029/2005JB003884

Steiner, M., Ogg, J., & Sandoval, J. (1987). Jurassic magnetostratigraphy, 3. Bathonian-Bajocian of Carcabuey, Sierra Harana and Campillo de Arenas (Subbetic Cordillera, southern Spain). *Earth and Planetary Science Letters*, *82*(3-4), 357–372. doi:10.1016/0012-821X(87)90209-3

Sumbler, M. G. (1984). The stratigraphy of the Bathonian White Limestone and Forest Marble Formations of Oxfordshire. *Proceedings of the Geologists' Association*, *95*(1), 51–64. doi:10.1016/S0016-7878(84)80020-6

Sumbler, M. (1991). The Fairford Coral Bed: new data on the White Limestone Formation (Bathonian) of the Gloucestershire Cotswolds. *Proceedings of the Geologists' Association*, *102*(1), 55–62. doi:10.1016/S0016-7878(08)80056-9

Sumbler, M. G., Cox, B. M., Cox, R. J., Wyatt, R. J., & Page, K. N. (2002). The Middle Jurassic stratigraphy of the Cotswolds. *In* B. M. Cox & M. G. Sumbler (Eds.) *British Middle Jurassic Stratigraphy: Geological Conservation Review Series, #26*. (pp. 113-226) Peterborough: Joint Nature Conservation Committee.

Sykes, R. M. (1975). The stratigraphy of the Callovian and Oxfordian stages (Middle-Upper Jurassic) in northern Scotland. *Scottish Journal of Geology*,*11*(1), 51-78. doi:10.1144/sjg11010051

Sykes, R. M., & Callomon, J. H. (1979). The Amoeboceras zonation of the Boreal upper Oxfordian. *Palaeontology*, *22*(4), 839-903.

Thierry, J., Marchand, D., Fortwengler, D., Bonnot, A., & Jardat, R. (2006). Les ammonites du Callovien–Oxfordien des sondages Andra dans l'Est du bassin de Paris: synthèse biochronostratigraphique, intérêts paléoécologique et paléobiogéographique. *Comptes Rendus Geoscience*, *338*(12), 834-853. doi:10.1016/j.crte.2006.05.005

Tivey, M. A., Sager, W. W., Lee, S.-M., & Tominaga, M. (2006). Origin of the Pacific Jurassic quiet zone. *Geology*, *34*(9), 789–792. doi:10.1130/G22894.1

Tominaga, M., Sager, W. W., Tivey, M. A., & Lee, S.-M. (2008). Deep-tow magnetic anomaly study of the Pacific Jurassic Quiet Zone and implications for the geomagnetic polarity reversal timescale and geomagnetic field behavior. *Journal of Geophysical Research*, *113*(B7), B07110+. doi:10.1029/2007JB005527

Tominaga, M., & Sager, W. W. (2010). Revised Pacific M-anomaly geomagnetic polarity timescale. *Geophysical Journal International, 182*(1) 203-232. doi:10.1111/j.1365-246X.2010.04619.x

Underhill, J. R. & Partington, M. A. (1993). Jurassic thermal doming and deflation in the North Sea: implications of the sequence stratigraphic evidence. *In* J. R. Parker (Ed.) *Petroleum Geology of Northwest Europe: Preoceedings of the 4th Conference.* (pp. 337-345) London: The Geological Society. doi:10.1144/0040337

Vine, F. J., & Wilson, J. T. (1965). Magnetic anomalies over a young oceanic ridge off Vancouver Island. *Science*, *150*(3695), 485-489.

Wierzbowski, A., Coe, A. L., Hounslow, M. W., Matyja, B. A., Ogg, J. G., Page, K. N., ... & Wright, J. K. (2006). A potential stratotype for the Oxfordian/Kimmeridgian boundary: Staffin Bay, Isle of Skye, UK. *Volumina Jurassica*, *4*(4), 17-33.

Wright, J. K. (1977). The Cornbrash Formation (Callovian) in North Yorkshire and Cleveland. *Proceedings of the Yorkshire Geological Society, 41* (27), 325–346.

Wyatt, R. J. (1996). A correlation of the Bathonian (Middle Jurassic) succession between Bath and Burford, and its relation to that near Oxford. *Proceedings of the Geologists' Association*, *107*(4), 299–322. doi:10.1016/S0016-7878(96)80017-4

Wyatt, R. J. (2002). Shipton-on-Cherwell cement works and whitehill farm quarry, Gibraltar, Oxfordshire (SP 473 177, SP 478 186). *In* B.M. Cox & M.G. Sumbler (Eds.) *British Middle Jurassic Stratigraphy* (pp. 222-226) Peterborough, UK: Joint Nature Conservation Committee

Zhang, C., & Ogg, J. G. (2003). An integrated paleomagnetic analysis program for stratigraphy labs and research projects. *Computers & Geosciences*, *29*(5), 613–625. doi:10.1016/S0098-3004(03)00034-7

Ziegler, A. M., Scotese, C. R., & Barrett, S. F. (1982). *Mesozoic and Cenozoic paleogeographic maps* (pp. 240-252). Springer: Berlin, Heidelberg.

Ziegler, P. A. (1975). Geologic evolution of the North Sea and its tectonic framework. *The American Association of Petroleum Geologists bulletin, 59*(7), 1073-1097

Ziegler, P. A. (1988). *Evolution of the Arctic-North Atlantic and the Western Tethys: AAPG Memoir, 43*. Tulsa, OK: Association of Petroleum Geologists.

Ziegler, P. A. (1992). European Cenozoic rift system. *Tectonophysics, 208*(1-3), 91-111. doi: 10.1016/0040-1951(92)90338-7

Ziegler, P. A. & Dézes, P. (2006). Crustal evolution of Western and Central Europe. *In* D. G. Gee & R. A. Stephenson (Eds.) *European Lithosphere Dynamics: Geological Society of London Memoirs, 32*, (pp. 43-56) Bath, UK: The Geological Society Publishing House.

APPENDIX

APPENDIX
MAGNETOSTRATIGRAPHY OF THE BATHONIAN-CALLOVIAN BOUNDARY INTERVAL: ALBSTADT DISTRICT, SWABIAN ALB, SW GERMANY

Summary report to the Callovian working group. Initially drafted in 1997 and revised here.

James Ogg *(Mesozoic Stratigraphy Lab, Dept. Earth & Atmospheric Science, Purdue University, West Lafayette, Indiana 47907-1397, USA)*

Gerd Dietl *(Staatliches Museum für Naturkunde, Rosenstein 1, D-70191 Stuttgart, Germany)*

and

Rachel Gipe (*Dept. Earth & Atmospheric Science, Purdue University, West Lafayette, Indiana 47907-1397, USA*)

A.1 Abstract

Magnetostratigraphy of the proposed Bathonian-Callovian boundary stratotype near Pfeffingen, Germany, suggests that the boundary level is a minor stratigraphic break coincident with a magnetic reveral. The condensed iron-oolite-rich section of basal Callovian and uppermost Bathonian near Albstadt exhibited a heavy normal-polarity magnetic overprint. Possible primary polarity was interpreted from the directional stability or drift towards a "reversed" polarity hemisphere upon progressive thermal demagnetization. This tentative magnetostratigraphy indicates reversed polarity for uppermost Bathonian (*hochstetteri* Horizon) and a normal-polarity zone overlain by a reversed-polarity zone for the lowermost Callovian (*keppleri* Horizon). The coincidence of a polarity reversal at both the biostratigraphic recognition (definition) of the Bathonian-Callovian boundary and a local irregular-bedding contact in this condensed facies strongly suggests that the boundary interval is a brief hiatus in sediment accumulation. However, the associated magnetic reversal will provide a useful secondary global correlation tool. This interpretation requires testing by acquiring reference magnetic polarity patterns from additional boundary intervals.

A.2 Proposed Bathonian-Callovian Boundary Stratotype of Albstadt District

The Bathonian-Callovian boundary is currently recognized in Sub-Boreal ammonite biostratratigraphy as the base of the *Kepplerites (Kepplerites) keppleri* Horizon of the *K. keppleri* Subzone, *Macrocephalites herveyi* Zone. The uppermost Bathonian is the *hockstetteri* horizon (var. *hockstetteri* of *Clydoniceras discus*) of the *C. discus* Subzone, *C. discus* Zone. The contact between these two biostratigraphic units is rarely preserved.

One locality with an apparently complete boundary at the resolution level of ammonite successions is in the forest preserve "Quellgebiet des Roschbachs" in the upper Eyach valley, about 1 km west of Pfeffingen village in the Albstadt district (48.4°N Lat, 9.0°E Long; about 30 km south of Tübingen) of the Swabian Alb region of SW Germany. Details of the stratigraphy and ammonite fauna from the "Roschbachs" section is described by Dietl (1994), and this region is being considered as the global stratotype for calibration of the Bathonian-Callovian boundary.

Two other requirements for such a global stratotype is the ability to correlate the ammonite-defined boundary by other biostratigraphic and non-biological stratigraphic methods, and the demonstration of a fairly continuous stratigraphic record across the boundary level within the resolution of current stratigraphic methods. Magnetostratigraphy was one component of a multi-discipline investigation of this "Roschbachs" boundary section.

The Macrocephalen-Oolith formation (Unit **e** of the Brown Jura facies) is a condensed facies of iron-oolite-bearing clay to marly limestone. The orangish-brown iron-oolite spherules are randomly distributed in gray to reddish-tan micritic marly limestone or brownish-gray clay. This lithology is easily eroded, therefore the complete "Roschbachs" section is only exposed by escavation, then is re-covered after sampling to prevent removal of its rich ammonite fauna by amateur fossil collectors. The sampled section has the same bed-units as the profile of Macrocephalen-Ooliths diagrammed by Dietl (1994; his Figure 4), but the relative thicknesses are different. Bedding is essentially horizontal.

In this section, the Macrocephalen-Oolith formation encompasses most of the *keppleri* Subzone (basal Callovian) within approximately 70 cm and the *hockstetteri* horizon (uppermost Bathonian) in the lowest 8-cm-thick bed. This stratigraphic interval is bounded by unconformities -- the *keppleri* Subzone is overlain by the *Kepplerities (Gowericeras) gowerianus* Subzone of the *Proplanulites koenigi* Zone implying omission of the two upper subzones of the *herveyi* Zone, and the *hockstetteri* Horizon overlies the *Hecticoceras (Prohecticoceras blanazense* Subzone of the *Oxycerites orbis* Zone implying omission of the majority of the *discus* Zone.

Paleomagnetic drilling by off-set spacing of 2.5-cm diameter cores obtained a nearly continuous record through the Macrocephalen-Oolith formation (24 minicores in 65 cm). Sampling also included the base of the overlying *koenigi* Zone (4 cores in the 10-cm-thick bed) and the underlying exposure of the *orbis* Zone (5 cores in the 30-cm interval).

A.3 Paleomagnetic Behavior, Polarity Interpretation and Mean Direction

All samples underwent progressive thermal demagnezation at 25-40° increments from 250°C through 430-480°C. Thermal demagnetization and measurement on a 3-axis cryogenic magnetometer were performed in a magnetic-shielded room at the paleomagnetic facility at the University of Michigan (laboratory of Rob Van der Voo). Susceptibility was measured after each heating step, and demagnetization was terminated for individual samples when viscous-magnetization effects became a substantial component of the residual magnetization.

Initial magnetizations were very strong, averaging about 10 mA/m, but rapidly declined to 5-20% of initial NRM after heating to 300-350°C. Interpretation of polarity and associated selection of steps for least-squares fitting of vectors for characteristic directions (procedure of Kirschvink, 1980) were based upon visual examination of vector and equal-area plots of the progressive demagnetization. Samples typically displayed quasi-stable characteristic directions from 350°C to 430°C. The mean characteristic vector had an intensity of 0.9 mA/m. With a few exceptions, heating beyond 430°C commonly resulted in acquisition of significant viscous magnetizations, probably associated with a reddening in color of the heated samples.

A possible magnetic mineralogy assemblage in these samples is: (1) goethite, which contributes to the rapidly removed magnetization at low thermal demagnetization step), (2) magnetite, which may be the carrier of characteristic directions in the dark marly matrix, and (3) hematite, which is present in different forms including the brownish iron oolites, a possible initial oxidation at the sediment surface of some reddish levels, the observed reddish weathering-alteration mottling of several samples which probably contributes to the pervasive secondary overprint, and the high-temperature onset of viscous magnetization associated with reddening of the lithologies (in turn, produced by dehydration and oxidation of iron-bearing clays). However, an accuarate characterization of the magnetic carriers requires further tests of magnetic behavior.

Half of the samples displayed a tight cluster of magnetizations centered at 6° declination and 63° inclination (alpha-95 = 4°; K = 107), and this is interpreted to represent the mean normal-polarity direction, even though the direction is very close to present magnetic field at the site

(0.6°E declination; 64.2° inclination). Only 3 samples yielded magnetizations with definite reversed-polarity characteristics; with a poorly constrained mean direction of 184° declination and -35° inclination.

Between these two end-members of "normal" and "reversed" clusters are a distributed array of samples that display partial or substantial progressive drift from the initial NRM direction toward the "reversed-polarity hemisphere". Many of these intermediate samples undergo "over-steepening" in inclinations from the "normal-polarity mean direction", followed by swings in declination away from the "normal-polarity mean direction". Such intermediate samples commonly occur in stratigraphic clusters, often adjacent to the more obvious reversed-polarity cores. On the basis of these behaviors and groupings, most of these intermediate-direction samples were assigned as "reversed polarity, with persistent secondary magnetization", and were excluded from computation of mean directions. An emphasis was placed on directional shifts occurring from 350°C through 430°C -- a steepening trend in inclination was interpreted as removal of a present-day normal-polarity vector from a primary reversed-polarity magnetization, and a shallowing trend while maintaining a northward declination was interpreted as a drift toward a primary normal-polarity magnetization.

This magnetic behavior of both normal-polarity and reversed-polarity samples indicates a persistent normal-polarity (present field) secondary magnetization that is only partially removed by thermal demagnetization prior to onset of significant spurious viscous components. Therefore, the mean normal-polarity direction is distorted by the secondary magnetization. Assuming that the secondary magnetization affects both the normal-polarity and the definite reversed-polarity samples in equal proportions, then combining the mean characteristic-direction vectors from each polarity will result in effective cancellation of the common secondary component. This vector-addition procedure yields a mean Callovian-Bathonian direction of 5° declination and 48° inclination (29°N paleolatitude; alpha-95 estimated as about 15°) [2013 reinterpretation: 3.3° declination, 50.0° inclination and 31° paleolatitude].

A.4 "Preferred" Magnetostratigraphy and Alternative Interpretations

These polarity interpretations and characteristic directions are displayed in the magnetostratigraphy diagram. Polarity rating of samples is based upon the individual demagnetization behavior, and ranges from well-defined "N" or "R" directions, to heavily

overprinted “NPP” or “RPP” samples that were omitted from mean pole computations, to samples with uncertain “N??” or “R??” or indeterminant “INT” polarity.

The upper Bathonian has predominantly normal polarity in the *blanazense* Subzone of the *orbis* Zone, with a stratigraphic hiatus to the overlying reversed-polarity zone of the *hochstetteri* Horizon of the uppermost *discus* Zone. The lower Callovian has two pairs of a normal-polarity zone followed by reversed polarity; the lower set is equivalent to the *keppleri* Horizon of basal Callovian, the upper set spans the following *quenstedti* Horizon. However, this upper reversed-polarity zone (upper quenstedti Horizon) is dominated by samples that have been interpreted as “reversed, with a heavy persistence of secondary normal overprint”. Above a major stratigraphic hiatus, the overlying *toricelli* Horizon of the *koenigi* Zone yielded normal-polarity characteristic directions.

There are several caveats to this interpretation of the magnetostratigraphy. Of the indicated 14 “reversed” polarity samples, only 4 yielded characteristic directions that are quasi-antipodal to the mean “normal”-polarity cluster. This lack of a clearly defined separation of “normal” and “reversed” polarity suggests at least three alternative interpretations of the polarity assignments.

(1) It is possible that the lesser-quality 10 “reversed” polarity samples are intermediate or indeterminant polarity and should be ignored in interpreting the magnetostratigraphy. This conservative approach would imply that the entire section is predominantly normal-polarity with 3 or 4 scattered reversed-polarity excursions. However, the problems with this alternative is the observed rapid drift toward a “true” reversed-polarity direction for several samples and the anomalously high northern paleolatitude (identical to current latitude) computed for the remaining “normal-polarity” Callovian strata -- both of these anomalies argue for a secondary Quaternary overprint.

(2) The interpretation of a heavy and persistent secondary overprint of normal-polarity could be extended to include many of the remaining “normal” polarity samples. For example, the three isolated “single-sample” normal-polarity levels within the upper *quenstedti* Horizon may merely be secondary-overprint remagnetized samples of an original reversed polarity. The dominance of “normal” polarity in all clay-rich facies intervals (e.g., Bed 2 at the outcrop top and Bed 7a) and at contacts of lime-rich beds to adjacent clay-rich facies (e.g., top and base of Bed 4, and base of Bed 6b) is suspicious. The clay-rich interbeds may act as conduits for enhanced weathering and associated secondary magnetization of the original lithology. Therefore, it is possible that the entire stratigraphic interval was originally reversed polarity, and all apparent

"normal"-polarity samples are merely inadequate removal of overprints. However, comparison of the degree of penetrative weathering on individual samples (based on visual description of discolorations, veins, etc.) and the corresponding magnetic behavior did not reveal an obvious correlation. Some of the more altered samples (reddish discoloration of the original grayish matrix) yielded definite reversed-polarity directions.

(3) This outcrop of condensed iron-oolite-rich facies containing at least two major stratigraphic gaps may have magnetizations that are primarily set during submarine hiatuses in deposition or during post-depositional diagenetic processes. A key question is the origin of the iron oolites that characterize this facies. The dispersed iron oolites in a fine-grained micritic or clayey matrix suggest an in-situ formation, rather than a sedimentary deposition of these millimeter-sized spherules. The chemistry and associated magnetization (if any) of these iron oolites would have been altered if these curious features had an iron-hydroxide precurser. Therefore, it is possible that the interpreted characteristic polarities are not synchronous with sediment deposition, and the resulting "magnetostratigraphy" is a local artifact of unusual processes within this condensed facies.

In 1997, there was no reliable magnetostratigraphic sections to provide a coeval record for comparison. The oldest oceanic crust in both the Atlantic and Pacific displays a magnetic "quiet zone" of low-amplitude or negligible magnetic anomalies that encompasses the Bathonian through Oxfordian stages. Deep-tow magnetometer surveys of the Late Callovian through Oxfordian portion of this "quiet zone" region in the Pacific (Sager et al., 1998) are consistent with compilations of Oxfordian magnetostratigraphy sections from Europe (Ogg and Coe, American Geophysical Union presentation, 1997), implying that the "quiet zone" consists of relatively close-spaced magnetic anomalies formed by a frequently reversing magnetic field. The Bathonian through Early Callovian portion of this region was not included in this deep-tow magnetometer survey, but it is probable that this time span is also characterized by frequent magnetic reversals. A few Early Callovian outcrops have yielded magnetostratigraphy that suggest mixed magnetic polarity, but these lack high-resolution ammonite stratigraphy (e.g., pilot studies in southern Poland (Ogg and Gutowski, 1996) and at the Isle of Skye in Scotland (Ogg and Coe, unpublished)). A paleomagnetic survey of a Bathonian-Callovian boundary section in southeastern France only indicated remagnetization or unstable magnetizations (Ogg, Atrops and Melendez, 1996, unpublished).

Additional works in the past few years have added the magnetostratigraphic sequence of the Bathonian-Callovian boundary as recorded in the Lower and Middle Volga region in Russia

including the Russian GSSP candidate in the Prosek section (eg. Guzhikov et al., 2010; Molostovsky & Eremin, 2008). Deep-tow surveys of the low-amplitude zone in the Pacific Jurassic have modeled the marine magnetic anomalies into the lower Callovian, corroborating with the signal previously modeled through anomaly M40 (Sager et al., 1998; Tominaga et al., 2008). The second paleomagnetic reference section spanning the Bathonian-Callovian boundary further corroborates the interpretation of the magnetostratigraphy. As a paleomagnetic reference section, further verification of the magnetostratigraphy from this single section from the Swabian Alb is still necessary.

A.5 Implications of "Preferred" Magnetostratigraphy for the Boundary Stratotype

The close-spaced sampling of this Albstadt section indicates that magnetic reversal boundaries are apparently coincident with the bed contacts associated with the Bathonian-Callovian boundary (base of *keppleri* Horizon at base of Bed 6a, although the lowest 3 cm of this bed was not sampled) and with the base of the *quenstedti* Horizon (base of Bed 4; although there is a 11 cm sampling gap that encompasses the underlying Bed 5 band of soft clay). This coincidence of bedding planes with two of the four polarity reversals strongly suggests the presence of brief hiatuses in deposition. Therefore, the exact Bathonian-Callovian boundary in this Albstadt section is suspected to incomplete at the resolution of this magnetostratigraphy.

However, the association of this Bathonian-Callovian boundary with the reversal boundary between an uppermost Bathonian reversed-polarity zone (*hockstetteri* Horizon) and a lowermost Callovian normal-polarity zone (lower half of *keppleri* Horizon), coupled with the pair of polarity zones within the overlying *quenstedti* Horizon, may provide a very high-resolution stratigraphic tool for global correlation of the Bathonian-Callovian boundary. Indeed, this polarity reversal boundary can serve as a secondary global definition for the Bathonian-Callovian boundary.

It is important that a second magnetostratigraphy reference study is obtained -- either from a duplicate Bathonian-Callovian boundary section or from separate outcrops containing an uppermost Bathonian *hockstetteri* Horizon and a basal Callovian *keppleri* Horizon. This would enable the verification of the magnetic polarity signature of the Bathonian-Callovian boundary in

this condensed Albstadt section. Potential magnetostratigraphy reference sections may be possible within the Swabian Alb or in coeval strata of England.

Once verified, then the "boundary" magnetic reversal will provide a secondary correlation tool that can be applied to non-fossiliferous strata and to oceanic reconstructions, thereby enabling an improved understanding of the global events that are associated with the biostratigraphic events at the Bathonian-Callovian boundary.

A.6 References

Dietl, G. (1994). Der hochstetteri-Horizont - ein Ammonitenfaunen-Horizont (Discus-Zone, Ober-Bathonium, Dogger) aus dem Schwäbischen Jura. *Stuttgarter Beiträge zur Naturkunde - Serie B (Geologie und Paläontologie)*, *202*, 1–39.

Guzhikov, A. Y., Pimenov, M. V., Malenkina, S. Y., Manikin, a. G., & Astarkin, S. V. (2010). Paleomagnetic, petromagnetic, and terrigenous—Mineralogical studies of Upper Bathonian—Lower Callovian sediments in the Prosek section, Nizhni Novgorod region. *Stratigraphy and Geological Correlation*, *18*(1), 42–62.

Kirschvink, J. L. (1980). The least-squares line and plane and the analysis of palaeomagnetic data. *Geophysical Journal International*, *62*(3), 699–718.

Molostovsky, E. A. & Eremin, V. N. (2008). Магнитостратиграфическая Схема Юрских Отложений Нижнего И Среднего Поволжья. *Бюллетень Московского Общества Испытателей Природы. Отдел Геологический, 83*(4), 43-53.

Ogg, J.G. and A.L. Coe (1997). Oxfordian magnetic polarity time scale (GP41A-12). *EOS Transactions, American Geophysical Union, 78*(46) Supplement F186.

Ogg, J.G., and J. Gutowski (1996). Synthesis of Oxfordian and lower Kimmeridgian magnetostratigraphy. *In* A. C. Riccardi (Ed.). Advances in Jurassic Research 2000. Proceedings of the 4th International Symposium on the Jurassic System: *GeoResearch Forum, 1-2* (406-414) Aedermannsdorf, Switzerland: Trans Tech Publications Ltd.

Sager, W. W., Weiss, C. J., Tivey, M. A., & Johnson, H. P. (1998). Geomagnetic polarity reversal model of deep-tow profiles from the Pacific Jurassic Quiet Zone. *Journal of Geophysical Research*, *103*(B3), 5269–5486.

Tominaga, M., Sager, W. W., Tivey, M. A., & Lee, S.-M. (2008). Deep-tow magnetic anomaly study of the Pacific Jurassic Quiet Zone and implications for the geomagnetic polarity reversal timescale and geomagnetic field behavior. *Journal of Geophysical Research*, *113*(B7), B07110+.